REPUBLIQUE ALGERIENNE DEMOCRATIQUE ET POPULAIRE

MINISTERE DE L'ENSEIGNEMENT SUPERIEUR ET DE LA RECHERCHE SCIENTIFIQUE

UNIVERSITE FERHAT ABBAS DE SETIF

THESE

Présentée à

LA FACULTE DES SCIENCES DE L'INGENIEUR
DEPARTEMENT DE GENIE DES PROCEDES

Pour obtenir

Le GRADE DE DOCTEUR D'ETAT

Option: Génie des Polymères

Par

Mr. BOUHELAL Said

"ETUDE DE LA RÉCUPÉRATION DES POLYOLÉFINES ET LEURS MÉLANGES"

Soutenue le: 30 / 06 / 2007
Devant la Commission d'Examen

Jury:

Président:	BELBACHIR Mohamed	Prof.	Univ. Es-senia Oran
Rapporteur:	BENACHOUR Djafer	Prof.	Université Ferhat ABBAS-Sétif
Examinateurs:			
	HADDAOUI Nacerddine	Prof.	Université Ferhat ABBAS-Sétif
	DJELLOULI Brahim	Prof.	Université Ferhat ABBAS-Sétif
	KACI Mustapha	Dr.	Université Abderrahmane Mira- Béjaia

Abstract

The present work deals with two parts . First part deals with reactive blending of isotactic polypropylene (iPP)/low density polyethylene (LDPE)/ ethylene propylene diene monomer(EPDM) and second part deals with the Reversibly crosslinked isotactic polypropylene (iPP) was prepared in the presence of dicumyl peroxide (DCP) and the investigation has been extended the iPP/LDPE blends to see the influence of the crosslinking process in the microstructure and the micro- and macromechanical properties of the modified blends.

The reactive blending of iPP/LDPE/EPDM was used to study the effects of peroxide oxy-radicals on melt miscibility in relation to chemical modification, i.e network crosslinking. Blends were prepared in presence of dicumyl peroxide (DCP), using a plastograph at 30 rpm rotor speed and at 200°C. The crosslinking reaction was evaluated using the Monsanto method. The peroxide effect increases the torque value as residency time in the plastograph is increased, and consequently, the overall viscosity increases . This is shown by capillary rheometry. The overall cristalline degree, as estimated by differencial scanning calorimetry (DSC), decreases , meaning that the mode of cristallisation is affected too. This is illustrated by the decrease of cristallisation temperature and spherulite size dimensions of iPP and LDPE. Impact strength results show a ductile-brittle behavior transition appearing for the equilibrium weight fraction of (iPP/LDPE) matrix. Scanning electronic microscopy (SEM) analysis shows a ductile fracture for compositions where each component of the matrix is predominant or major. The complex interpenetrating networks formed are accompagnied by some islands regions of iPP and LDPE. Such a structure is evaluated by combining results of DSC and dynamical mechanical thermal analysis (DMTA). The binary blends based on LDPE/EPDM offer interesting materials (from the mechanical point of view); this is not the case for the reactive binary blends based on iPP/EPDM . Finally , the ternary reactive blends of iPP/LDPE and 20 phr EPDM overcome the problem of compatibility with an increase in the ductile behavior and a larger visco-elastic domain, particularly when LDPE is the major component.

Concerning the second part of the reversibly crosslinked iPP, it was prepared in the presence of dicumyl peroxide (DCP). The effects of the peroxide oxy-radicals in the melt were investigated in relation to the modification of the polymer. The dynamic rheology analysis of the crosslinking process was carried out by using a plastograph. The crosslinking reaction was evaluated by the Monsanto method. The resulting structure of the modified samples was studied by means of Infra-red (FTIR) , differential scanning calorimetry (DSC), wide-angle X-ray scattering (WAXS), dynamical mechanical thermal analysis (DMTA), microhardness and mechanical properties. The degree of crystallinity of the modified iPP, derived from DSC and WAXS, remains almost unchanged, i.e., the crystalline structure is unaffected, though the lamellar thickness slightly decreases. Some mechanical properties of the crosslinked iPP, in particular, the impact strength, are greatly improved with reference to the properties of the unmodified material. The impact strength shows a brittle-ductile behavior transition appearing in the modified iPP for all the crosslinking agents studied. We have extended the investigation to analyse the generated ethylenic chains by means of DMTA, DSC, and FTIR. More than that, this crosslinking method was extended to the blends based on iPP/LDPE by using WAXS, DSC, microhadness and tensile experiments. The differents compulations shows an academic and industrial interest.

Introduction

The present work deals with the study of recycling of polyolefin's. Based on the statistical data, the Polyethylenes and Polypropylenes represent almost the major part of the total thermoplastic materials consumed over the world, and enclosing all activities sectors [1]. More than three decades, blending of these two materials has been the subject of intensive research in both academic and industrial laboratories but without significant success. The main goal of blending is to obtain "new materials" with interesting properties such as mechanical properties, enhancement of impact strength at low temperature, and, last but not least, improvement of processability. Blending is also one road to solve plastics recovery problem.

The most relevant point in our study is the reactive blending approach. There are fundamental differences between conventional blending and the reactive blending; where covalent bonds are involved. It means that we assist to new generated structure, involving the formation of networks and modifying the morphologies of individual polymers by combination. The combination of systems composed of relatively flexible soft segments and stiff hard segments will lead to useful and stable phase. This is possible by links formed in the presence of radicals or the macro-radicals. This relatively new topic has become, over the last decade, one of the main research subject for academic as well as industrial laboratories. Reactive processing is capital for further research not especially to look for new polymers but also new interesting blends and especially for plastics recycling and environmental concerns. Now, we assist to the environmental policy and the research could not be excluded from this context. The new tendencies are based on academic method and practical industrial needs. Our experimental protocol, as reported and described in this thesis, contributes to a better understanding of industrial, economical and environmental points of view related to polyolefin's applications.

This thesis is organized into four parts: one theoretical part and three experimental ones. The theory part starts with a summarized history of polymers, from the natural rubber used by the Incas in the 1500's up to the introduction of advanced and emerging materials of the 21st century. The second part deals with the materials used and the morphologies of each semi-crystalline material. The third part deals with

polymer blends, including the different methods and techniques used to prepare them. In that part, we have judged that the state of recycling is the most appropriate chapter to show the challenges and the importance of our study and the plastics recycling industry, for that purpose, we are referring to the USA example since the USA are giving a great importance to recycling (there is even an American Recycling Council) [2],

We are presenting the most recent results based on the usefull studies on the reactive compatibilizer EPDM using the most appropriate technique: reactive extrusion , which is in reality replacing conventional single extrusion. The second part deals with the some innovative results that permitted us to have an US patent: it is based on the reversibly crosslinking reaction and continuation to our results , a deep study was done on, this is the third part of experimental study, the forth and last part is dealing with the use of the newest techniques for the iPP/LDPE blends. We are still working on the effect of doping in one case and thermo-mechanical degradation by intensive shearing in the other case.

I- Most important events in the history of polymer science.

Natural polymeric materials have been used since the apparition of man on earth. Synthetic polymers appeared in the 1500's when Incas used a modified natural rubber latex to make balls to play with…The synthesis of urea by Wöhlert (in Hambourg in 1828) was a great relevant result at. a laboratory scale. The polymer term was introduced for the first time in 1833 (by Berzelius), and it took a century to get accepted by the scientic community (Staudinger, in1924.)

The most important periods and events in the history of polymer science are :

1828 : -**WÖHLER** synthetized Urea, first time use of the polymer appelation

1838 : **Regnault** synthesized accidently the first polymer (PVC) by exposition to the light, and , in 1839 , **Simon** noticed the solidification of styrene.

1839 : Vulganization of natural rubber by **Goodyear** for manifacturing bycycle and car tires

1845 : **Schönber** discovered the nitrocellulose (which was directly used for military application)., In the same year, **Hofman** and **Blyth** identified the polymerization reaction of styrene.

1847 : **Berzelius** synthesized a polyester from glycerine and tartic acid.

1859 : **Joule** confirmed the origin of rubber elasticity .

1869 : **Hyatt celluloid brothers** manufactured the the first synthetic plastic material at an industrial scale : the monomer was modified cellulose dinitrate.

1900 : In this century, we can find different industrial products such as nitrocellulose, « silk cellulosique » known as Chardonnet, acetate, Dunlop air chamber, PMMA (1902 by Röhm and Haas)… oOher trade marks such as Perpex, Lucite.

In 1907, Baekeland patented the bakelite (curing of phenol /formaldehyde). Nowdays, the thermoset materials are very important. Buna, BASF, and Bayer developped the most important rubber materials.

1924 : Staudinger gave and explained the « macromolecule » concept which replaced the « colloidal » particle idea that was used to explain the particular properties os materials such as : cellulose, amidon and natural rubber…

1920-1930 : emergency of the « polymer physics science « : differents analytical methods were then used such as X-Rays, Viscosimetry in solution. Svedberg showed the existance of macromolecular substrances by ultracentrifugation.

From the industrial point of view, the thermoset materials were developped.

1930-1942 : Carothers set the principal basis of polyamide polycondensation reaction. Dupont compagny (1939) manufactured synthetic fibers from PA 6,6. In the same period, we observed the apparition of first thermoplastic materials : PS and PVC.(IG-Ludwigshafen, 1930/31) ; polyurethane,(IG-Bayer, 1937) ; PA 6 (Schlack 1938), LDPE (ICI 1939) ,PTFE (Dupont compagny 1940)…

In parallel, polymer physics has known a big development : three principal aspects were established :

a) dependance of macromolecular size on thermodynamics and viscosimetry of solution. Differents definitions and techniques were developped to measure molecular weights .
b) The analysis of cristalline structure and the morphology in different aspects.
c) The explanation of the origin of viscoelastic behavior through the use of different mathematical models.

1940-1970 : this period, could be considered as the golden period for “Polymer Science and Engineering ”., from the academic as well as the industrial side. Most of important progress of mode, technics, systems of differents routes of polymerizations by introduction of coordinated metal catalyst. [2]Two of the most important accommodate polymers used until nowdays, polyethylene and polypropylene (**Ziegler and Natta, Nobel price 1963**) also the engineering materials such as PUR, ABS, SAN, PET, POM, BPAPC, PTFE ,PBT, thermoset materials such as epoxy and so on…; have penetrated the automobile, aeronautics, agriculture, medical, engineering… markets with rapid and convenient substitution of “conventional” materials such as wood, ceramics, metals…

The most important studies and discoveries during this period were : a thorough investigation of conformations and configurations; the discovery of lamellae morphology in crystalline polymers (**Keller, Fisher and Till).** I the field of fracture mechanics, the significant and relevant aspects of crazes, cracks and fracture mechanisms were assessed (**Hsioo, Sauer, Kambour**).

1970-1995 :

It was the period of intensive works on simulation (introduction of powerfull computers), the emergence of new physical, mathematical and new characterization methods of investigations : Neutrons diffusion , X rays, RMN, FTIR, AFM … New developped thermodynamics theories and physical approaches (**Benoît, Strein,**

Fischer, Zachmann) have contributed to better understanding the polymer physics The reptation models **(Gennes, Doi, Edwards)** and solid thermodynamics contribution (**Kovacs, Mandelkerm, Hoffman and Wunderlich)** have given new essors and knowlegde on diffusion, adhesion, compatibility, glass transition, phase separation and cristallisation… Numerical simulation and modelization (**Binder, Monnerie, Suter**) and theoretical approaches (**Leibler, Cloizeaux**) were precious support and tools for analysis of structures… The progress was also marked by the appearance of solid polymerization (**Wegner, H.F.Mark, Ringsdorf**)**,… Kaminski** had prepared new catalysts for engineering polymers, temperature resistant, intrinsic conductors, functional, photosensitives, biodegradables polymeric materials…
Polymer based materials can be multifunctional, based on the demands of emerging technologies, and are related to several interdisciplinary fields : chemistry, physics, biology, engineering…. The economical importance of polymers is related to their wide range of uses and their applications is so many interesting and different sectors

I-1 Materials of 21 st century : polymer based NANOCOMPOSITES

Industrial nations regard the development of new and improved materials by the design of appropriate engineering and scientifics devices, the understanding of mechanisms or structures, and the development of new methodologies for materials selection with regards to environmental impact…. Many nations have promoted government-backed initiatives for the development and exploitation of new materials that generally include « high-performance » composites, new engineering ceramics, high-strength polymers, glassy metals, and new high-temperature alloys.The recent development of nanotechnologies brings a new class of materials : NANOCOMPOSITES. This type of materials is dominated by polymer based systems So, the challenge is still here : produce innovative polymer matrices for new and environment friendly nanomaterials ; a good exemple is to produce polyolefin/clay nanoparticles nanocomposites for heat resistant materials… This could be achieved through the use of modified polyolefin matrices…

POLYOLEFINS

Introduction

Polyolefins comprise the largest portion of the world commercial polymers. The oldest crystalline polyolefin is branched low density polyethylene (LDPE). LDPE contains varying amounts of short chain and long chain branches and has a crystalline melting point of about 110°C. Linear high density polyethylene(HDPE) consists of almost all linear ethylene unit and has a crystalline melting point of about 135°C. Linear low density polyethylene (LLDPE) contains significant amounts of short chain branches by adding small amounts of comonomers such as butene-1,hexene-1,octene-1, or 4-methyl pentene-1. There are also medium density form (MDPE) and ultra low density form (ULDPE).

Polypropylene can exist in atactic, isotactic, and syndiotactic forms. The first synthesized polypropylene had an atactic form. It is an unvulcanizable elastomer and has few practical applications. Isotactic polypropylene has the asymmetric carbon atoms with the same *d*- or *l*- configurations and a crystalline melting temperature of about 165°C. It was first synthesized in 1955 by Natta et al [1] and has become an important commercial polymer since the late 1950's. In recent years, isotactic polypropylene having various tacticity levels has become commercially available using métallocene catalysts [2].

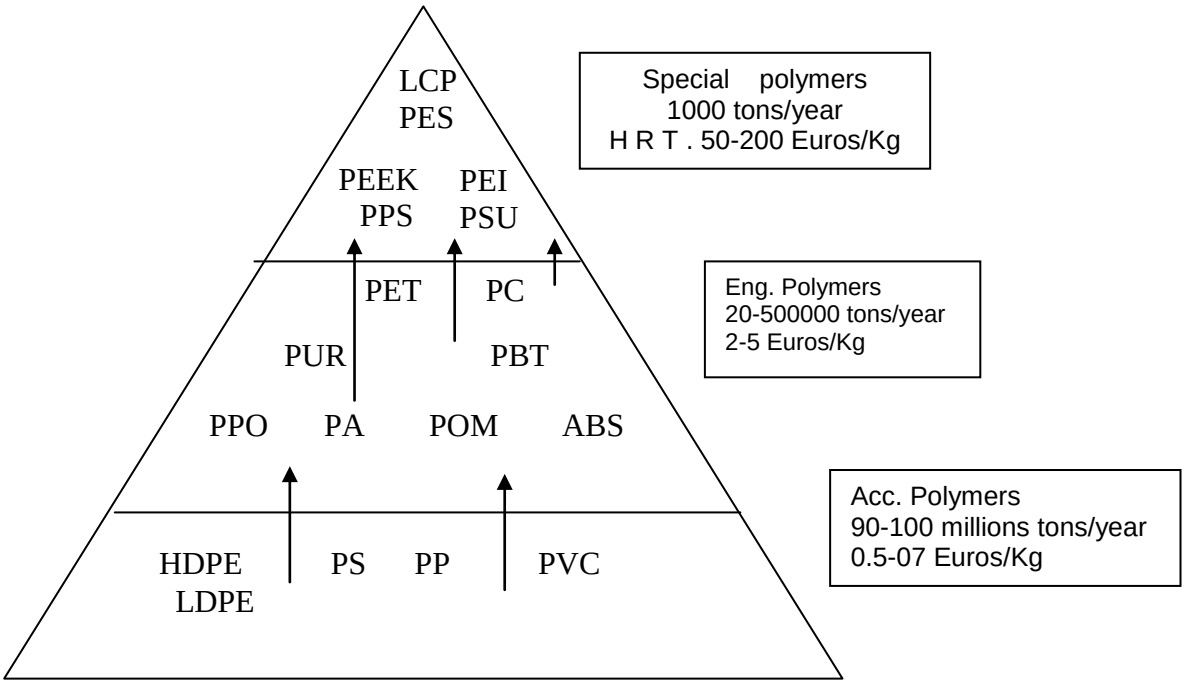

Fig 1 : Diagram of consommation of polymer materials [3]

From the above diagram [3], one can appreciate the challenge and the interest of the use of polyolefin materials compared to other polymeric materials. The future of these polyolefin materials is still considered bright due to possible extension of their properties and applications through chemical modifications and blending, thus they will continue to have a large part among the engineering materials.

Polyolefin structure

Introduction :

The structure of polyolefin materials, including polyethylene, isotactic polypropylene and isotactic polybutene-1 is of great importance and present various polymorphic crystal structures. The cristallization, morphology and orientation development of these polymers are strongly dependent to polymer processing applications example : melt spinning, tubular blown film extrusion, compression molding and injection molding.

Some polyolefins exhibit polymorphic crystallization behavior during processing. We find the relationships of the structure with stress level, cooling rate, and material characters (i.e..crystalization rate and sterio-regularity). It could be considered for

some polyolefins that the structural transformation processes ocurring as function of time or involving some structure modification as was our case: example of reactive extrusion or reactive crosslinking processes. This involve transformation of a less stable form of the (form II to form I) as was the case of polybutene-1 and induced cristalization of β form cristalization for isotactic polypropylene, or some mesomorph (smectic) form during ageing , annealing or caused by chemical modification as was the case of chemical crosslinking process.

1) Polyethylene Morphology

Polyethylene generally crystallizes into an orthorhombic unit cell with parallel methylene ($-CH_2-$) chains with all trans chain conformations. This type of crystal structure was first found by Muller in 1928 for n-paraffins. Muller later found that many n-paraffins transformed to a hexagonal unit cell at temperatures near their melting points. Subsequently, Muller and Lonsdale found a triclinic structure in even n-paraffins with low molecular weights.

After LDPE was first produced by ICI in the 1930's, its crystal structure was investigated by C.W.Bunn of the firm. He confirmed the Muller orthorhombic structure and gave the unit cell dimensions of a=7.40 Å,b=4.93Å,and c=2.53Å. the second generation of studies of the crystal structure were made in the 1960's with the new developed linear polyethylene, HDPE. These had the same unit cell with all trans chain conformations as found by Muller and Bunn.

The crystalline structure of polyethylene copolymers with small amounts of olefinic comonomers were also investigated, Swan of union Carbide compared the crystal structure of 100" linear polyethylene with those copolymers containing rondomly inserted propylene, butene-1, pentene-1, hexane-1, and heptene-1 comonomers. The propylene copolymers showed substantial increases of the a-axis dimension, from 7.42Å to 7.92Å, as propylene content increased. This is apparently because propylene units can be incorporated into the crystalline lattices. For the copolymers with larger comonomers (butene-1, pentene-1, hexene-1 and heptene-1), the dimensions of a-,b-,and c-axes are independent of comonomer content.

At high pressures, HDPE melt crystallizes into a hexagonal crystalline form but this crystalline form transforms to the orthorhombic structure at lower pressures and temperatures.

2) Isotactic polypropylene morphology:

Isotactic polypropylene was found to be polymorphic, exhibiting α-, ß-, and γ-crystalline forms as well as a mesomorphic (smectic) structure. The most stable form seems to be the α-structure, determined by Natta and Corradini. It has a monoclinic into unit cell dimensions (a=6.65Å, b=20.96Å, c=6.50Å, and ß=99.3°). The c- axis corresponds to polymer chain or helix axis; The 3/1 positive and negative helices of trans-gauche$^+$ trans and trans-gauche$^-$ trans chain conformations are arranged in a balanced manner in unit cell.

The ß-crystalline form was first identified for the first time in 1960. it exhibits wide-angle X-ray diffraction (WAXD) reflections at d-spacing of 5.53Å and 4.17Å. it has been realized since the paper of keith and al, that the ß-form polypropylene has a hexagonal unit cell. The ß-crystalline form can also be induced by a range of nucleating agents or chemical modification as will be discussed in our present study.

The γ-crystalline was first observed by Adding and Beintema and has since been the subject of extensive study. They proposed an orthorhombic unit cell with a=8.54 Å, b=9.93 Å, and c=42.41 Å. In the γ-form unit cell, there co-exist macromolecules with non-parallel chain axes which make an angle of 81°. In metallocene catalyst isotactic polypropylenes containing significant amounts of sterio-irregularities, the γ-form crystal is predominantly formed at high crystallization temperatures.

Mesomorphic (smectic) isotactic polypropylene was first prepared by Nattaet al. by quenching molten isotactic polypropylene in ice water. This form seems to consist of a disordered array of the same 3/1 helices. This mesomorphic form exhibits mechanical properties similar to crystalline polypropylene but gives no sharp X-ray diffraction peaks. When annealed at temperatures above about 80°C, it transforms to the monoclinic α-form.

Table 1. Crystal Structure of Various Polyolefins.

Polymer	Crystallization form	Chain Conformation	Unit cells (length: Å)	WAWD peaks (Å)
Polyethylene	Orthorhombic form	All trans	Orthorhombic ($a=7.40, b=4.93, c=2.53$)	(110) (200) (020)
	Hexagonal form	All trans	Hexagonal ($a=4.80, c=2.45$)	
Isotactic Polypropylene	α-Form	3/1 helix (tg^+) or(tg^-)	Monoclinic ($a=6.65, b=20.96, c=6.50$, ß=99.3°)	6.26(110) 5.19(040) 4.77(130) 4.19(111)
	ß-Form	3/1 helix (tg^+) or(tg^-)	Hexagonal ($a=12.74, c=6.35$)	5.53(200) 4.17(201)
	γ-Form	3/1 helix (tg^+) or(tg^-)	Orthorhombic ($a=68.54, b=9.93, c=42.51$)	6.37(111) 5.29(008) 4.42(117) 4.19(202)
	Mesomorph (smectic)	3/1 helix (tg^+) or(tg^-)	-	5.99 4.19

Crystallization, orientation and lamellar structure

Since the polymers are never completely crystalline than the crystallization of polyolefins under quiescent conditions is generally nucleated by nucleators or heterogeneous impurities in the system which may include catalyst residues and added nucleating agents. Some inorganic additives such as calcite, clay, and talc can act as nucleating agent. Crystallization mechanism is argued to be the competitive effects of cooling rate and crystallization rate or in others words the growing rate

which grows in perpendicular specific direction to center known as nucleon. The unit repeat cell known as lattice developing in tree dimensions which rise to the formation of spherulites: this spherulite could take a shape of disc, rod or perfect spheres and are strongly dependant on preferential growing direction axes (x,y,z). In most cases there are two preferential direction and the shape looks like the disc or rod in most cases for the crystalline polymers and they are called lamelleas crystal structure.

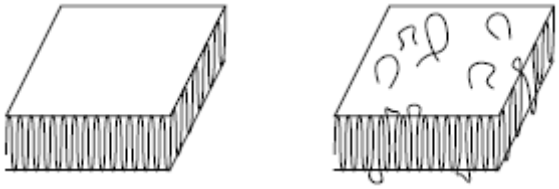

Fig 2 : Lamellae models examples

These lamellae were about 100 Å thick. The dimensions are strongly dependant on the structure configuration and conformation also orientation induced during the quiescent melt and which are determined by the crystallization conditions of the process and starting melt temperature. Spherulites formation of polyolefins materials have long been known to form negative spherulites, *i.e.* spherulites where the angular refractive index (n_θ) is greater than the radial refractive index (n_T), The different observations reported by many authors subjected that there intercrossing lamellae structure almost normal to the surface of the main lamellae. This is often known as secondary crystallization or epitaxial lamellae branching. This epiculiar phenomenon is well known as Shish-Kebab model.

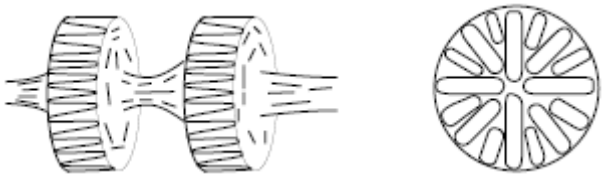

Fig 3: Representation of Shish-Kebab model

The crystallization mechanism of thick, oriented thin film and fibber of the polyolefins show differents crystal structure and sometimes there is transition to one

configuration to more stable configuration or polymorphisms and are processing dependances. Crystalline polyolefins possess in general various polymorphic crystal structures as well as mesomorphic structure in some polymers. The structure in a fabricated shape may vary with polymer processing method, processing conditions and material characters. In various polymer processing operations, the common governing factors to determine the structure are generally melt stress level at the position of solidification, cooling rate and crystallization characters of polymer. Each polymer processing operation gives different stress and cooling rate history, which leads to different structures. A structure overview in various processing operations of polyolefins is given in table 2 [ ].

Table 2: Polymorphic Crystallization in Polyolefins Processings

Polymer	Melt Spinning	Tubular Blown Film	Injection Molding	High Melt Pressure
Polyethylene	**Orthorhombic**	**Orthorhombic**	**Orthorhombic**	**Hexagonal**
Isotactic Polypropylene	**A-monoclinic Mesomorphic**	**α-Monoclinic**	**α-Monoclinic ß-Hexagonal**	**γ-Triclinic**

Due to high cooling rates during polymer processing or for other reasons, thermodynamically less stable structures are sometimes obtained *i.e.:* the mesomorphic form in isotactic polypropylene, the planar zigzag form in syndiotactic polypropylene. These less stable forms will be transformed into a more stable crystalline form during ageing or annealing. The lamellae twisting and epitaxial lamellae branching in some α-polyolefins act in opposite sense than the crystalline chain-axis orientation levels; the syndio is more regular than the iso and the linear is more regular and stable than the branched one

Polymer blends

Introduction

Polymer blends, which may be defined as ‘’any combination of two or more polymer resulting from a common processing step, are combined or blended in fluid state’’ [ ]. The first question is: are the polymers miscible?

We can distinguish between two cases:

- Miscible; then a real blend is formed on a molecular scale; the individual components have “disappeared”

- Immiscible; we have a dispersion in which both components retain their own identity.

Both types of blends are being used and are commercially available. The original idea was of gaining extra performance by blending. The pioneers blends were the blends based on the rubbers where they predates those of thermoplastics by nearly a centery. However, development of processing technology permited the rapid penetration of blends in the market. New generation of engineering plastics materials appeared: defined as the material capable of being formed to precise and stable dimensions, exhibiting high performance at the continuous use temperature above 100°C, and having tensile strength in excess of 40 MPa. Reading the patents based on blends , one may attempt to identify the reasons for blending and the means by which these goals were achieved. We assist to more than 5000 patents (in last 20 years) based on engineering blends and most of them are commercial, the main owneers are major suppliers and big compagnies (table N° shows the different properties attempt).

Table 3 : Principal Properties claimed in blend patents [ ]

N°	Property	Frequency %
1	High impact strengh	38
2	Processability	18
3	Tensile strengh	11
4	Rigidity/modulus	8
5	Heat distortion temp. HDT	8
6	Flammability	4
7	Solvent resistance	4
8	Thermal stability	3
9	Dimensional stability	3
10	Elongation	2
11	Gloss	2
12	Others	4

It is apparent that toughening and processability are the major concerns of the patents issued, the second important reason includes the strength, modulus and heat deflection temperature. The third group of concerns includes the flammability, solvent resistance as well as thermal and dimensional stability.

There is no doubt that the main reason for blending, compounding and reinfortcing is economy. If a material can be generated at a lower cost with properties meeting specifications the manufacturer must use it to remain competitive. In general the following economy-related reasons can be listed:

- Extending engineering resin performance by diluting it with a low cost polymer.
- Developing materials with a full set of desired properties
- Forming a high performance blend from synergistically interacting polymers.
- Adjusting the composition of the blend to customer specifications.
- Recycling industrial and/or municipal plastics scraps.

In most cases polymer pairs are immiscible. Dispersions occur most ofen, and real mixtures are exceptions. But the methods of blending plays a major role ; we can list the most important preparation methods of polymer blends:

- Mechanical mixing
- Dissolution in co-solvent then film casting, freeze or spray drying
- Latex blending

- Fine powders mixing
- Use of monomer(s) as solvent for another blend component then polymerization as in IPN's or HIPS manufacture
- Diverse other methods of IPN technology

For economic reasons mechanical blending predominates, beside that the highly dispersion is optimized by high performance blends machine and the most important equipment obviously should be extruders as continuous mixers. Other mechanical mixers are of so important such as Batch mixers and special machines; the following table report the type and the functions for compounders.

Table 4 : Different mixing processes used for blends mixing.

Machine	Function
Continuous Mixers	
-Twin-screw extruder	*Primary compounder*
-Twin-shaft intensive mixers	*Primary compounder*
-Disk extruder	*Adaptable for compounder*
-Single screw extruder	*Second choice*
-Single shaft mixer	*Second choice*
-Motionless mixer	*Add-on*
-RAPRA CTM-mixer	*Add-on*
-DYNAMIC melt mixer	*Add-on*
Batch Mixers	
-Roll mills	*Laboratory or short runs*
-Internal sigma-blade mixers	*Laboratory or short runs*
-Kinetic energy mixers	*Speciality or short runs*
Special Machines	
-Plastoficator Patfoort	*Blending or recycling*
-Reverser	*Recycling*
-Multi-stage systems	*Large volume, primary*

In practice, the first and second choice are indicated in the following table based on the advantages and disadvantages of typical and most popular equipments widely used :

Table 5 : Advantages/disadvantages of different machines used for blends mixing.

Machine	Advantages	Disadvantages
Twin-screw extruder	Uniform high shear stress flow, short residence time. Self-cleaning, flexibility and ease of change	Capital cost
Single-screw extruder	Cost, availability, flexibility for modification of screws and add-ons	Poor control, low rate of shearing, long residence time, deap-spaces
Internal mixer	Uniformity of stress history, control	Capital and operational cost. Long cycle, batch to batch variation

Polymer blends have increasing technological importance because they can combine mechanical, thermal, or other useful resulting properties from different polymers to obtain materials that are unavailable from the constituents alone.

A blend's physical properties depend on its miscibility, composition, structure, molecular state of dispersion, the morphology of two phase mixtures, adhesion between phases and the kinetics of blending. In most cases, since it is not possible to get direct determination of either phase diagram, it could be taken as measures of apparent properties such as the measures of dependency of glass transition temperature or the Heat distorsion temperature (HDT) as simplest measurement techniques. It is noticed that provides similar dependency curves; as shown in the following figures that predict the general cases of different phase diagrams.

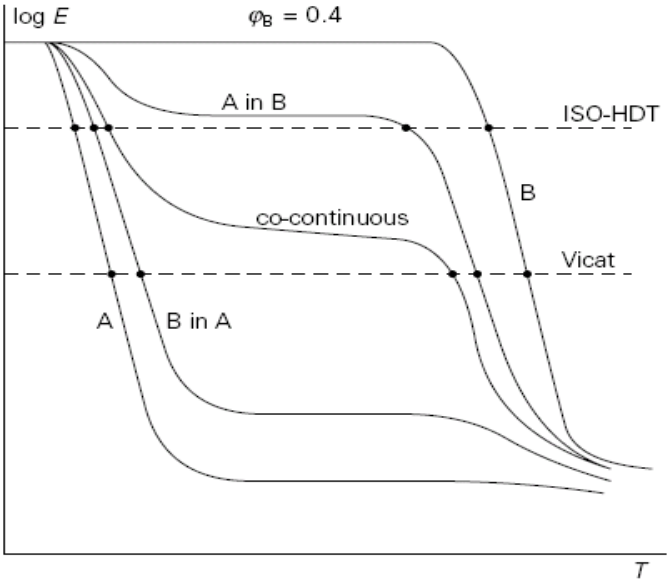

Fig 4 : Effect of softening temperature on the morphology on the softening temperature

From this representation, one can distinguish that the extreme case considered is the Heterogeneous blends, the upper case B and lower case A: where the curve does not show any sign of the transition but the behaviour of the individual components.

The second case holds for the other extreme case; it denotes the behaviour of a pure dispersion in which A and B retain their own individuality is called the co-continuous phase;

The third case: represents the intermediate cases: indicates partial miscibility; we see a two-phase system of AB blends with different behaviours of A in B.

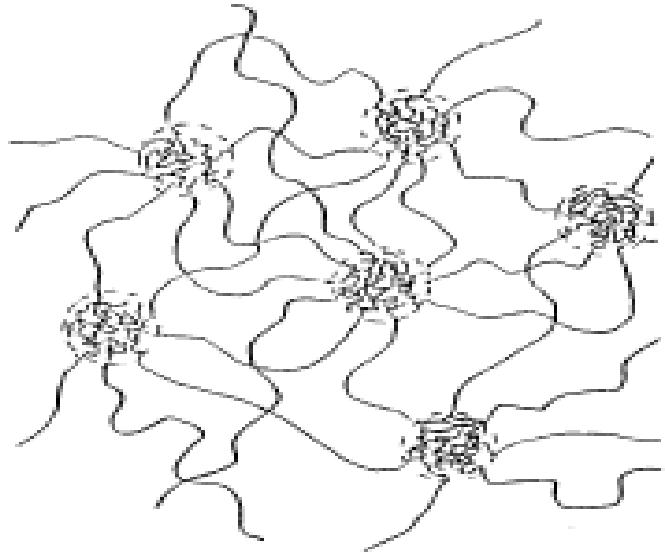

Fig 5 : Compatible phase of binary blend

In fact this factor plays an important role, in the blending process the domain sizes have to be sufficiently reduced before complete mixing by diffusion can take place.
Diffusion is a slow process, so that homogeneous mixing can only be reached after a long time of mixing. This situation is less complicated by addition of some coupling or compatibilizer agents … In fact, the enthalpy of mixing should be negative or exothermic for a mixture. This condition can be achieved if polar groups in the polymer interact in certain ways. These interactions may arise from various mechanisms such a dipole-dipole forces or ionic interactions. Few, if any, polymeric blends exist in a thermodynamic equilibrium state. Some thermodynamic compatibility or chemical links such as grafting, crosslinking, or an interpenetrating network formation should be present in a stable blend. Figure N° illustrate the network region at. Equilibrium state.

However, some compatibilizers chemical species, usually block or graft copolymers and ionomers, can be used to improve miscibility usually because their segments are identical to those of polymers being mixed. They affect the properties of polymer, polymer melt and influence the polymer's dispersion in a non solvent. Dispersing additives such as fillers and reinforcing agents can also be enhanced by compatibilizers at the polymer additive interphase.
The desirable effects can be obtained if one segment from a block copolymer is miscible or adds to one of the phase.

Future Outlook :

Advanced polymer blend deals with compatibilizers that can be formed in situ. It is considered as a new approach to solve the blending compatibilty problems, it is achieved by modifying the mixture's components in such a way that one of the polymer reacts with the other. For the instance, when the polypropylene is modified by the maleic anhydride in presence of decomposing organic peroxide and given polar polymer resin is added to modified polypropylene a good blend could be achieved. Because the polyolefins and engineering polymers have desirable properties, blending these components is of considerable interest. Several studies focused on compatibilizing iPP with other polyolefins or different thermoplastic materials [ ]. Recently, there is development of reactive processing and more recent view is synthesized of functionalized polymer with different amounts of polar groups but many problems arise from the difficulties of getting homogeneous distribution of the functional groups along the macromolecular chain.

For this purpose and from our recent finding, obviously the reactive extrusion is the most important process to optimize and monitoring the compounding. It provides desirable blends compatibizers, the new polymer blends could be achieved with an interesting properties and could be the ideal way to solve and simplify the recycling or the recovery of plastic materials.

State of Plastic Recycling
(The USA are cited as an exemple)

Plastics recycling has become already an established industry in most developed countries (as in the USA, Canada and the European Union), and is becoming so, slowly but surely in developing countries (as in Algeria, with the ENPC industrial Unit TRECYPLAST in Rouiba near Algiers). For instance, in USA, the number of companies handling and reclaiming post-consumer plastics jumped from 310 in 1986 to 1,677 in 1999, and the American Plastics Council (APC) believes that the recycling of plastics will become a more efficient and mature segment of the US economy (ref.)

All over the world, the capacity to process materials and the market demand for the recovered plastics both currently exceed the amount of post-consumer. Each year the amount of recycled plastics increases by millions of kilos while the recycling rate has stabilized around 23%. Actually, markets for recycled plastics are stable in most areas and expanding in many others. Industry of recycled plastics is also beginning to hit its stride, and new ASTM (American Society for Testing and Materials) standards and test methods are paving the way for use of these materials in structural applications.For many products, the switch to plastic means longer life and less maintenance, which translates to lower cost over the life of the product.

As an illustrating example, the US American Plastics Council (APC) has initiated an "All Plastic Bottle Collection Program" to increase recycling of plastic bottles and will work with communities to educate consumers in that sense. Research has shown that the simplified message "recycle all of your plastic bottles" significantly increases collection of post-consumer plastic bottles. The program has the support of several other industry trade associations such as the Association of Post Consumer Plastics Recyclers (APR), the National Association for PET Container Resources (NAPCOR), and the National Soft Drink Association (NSDA).

Recycled materials compete with virgin materials. The cost-effective recycling of new packages (for example) will require renewed education for households, recyclables collectors, the Materials Recovery Facilities and handlers sorting plastic, and the

processors. The end result will be a more dynamic industry poised to recover more valuable resources.

Handling:

After plastics are collected, they are delivered to a handler for sorting (if necessary) and densification.

- **Sorting:** Most collection programs today are multi-material, commingled programs. This means that plastics are collected with other recyclable packaging such as steel, glass and aluminum. In these programs, plastics will need to be separated - or sorted - from the other materials before they can be sent to market. Even if plastics are delivered in a separate stream, they still may need to be sorted by resin type (e.g., PET, HDPE) and to remove other forms of contamination. Today, sorting is performed either in a manual system, where plastic bottles and containers pass along a conveyor belt and are sorted by hand or in an automated system, which uses advanced technology (e.g., infrared identification or X-ray) to identify plastic containers by resin type and/or color.

- **Densification:** Because it takes only a little bit of plastic to produce large volume bottles, e.g. a milk jug, empty plastic bottles have a high "volume to weight" ratio. High volume-to-weight ratios translate into high shipping costs. Therefore, once plastics are sorted, handlers will densify them prior to shipment. Baling (using a vertical or horizontal baler) is the most common means of densification, although some handlers granulate, or grind, plastics. The densification method selected usually depends on the specifications required by the handler's market.

Reclamation:

Reclamation is the step where sorted and densified plastics are converted into flakes or pellets, which can then be used to manufacture new products. (Pellets and flakes are the two forms in which plastic feedstocks are commonly sold.) Flakes are made

by feeding plastic articles (e.g., bottles) into a granulator where they are chopped into small uniform-sized chips of material.

End-Use:

Once the plastic is in flake or pellet form, it can then be sold to manufactures to be made into new products. These include bottles and containers, clothing, automotive accessories, bags, bins, carpet, plastic lumber, film and sheet, hospital supplies, housewares, packaging, shipping supplies, toys and more. More than 1,300 products, made from or packaged in recycled plastics, are listed in APC's online Recycled Plastic Products Directory.

It is important to keep in mind that these components - although common to all plastic recycling systems - may occur in a slightly different order. It also is important to recognize that one facility or company may perform multiple roles in the system. For example, a company may fulfill the role of both plastics handler and reclaimer, or the role of both reclaimer and end-user. In general, however, the four components described (guidance for identification, separation, densification, transport and marketing of plastic recovered) must occur at some point in the system in order to recover plastics for use in manufacturing recycled plastic products. These efforts resulted in environmental benefits.

As good example of environmental friendly: Vinyl Mineral Bottles? It may not sound like it is the fashionable thing to do, but clothing manufactured out of post-consumer recycled PVC could just become the next "big thing" in the fashion industry. Rhovyl, a French clothing manufacturer and Elf Atochem, a French additives company, are working together to develop technology to transform old bottles into new clothing. They have created fashionable sweaters, as well as scarves and socks, with fibers used to produce the yarn coming from reclaimed PVC mineral water bottles. Approximately 27 bottles are needed to produce one sweater and the fiber is combined with wool in a 70/30 percent vinyl/wool blend. France uses approximately four billion vinyl bottles annually and thanks to innovative recycling techniques such as this one, half of the bottles are being recycled.

Future Outlook

Advanced recycling of plastics represents a significant technological advancement that in the case of some polymers is already supplementing existing mechanical recycling processes. These processes signal a significant technical advancement in plastics recycling because the products, after purification, are identical to current feedstocks and monomers used to produce new plastics.
This recent development in plastics recycling shows promise toward achieving the industry's goal of increasing the environmentally and economically sound recovery of plastics, and may someday provide viable recycling options beyond conventional mechanical recycling for many more types of post-consumer plastics.

To illustrate the development one product recycling and reuse industry, let us take the american PET bottles recycling program.

INTRODUCTION

The 2004 National Post~Consumer Plastics Recycling Report is the 15thannual APC Plastics Recycling Study. This Study was a cooperative effort between the American Plastics Council (APC), the Association of Post Consumer Plastics Recyclers (APR), and the American Beverage Association (ABA). Designed to quantify the amount of and the rate at which post~consumer plastic bottles were recycled in calendar year 2004, the Study was conducted by the engineering consulting firm of R. W. Beck, Inc. (R. W. Beck). Overall, total post~consumer plastic bottle recycling increased 247 million pounds in 2004 to anall time high of 1,915 million pounds. The increase continues the historical trend of more pounds collected each year as the pounds of plastic bottles available for recycling continues to grow.

- Today PET is used to package a wide variety of beverages in addition to soft drinks (water, juice, tea, isotonics, and beer) other foods (peanut butter, ketchup, edible oils, applesauce, etc.) and other products. These products demand a variety of bottle designs and sizes, a wide range of pigments, unique label materials, and barrier coatings, layers and blends that are combined with the PET to make a marketable and functional package.
- The PET bottle market has grown to represent 55% of the plastic bottle

market (up from 54% in 2003, and 53% in 2002), and the recycled bottle stream has shifted to a 53% PET/47% HDPE ratio from the 51%PET/49% HDPE in 2003 (Figure 7).

- The PET market, previously predominantly soft drink bottles, continued to shift to water, juice, tea and other types of beverages and foods. The sale of these products in PET “custom”bottles now represents nearly 63% of the total PET bottles sold.
- HDPE, used to package a variety of products from milkand juice to motor oil and shampoo, has not undergone the same degree of change in market demographics and therefore has experienced more consistent recycling dynamics.
- HDPE bottled products continue to be consumed primarily at home and near a recycling bin as evidenced by its continuing strong recycling rate of nearly 26%
- . Recovery of bottles for products consumed outside of the kitchen (e.g. bathroom, garage, laundry room, etc.) continues to be a challenge as consumers forget these bottles are recyclable.

Fig 7 : 2004 Plastic Bottle Production and Recycling Composition by Resin Type

Other includes PVC, LDPE/LLDPE, and PP; data was not collected for PS in 2004.

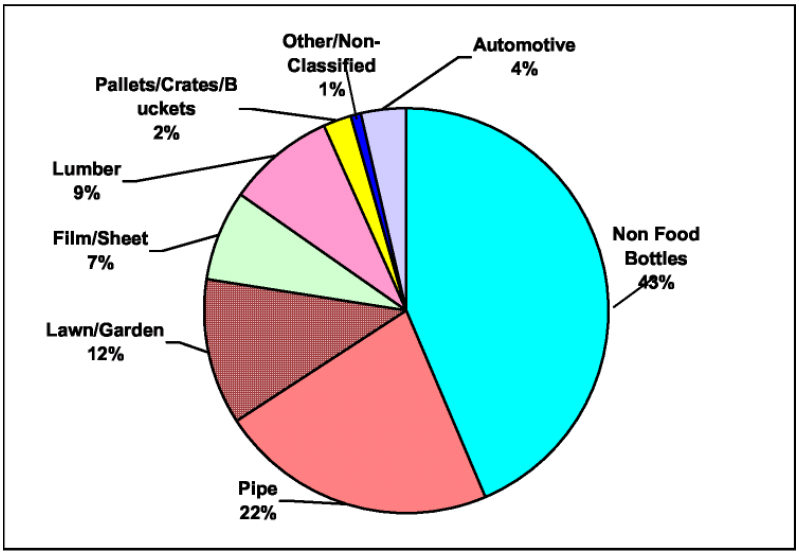

Fig 8 : Domestic Recycled HDPE Bottle End Use

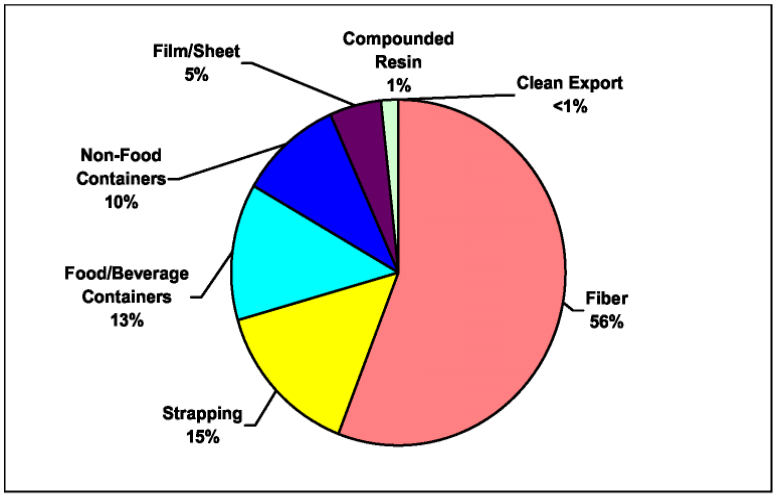

Source: R. W. Beck, Inc.

Fig 9 : Domestic Recycled PET Bottle End Use

EXPORT MARKETS

- 372 million pounds of PET bottles (37.1% of the total recovered for recycling) and 145 million pounds of HDPE bottles (16.0% of the total recovered) were exported for recycling in other countries. These quantities may be underrepresented due to the large number of export brokers handling the material, which results in difficulty in accurately tracking the movement of the material.

- Export markets for post~consumer plastic bottles were again strong for the year. The slight decline from 38.3% in 2003 to 37.1% in 2004 for PET pounds exported may have been due in part to actions taken by the Chinese government to enforce restrictions on the import of post consumer plastic bales.

Waste Evaluation

That's how much solid waste is generated by each man, woman and child in the United States. This waste includes substantial amounts of paper and cardboard (40%), as well as yard waste (18%), metals (9%), plastic (8%) and other products. Where does it all go? How much its cost? The answer: more than 70% of this material is buried directly in the ground-in disposal facilities known as landfills."

Reactive Extrusion

Introduction

Reactive Extrusion (REX) is an extruder-conducted process that involves a chemical reaction of the feed polymer. The feed polymer is modified by:

- changing its molecular weight
- grafting or adding a functional monomer to the polymer
- reactive combination of one polymer with another.

REX is primarily used to produce new polymers by chemical modification of existing polymers.It can involve also the direct polymerization of monomers to a new grafted polymer.

The REX extruder provides the environment for melting, mixing and reaction of the polymer and additives. In other words, it could be considered as reactor. The adequate residence time at the proper temperature must be provided for the reaction to take place. The extruder conditions must be controlled to allow the proper reaction. Twin-screw extruders are generally used in the REX process. It could be considered also as micro-reactor when the nanocomposites are involved and also for the reaction in situ. The advantage of this extruder type is that we can control total process in one step.

Polymer modification via REX is intended to produce chemical changes that improve the properties of the modified material such as enhanced thermal stability, higher mechanical strength, good elongation, higher adhesive strength and other mechanical properties.

During the last 30 years, the number of polymers created via new routes of polymerization has been decreased.

Metallocene-catalyzed polymers are among the few of ones that have been found significant success. In order to fill the new performance needs of plastic materials, the use of REX techniques has become a method of choice. In general, it is less expensive to develop new polymer properties by modifying existing polymers by REX than to develop new polymers based on new polymerization routes, adding to that the modification and the conversion to end product happens at same time and in one step, which is attractive advantage.

Brief History of REX Technology

Reactive Extrusion processing emerged in the 1960s and 1970s. Single-screw extruders were first used in studies of polymer chain breaking and grafting of monomers to polyolefins. Several REX patents were published concerning these processes. Commercial extrusion plants started producing new polymers via REX in the late 1970s. Twin-screw extruder technology, evolving at that time, was better able to meet the demands on polymeric materials obtained by REX. The 1980s witnessed a great proliferation of papers and the commercialization of many REX applications.

Resin companies installed lab extruders and developed the process technology to make many different alloys and blends and grafted monomers via REX.

Large resin companies—Exxon, BP, Shell, DuPont, Dow, Rohm & Haas and others—developed new modified polymers with active functional groups. A partial list of these functionalized polymers is given in *Table 1*. Patents covering the technology and manufacturing of several of these polymers are given in references [ ].

Table 6 : Commercial Functionalized Polymers.

Product	Base Polymer	Functionality
RPS	PS	Oxazoline
EAA	LDPE	Acid
SAA	PS	Acid
VAMAC	Acrylic rubber	Acid
SURLYN	EMA-ionomer	Acid
NUCREL	EMAA	Acid
ELVAX	EVA	Acid
HYCAR	B/AN	Acid/Amine
PAXON	NYLON	Acid
PROFAX	PP	Anhydride
POLYBOND	PE, PP, EPDM	Acid
PLEXAR	PE, PP, EVA	Anhydride
MODIC	PP	Anhydride
CADON	PS	Anhydride
DYLARK	PS	Anhydride
ARLOY	PC/SMA	Anhydride
KRATON	F SBS	Anhydride
EXCELLOR	PP, EP, EPR	Anhydride
VITEL	PET	Acid
EXL	PMMA	Imide/Acid

Many new alloy and blend polymers made by reactive compatibilization appeared in the late 1980s and early 1990s. The Alloys & Blends Special Interest Group of SPE

was formed in 1988. In the early 1990s, numerous REX-related papers presented at the SPE ANTEC meetings confirmed the wide scope and opportunities in REX processing. Papers from both industry and universities were published. Then a shift occurred so that more than 90% of the papers were presented by university authors.

Today, many new products are REX produced via reactive alloying and blending. A good review of Reactive Extrusion processing can be found in the book published in 1992 by Xanthos [ ]. The review article by Tzoganakis [ ]

Types of REX Processes

There are many types of REX processes. They differ by the type of reaction that takes place and by the polymer and additives that are reacting. We can consider the controlled degradation of Polymers, It involves the breaking down of large polymer chains to smaller chains. This reaction is typically caused by an organic peroxide, which thermally decomposes and forms active free radicals. They, in turn, react with the polymer chain and break it. Polyolefins and copolymers of olefins are frequently used as the base polymer for this REX process, which is also called “viscosity breaking” or “controlled rheology” processing, The chain length reduction of high molecular weight polypropylene is a typical process. Peroxide is mixed with the PP feed, or is fed as a separate stream after the PP is melted. The temperature is controlled to decompose the peroxide. A specific amount of peroxide is added to give the desired molecular weight reduction. A narrower molecular weight distribution is also achieved. Experimental studies of this process using a single-screw extruder were conducted by Pabedinskas [ ] and Tzoganakis [ ] , our previous work was dealing with the controlled degradation of iPP by controlling the oxy radical attack , compared to the work of Tzoganakis it could be considered as much more interesting since the control of the degradation is more accurate [These de magister].

Second important conserns of using the Rex is the Grafting Monomers Onto Polymers. It allows the base polymer to achieve enhanced physical properties and can create a new polymer with an attached functional reactive

group. This modification can improve polymer adhesion to mineral fillers, glass fibers, metal, and other polymers.

Polyolefins represent the most common polymers modified by grafting reactions. When the polyolefin is attacked by a peroxide initiator, an active free radical is created that can react with the monomer and attach it to the polymer.

The monomer being grafted must have a reactive group, usually an unsaturated double bond. This will react with the free radical on the polymer chain. A second functional group on the monomer will add new properties to the grafted polymer.

A typical commercial example of this process is grafting maleic anhydride (MA) monomer to a polypropylene polymer. The reactive extruder process steps are:

• melting the PP.

• adding and mixing liquid MA into the PP.

• adding and mixing a peroxide initiator into the melt.

• reaction of the peroxide with the PP polymer backbone.

• adding MA to the free radical on the PP backbone.

• devolatilization of the residual products and excess monomer.

• pumping the product out of the extruder.

A diagram of this REX process is represented in the following figure .

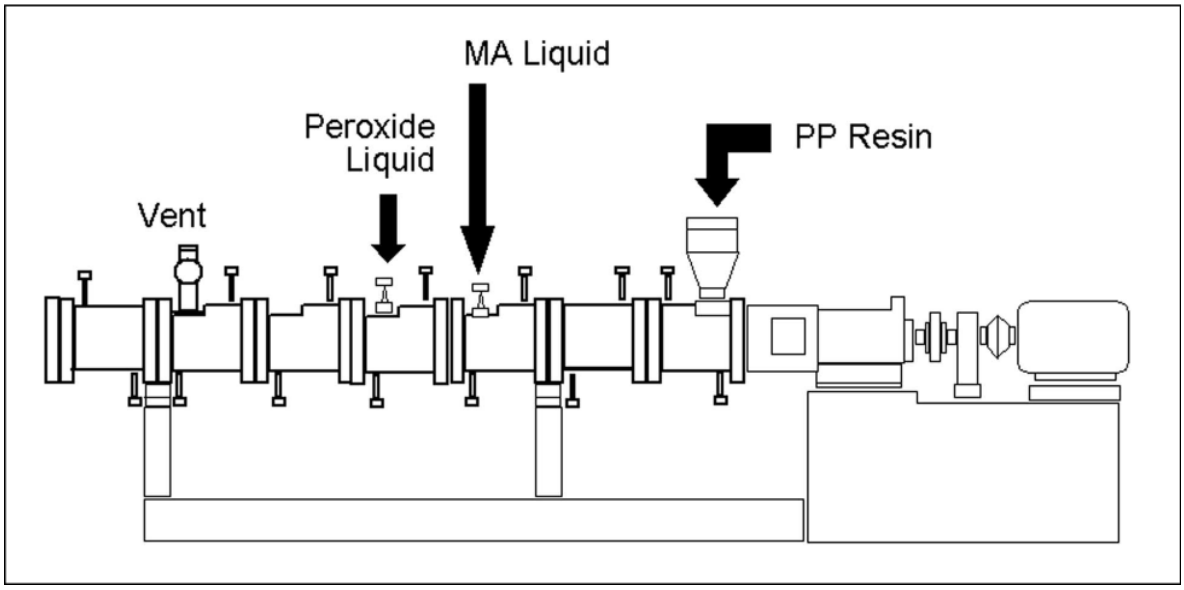

Fig 6 : Reactive extruder for grafting process.

Control of the reaction in the extruder is accomplished by controlling the polymer temperature, the reaction rate and the order in which the ingredients are added. Sometimes the peroxide is added in smaller amounts over two or three ports to reduce its concentration in the extruder and minimize harmful side reactions. The reactions are fast, and a short residence time is normal.

The key steps in the process are:

- complete mixing of the monomer with the polymer before the peroxide is introduced.
- complete mixing of the peroxide at its addition point.

References :

1) Hans-Henning Kausch, Nicole heymans, Christopher John Plummer and Pierre decroly ; *TRAITE DES MATERIAUX, Matériaux polymères : propriétés mécaniques et physiques* ; Vol N°**14**, Chap.I, (2001), 34-39.

2) SEARCH SITES
PlasticsResource.com; and All APC Sites Plastics.org AmericanPlasticsCouncil.org

Christian Janot et Bernhard IIschner ;*TRAITE DES MATERIAUX, Matériaux émergents* ; Vol N°**19** Chap I, 3,4, p(4-35-57-159).

6) Leszek A. Utracki ;*Polymer alloys and blends*, Chap1, 2,3, New york : Carl Hanser verlag, (1989), pp (1-29, 202).

7) Engineering materials 2 ; Michael F. Ashby and David R. H. Jones ; Chaps B and C ; Planta Tree (GB) (1998), p(161- 219).

3) J.A. Brydson , *Plastics Materials*, Chaps 1,2,5,10,11 ; Seven edition Butterworth-Heinemann (1999).

P.M.Ajayan, L.S. Schadler and P.V. Braun ; *Nanocomposite Science and Technology*, Chap 2, Wiley-VCH. Verlag Gmbh and Co.KGaA (2003).

4) Charles E. Carraher ; *Polymer Chemistry*; Chap 1, 15, Marcel Dekker, Inc (2003).

Robert O. Ebewele ; *Polymer Science and Technology* ; Chap 1,5,10 ; CRC. Press.LLC.(2000).

5) Atul. R. Khare, Stanley P. Westphal, Michael T.K. Ling, Chuan Qin, Lecon Woo; *Thermochimica Acta*,**358** (2000) 155-160.

B.G.Soares, M.S.M. Almeida, C. Ranganathaiah, M.V. Deepa Urs, Siddaramaiah ;*Polymer testing,* **26** (2007) 88-94.

M.S.hedenqvist, A. Backman, M. gallastedt, R.H. Boyd, U.W. Gedde ; *Composites Science and Technology* ; **66** (2006) 2350-2359.

Hong Yang, Xiaoqing Zhang, Cheng Qu, Bo Li, Lijuan Zhang, Qin Zhang, Qiang Fu; *Polymer* **48** (2007) 860-869.

Ying Xu, Bao-Ku Zhu, You-yi Xu ; *Desalination* **189** (2006) 165-169.

Fernando Wypych, Kestur Gundappa Satyanarayana; *Journal of Colloid and Interface Science,* **285** (2005) 532-543.

R. Nowacki, B. Piorkowska, A. Galeski, J.M. Haudin ; *Polymer* **45** (2004) 4877-4892.

Dongyan Wang, Charles A. Wilkie ; *Polymer Degradation and Stability* **80** (2003) 171-182.

M. Abdul Kader and Changwoon Nah ; *Polymer* **45** (2004) 2237-2247.
K.A. Moly, H.J. Radusch, R. Androsh, S.S. Bhagawan, S. Thomas; European *polymer Journal* **41** (2005) 1410-1419.

Ralf Lach, Lada Antonova Gyurova, Wolfgang Grellmann; *Polymer testing* **26** (2007) 51-59.

Kalpana S. Katti; *Colloids ans Surfaces B* : *Biointerfaces* **39** (2004) 133-142.

9) Masoud Frounchi, Susan Dadbin, Zahra Salehpour, Mohsen Noferesti ; *Journal of Membranes Science* **282** (2006) 142-148.

E. Ritzhaupt-Kleissl, J. Hausselt, T. Hanemann; *Materials Science and Engineering* **C 26** (2006) 1067-1071.

8) S.-M. Lai, F.-C. Chiu, T.-Y. Chiu; *European Polymer Journal* **41** (2005) 3031-3041

W. Belguicem ,These de Magister, Univ. Setif. (1998)

2) SEARCH SITES
PlasticsResource.com; and All APC Sites Plastics.org AmericanPlasticsCouncil.org

Experimental methods and techniques

Introduction

The aim was to achieve a compatible polyolefin blends in order to contribute to the recovery plastics materials by recycling instead of doing the incineration; using this method in order to be environmental friendly, so it is important of nowdays to think for saving our enviroment. Many years ago , the recycling were an expensive methods then the recent approaches let use to say that the use of new efficient compatibilizers such as ionomers or advanced industrial equipments or simply the the new conscient and volonty gouvernomental leaders to share this important problem by introducing a legislative and law of use and reuse of this kind of materials are of great jump for an environmental interest. More than that we could consider that the road choisen is promoting and we can say that the new research approaches are promoting the recycling of the plastics materials in such a way to hand up with advanced recycling method or technique taking into account the environmental interest.

Our works dealing with the recent approach related to industrial interest which consist of the study using reactive extrusion and compatibizer (EPDM) in order to form strongh stable links even convalent bonds or stable interpenetrating networks. The idea was to cumpute the high shearing provided by thermomechanical mixing in melt state and the formation of macroradicals provided by decomposition of oxy radicals as homolytic reaction which provide such a medium capable to combine these macroradicals in rondom way . This phenomena has to be realyzed in very short residence time at melt state in closed cells and under high presure.This works was achieved by using a single screw extruder. In order to control the hole chemical process the experimental protocol was set up in such a way to give good description of the melt behaviour and the consequency the impact of this reactive extrusion on the structure and morphology and the properties. It is clear enough that succeeding in forming a network by setting right experimental conditions and balancing between differents kinetics reactions for all components is an important aspect and particularity and most important agent which play an major role is the peroxide as oxy radical source which in general case present very short half life time. In general, of

course the more accurates and interesting studies are to be by using twin srew reactive extruder with probably better statistically an stable overall.

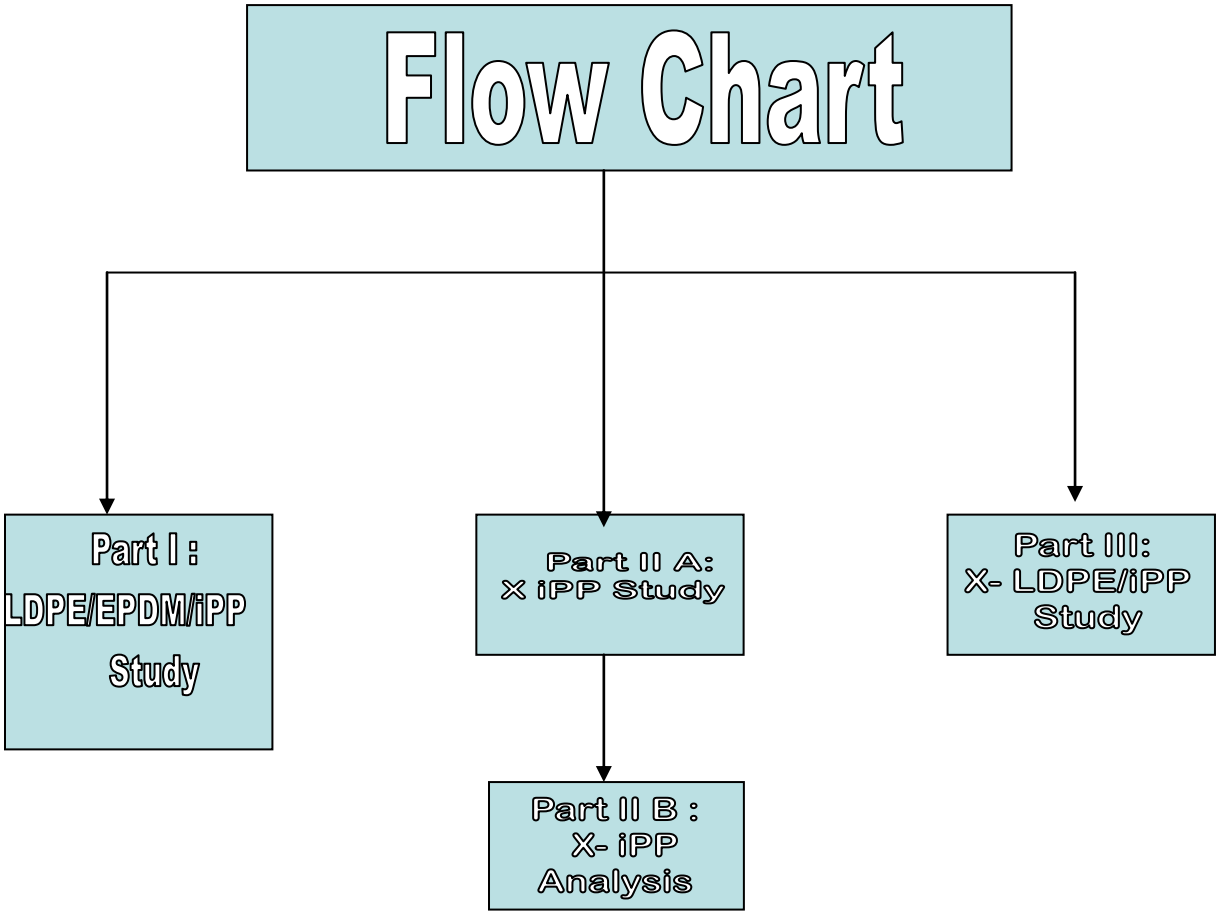

Dynamic Rheologic Analysis (D R A) Techniques.

For the dynamic rheological analysis (DRA), a Brabender-type plastogragh was used. The processability of LDPE/iPP/20 phr of EPDM blends has been evaluated measuring the torque required to mix the molten components in a heated chamber at 200°C. The torque-time evolution, carried out for each component of ternary blends, in presence of aggressive oxy-radicals provided by peroxide decomposition, is studied since each component may react in the melt state. To clarify the role of each component in the ternary blends, the effect of the EPDM on iPP and on LDPE was investigated first.

For the second part of this present study the dynamic rheological analysis (DRA), a Brabender-type plastogragh was used too. The processability of the iPP blends has been evaluated by measuring the torque (torque = moment of force) required to mix the molten components in a heated chamber at 200°C at a rotor speed of 30 rpm. To clarify the role of each component in the blends, the torque-time evolution was firstly measured for the neat peroxide as the first part of this study, then for each couple peroxide/accelerator, and finally for every crosslinking agent, i.e., peroxide/sulfur/accelerator. Fig. 1 shows a typical curve illustrating the different steps of the torque-time evolution for a crosslinked isotactic polypropylene material and also for the different blends compositions based on iPP/LDPE with differents crosslinking agents compositions. In this figure, the most important and characteristic points are:

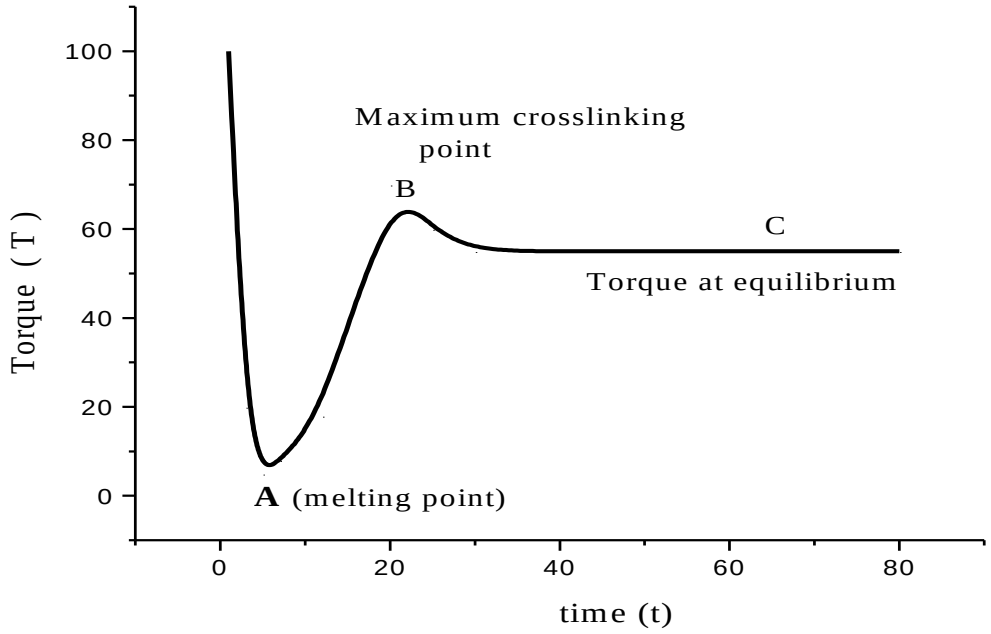

Fig 1: Torque–time evolution for a crosslinked polyolefin material.

A: starting point of the melt.

B: maximum crosslinking point.

C: equilibrium point.

At the beginning, the polymer melts and the torque decreases to a minimum value T_A. As the crosslinking begins, the torque increases to a maximum value T_B. After that, a small decrease of torque is observed, reaching a final stable plateau at point C, usually higher than A. The logarithm of $(T_t - T_A)$ is plotted as a function of time, T_t signifying the torque value at the time t. When the path of this curve is nearly linear, the crosslinking reaction is of 1^{st} order and comprises the main reaction. However, this is only true for polyolefins with secondary carbons, such as polyethylene, under the action of a peroxide [2].

Thermal Analysis

DSC and DMTA are one of experimental techniques which investigate the behavior of materials samples as a function of temperature. In the first case we determine the enthalpy property (DSC) and in second case (DMTA) known also as TMA, and DMA, we determine the deformation property. From the enthalpy and deformation properties one may relate to structure properties such as Transition temperature Tg, fusion temperature Tm, crystallization temperature Tc, and micro mechanical properties and relaxation.

From DSC analysis we have determine the micro-structure properties such as the lamella thickness by using Thomson-Gibbs equations according to the following formula and correlates this results with the microhardness results:

$$T_m = T_m^0 [1-(2\sigma_e / \Delta H_m^\infty l_c)]$$

T_m : The melting temperature

T_m^0 : The absolute melting enthalpie

σ_e : The surface free energy

ΔH_m^∞: The 100% pure melting enthalpie

l_c : The Lamella thichness in nm.

Optical Analysis

The optical OM and SEM microscopes provide the investigation with a highly magnification marge of the surface of a material that is very similar to what one would espect if one could actually see the surface visually. These techniques tend to simplfy image interpretation considerably. The difference is that the SEM approach a few nm and can operate at magnification that are easily adjusted from about 10 x – 300,000 x whereas the OM has limited magnification , but good to study the spherulite dimensions and the growing spherulite dimentions in dynamics regime.

X- Ray Diffraction

X- ray diffraction(XRD) is a powerful technique used to uniquely the crystalline phases present in materials and to measure the structural properties (strain state, grain size, epitaxy, phase composition, preferred orientation, and defect structure) of these phases. XRD is also used to determine the thickness of thin films and multilayers, and atomic arrangements in amorphous materials and at interfaces.

XRD offers umparralleled occurancy in the measurement of atomic spacing and is the technique of choice for determining strain states in thin films. XRD is noncontact and nondestructive, which makes it ideal for in situ studies. The intensities measured with XRD can provide quantitative, accurate information on the atomic arrangements at interfaces.

FTIR

The Infrared spectroscopy is considered as one of the few techniques tha can provide information about the chemical bonding in a materials, it is particularly useful for the nondestructive analysis of solids and thin films, for which there are few alternative methods. Chemical bonds very widely in their sensitivity to probing by infrared techniques. For example, carbon-sulphur bonds often give no infrared signal, and cannot be detected at any concentration, while with FTIR the signal is intense enough to be detected. Thus the potential utility of infrared and particularly FTIR is a function of the chemical bond of interest and qualitative-quantitative identification and analysis. Because most of recent developments in the field have been attendant to FTIR technology. In many respect, FTIR is a “science of accessories” but in our case is useful method to evaluate the generated ethylenic chain and the new bonds caused by the reactive crosslinked reaction for isotactic polypropylene where the carbonsulphur and carbon-nitrogene bonds are analysed.

Microhardness study

The microhardness is relatively a new approach techniques to polymer science and one of the simplest method of characterization of solid macromolecular materials. It consist of the uses a diamond pyramid indenter which penetrates surface of a specimen (very small scale) upon application of a given load at a constant rate.

During an indentation cycle the following effects must be distinguished:

a) An elastic deformation upon removal of the load leading to a recovery of the indentation.
b) A permanent plastic deformation (mesure of hardness).
c) A time dependent contribution during loading.
d) A long delayed recovery of indentation after load removal (viscoelastic relaxation)

From a macroscopic point of view, hardness is directly correlated to the yield stress of the material by the following expression:

$H= 3\sigma_y$

Concerning the microhardness (H) of polymer relating to microstrucure. The dependence of H on structure parameters, such as degree of crystallinity and lamellar thickness, are of great useful results.

In our case, we use the reduced empirical relationships is as follows

First let take this conditions: (Tg < T < Tm) i.e that Ha << Hc:

Than :

$H = \alpha H_c$

The *H*-value was derived from the residual projected area of indentation according to: $H = kP/d^2$. In this expression, *d* is the length of the impression diagonal in meters, *P* is the contact load applied in N, and *k* is a geometrical factor equal to 1.854. Loads of 0.25, 0.5, and 1 N were used. The loading cycle was 0.1 min. 8-10 indentations were made on each sample, and the results were averaged.

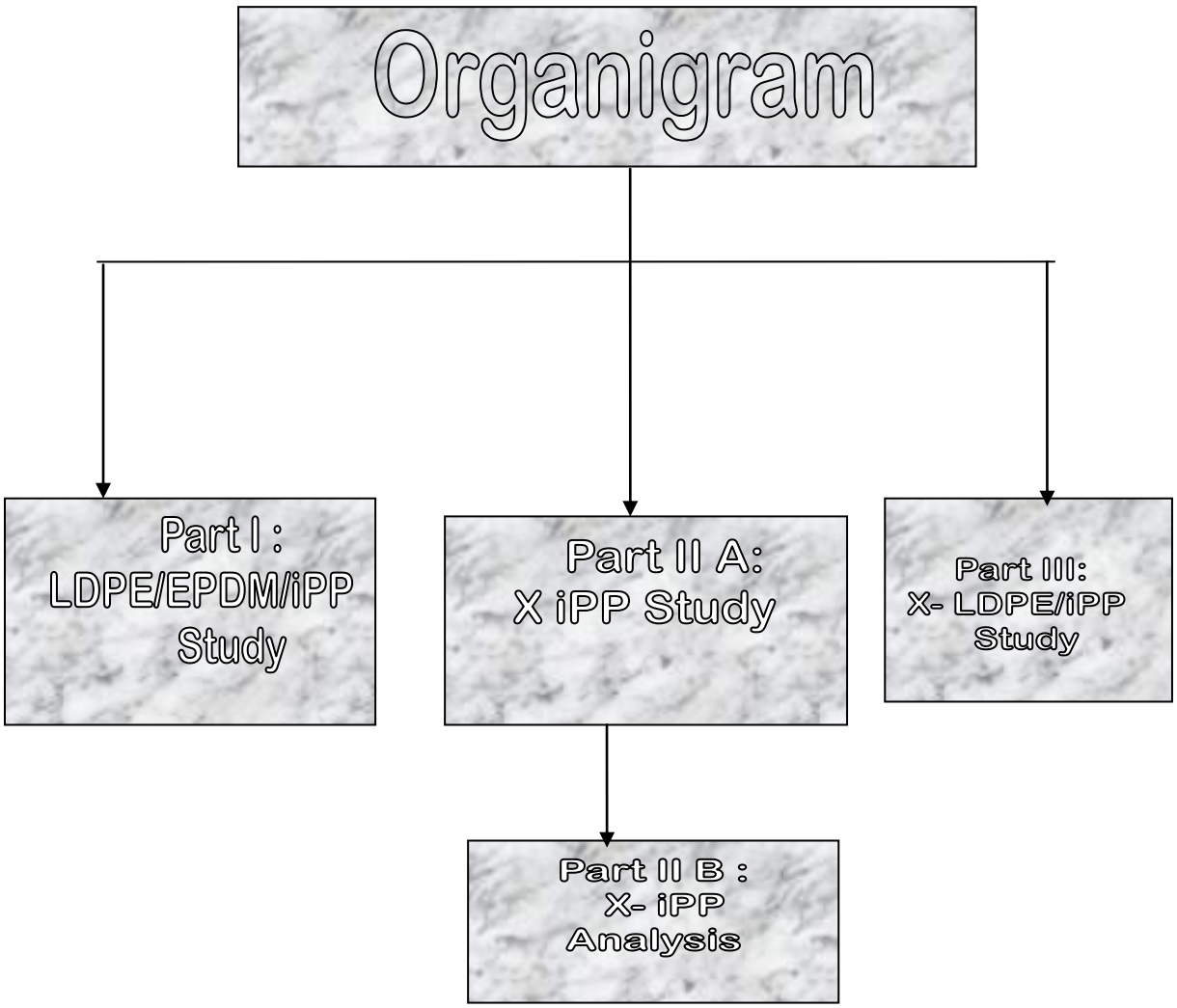
Organigram
Part I : LDPE/EPDM/iPP Study
Part II A: X iPP Study
Part III: X- LDPE/iPP Study
Part II B : X- iPP Analysis

Part I: Study of ternary blends (iPP)/ (LDPE)/ (EPDM).

Introduction:

Plastic waste has become an important global issue in the recent years. This issue has emerged following rising concerns about environmental pollution and limited handfull space. Some countries are solving this problem with special legislative measures, which impose to industries the elimination of wastes they generate. On the other hand, the economical viability of recycling depends on environmental laws which may vary from one country to the other depending on specific and national legislation .

Thermoplastic polymers will be conveniently recycled provided that appropriate treatments are used. Polyolefin such as polyethylene (PE) and iPP, with respectively growing ratio of 2 and 6 % per year, represent a large amount of produced and consumed thermoplastic materials. To make useful and compatible blends, compatibilizer materials must be added to overcome the problem of immiscibility between iPP and PE, and thus to obtain recycled materials with acceptable properties. Compatibilizers can be mainly classified as follows:

1) non-reactive; random, graft and block copolymers, varying for the nature , that should have polarity similar to the blend components. II) reactive compatibilizers: although EPDM copolymers are classified as non-reactive, reactive blending is achieved in presence of a peroxide as radicals source [1]. Peroxide induces radical reactions involving three steps; a) cleavage of the peroxide, b) formation of macroradicals, c) combination of different macroradicals with chain termination. The final polymer blend will have a graft, block, random copolymers or interpenetrating network structure. Therefore, the structure and morphologies of the blend components are changed, thus affecting the mechanical properties. Preparations of such complex blends demand well understood and correctly predicted reactive mechanisms: a firm control of the processing conditions is needed in order to optimize the final properties of the blends. A homogeneous and fine dispersion of EPDM in PE/iPP blends leads to advantageous crosslinks which stabilize the phase structure of the blend preventing the demixing during further processing operation or industrial applications.

This part of our work deals with LDPE/iPP blends compatibilized with EPDM in presence of a peroxide (DCP). Combining different characterization techniques allowed us to correlate rheological, mechanical, thermal and morphological properties of such blends, and to make predictions for a useful industrial recycling.

EXPERIMENTAL PART

Materials used : LDPE: B21 sak , ENIP, Skikda, Algeria.

iPP : Sabic-Vestolen 9000-67404, supplied by Chemische Werke Hüls?, Germany.

EPDM: Mordel 2744, hexadienne type, Dupont,USA.

Peroxide: DCP , Dicumyl peroxide (mixed with 40% of phthalate).

Blends preparation:

First blend components were mixed, in solid state, using a small quantity of vegetal oil in order to wet and improve the dispersion of fine powder of peroxide within the granulas of LDPE and iPP. Then, the obtained mixture was introduced in a single screw extrusion. The extrusion cycle was repeated twice in order to achieve a homogeneous blend. Injection and compresion molding machines were used to obtain samples for the different tests.

DSC analysis:

Two method were used in order to determine the fusion enthalpy (ΔH_f), the melting temperature (T_{melt}) and the crystalline temperature (T_{crist}) . Then degrees of crystallinity were calculated using the theoretical enthalpies fusion values for 100% crystalline polymers [1,3] : for 100% crystalline PE the enthalpy fusion is equal to 277 J/g , and for the 100% crystalline iPP the enthalpy of fusion is equal to 210 J/g.

The conditions of the first method are : first run : -120°C to 200°C at 10.00°C/min
200°C - maintained for 10 min
200.°C to –120°C at -50°C/min
second run: -120°C to 200°C at 10.00°C/min

The conditions of the second method are: 25°C to 200°C at 20.00°C/min
200°C to 25°C at –10.00°C/min

Optical microscopy (OM).

Light microscopy was performed using an Olympus apparatus equipped with a hot stage and photography equipments connected to a computer. The specimens were cut from compression molding sheets and squeezed between two glass slides to obtain very thin films. The specimens were heated from room temperature to 200°C at a rate of 20°C/min, then kept at that temperature for 10 min to ensure uniform melting, and finally cooled to room temperature at a rate of -10°C/min.

Scanning Electron Microscopy (SEM).

The scanning electron microscopy analysis was performed by means of a Philips 501 apparatus. Specimens were cut from compression molded sheets, and cooled in liquid nitrogen before to being fractured. The metallization of the fractured surface was carried out in a metallizer.

Dynamical Mechanical Thermal Analysis (DMTA).

Tangent δ , logarithm of real modulus and glass transition temperature (Tg) of samples blends were measured using a DMTA apparatus (Rheometric Scientific MK III). Data were recordered in the tensile mode from –150°C to 200°C using a scanning rate of 5°C/min and a frequency of 3Hz.

Steady state capillary rheometer.

The apparent viscosity, and corrected viscosity were measured according to the power law model, using a die with a length/diameter ratio L/D= 30 and applying Rabinowitch correction to obtain viscosity values. Die have conical feeding shape and flat exit shape . The processing temperature was 200°C.

Impact strength test.

The impact strength test was carried out in a device equipped with a control temperature unit varying from –20°C to room temperature. Specimen were prepared by compression molding. Notched (1/3 deep) and non-notched specimens

were submitted to Izod strength testing: resiliencies a_n , a_k and K values were calculated using a hammer of 4 Joules. Measurements were carried out at –15°C and at room temperature according to the ISO 190 R norm.

Results and discusion

Dynamical Rheological Analysis (DRA)

The torque-time evolution carried out for ternary blends based on iPP/LDPE matrix and the EPDM in presence of aggressive oxy-radicals, reveals complex crosslinking reactions involving the different components. These reactions occur simultaneously, in the melt state. This approach is used to assess the contribution of each component (iPP, LDPE and EPDM) and the way it reacts with the others.

The torque-time rheometer was used for each component separately, as well as for binary and for ternary blends. Using the method developped by Harpell and Walrod , i.e. plotting the logarithm of the velocity constant k as function of 1/T, indicates that the crosslinking reaction kinetics follows an Arrhenius law type of function. This crosslinking reaction involving all components iPP, LDPE and EPDM, in presence of peroxide, showed a non-linear behavior. This means that the reaction order is different from the 1^{st} order, and that the presence of different materials will significantly influence the kinetics of a complex crosslinking reaction. The resulting blend structure of these ternary blends could rather be considered as that of an interpenetrating network (IPN).

a) Pure components

The experimental results of torque-time evolution (see Figure 2), shows that the torque of iPP/EPDM in presence of peroxide will decrease continuously until it reaches a plateau and is lower than that of pure iPP ; this is due to the macro-radical attack by peroxide radicals (particularly at tertiary carbons of iPP which are the more reactive sites) to form macroradicals by disproportionation or by cyclisation of the end groups. Consequently, there is a decrease of molecular weight (M_w). It is noticed that the higher peroxide concentration [P] , the lower will be the torque value and means that lower will be the viscosity and this is directly related to molecular weight (M_w) . Such a result has been observed in a previous study on iPP/EPDM [2] .

On the other hand**,** in other works based on LDPE in presence of peroxide, an increase in torque was observed and crosslinking reactions occurred [2] . Thus, M_w will be very low. By using the p-xylene solvent , swelling is observed instead of dissolution as it is the case for iPP.

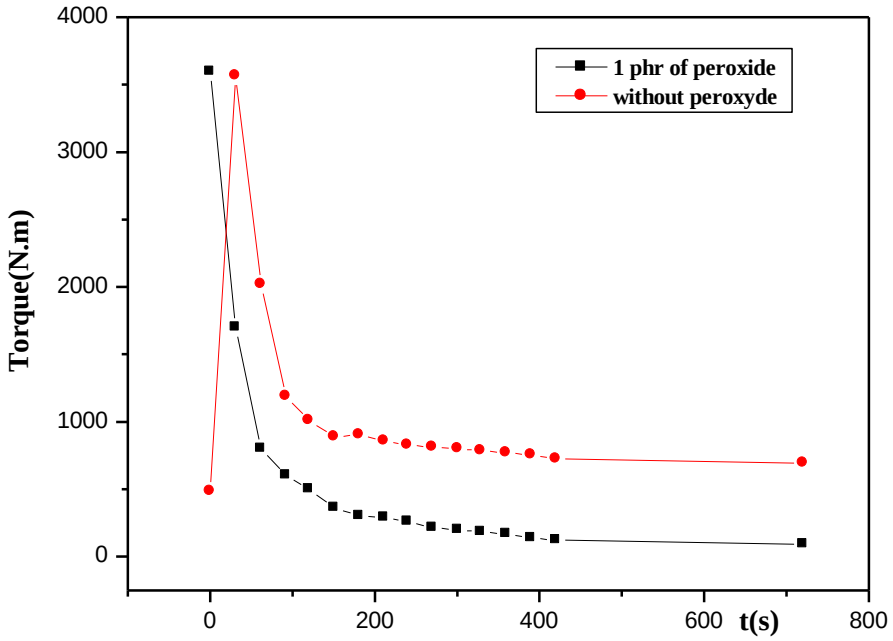

Figure I 1 : Comparison of torque as function of time for blends based on iPP/20 pcr of EPDM in presence of peroxyde at T=200°C

The experimental results concerning LDPE, show an increase of torque at T_B followed by partial decrease to point C. Equilibrium will take place at longer processing time. From the experimental results, it is noticed that T_B values increase as [P] increases, and, at the same time, the difference $[T_B - T_C]$ will be lower, whereas T_C increases. As [P] increases, the propagation rate will also increase; therefore, more crosslinks will be formed at shorter times. This fast crosslinking reaction will result in a higher degree of crosslinking. In this case, the overall network formed will be more difficult to destroy.

b) Binary blends

Torque-time evolution for binary blends based on iPP or LDPE and reactive EPDM is shown in Figures 2 and 3. From these results, it can be concluded that peroxide radicals activate the unsaturated double bond of EPDM. Beside that, it is found that with LDPE, the peroxide act in similar way and form LDPE macroradicals by abstraction of H from secondary or primary carbon due to the high branching degree of LDPE. It is obvious that the abstraction of H will involve secondary carbons, and it is noticed that the rate of termination is faster according to crosslinking speed represented by time value [$t_B - t_A$] or by calculation of the reaction constant by using Monsanto method. This result is also observed in the case of EPDM in presence of peroxide. The torque-time evolution of binary blends of LDPE/EPDM shows that the T_B increases as LDPE content increases, and T_C will go to a higher value. This could be due to the junction points of the networks (derived from LDPE macromolecules), unsaturated double bond and the combination of LDPE and EPDM ethylenic macroradicals.

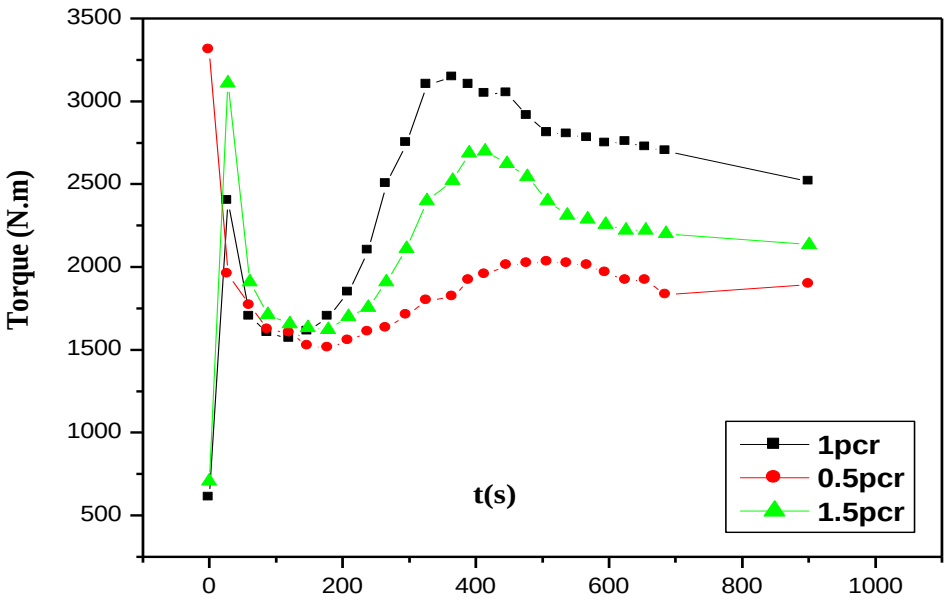

Fig I. 2 :Variation of torque as function of time for blends (PEBD/EPDM) for different peroxide concentrations at T= 180°C

Moreover, from the DMTA analysis, the 0/100/20 of iPP/LDPE/EPDM blend shows a formation of a propylenic part even if the iPP is not used. This is due to β scission of propylenic part of EPDM. This propylenic chain formed has low M_w according to Ethylenic/Propylenic ratio in EPDM: it interferes in the torque value acting as a lubricant. (The amount of PP formed depends on [P] and M_w of PP content in EPDM.) At this stage, the torque value does not correspond to crosslinks involved. The value of torque and T_c are also closely dependant on Ethylenic/Propylenic ratio rather than on terpolymer efficiency. One should take into consideraton of the effect of each part of EPDM's compositions. The torque-time investigation such as T_B , T_C values are very useful to predict the M_w effect qualitatively. There is no direct way to evaluate the M_w of PP neither its amount since the different components of blends are soluble in ortho, para, and metha-xylene solvants.

The experimental result based on iPP/EPDM in presence of peroxide shows that there is no point B, this is mainly due to high amount of low M_w of PP chains generated by β scission of PP and propylenic part of EPDM. A rapid solubility test using para-xylene shows that there is partial swelling of the blends due mainly to reactions of unsaturated double bonds of hexadiene present in EPDM and also to crosslinking of ethylenic part of EPDM. It should be mentioned that the anti-oxidant or anti-ozone additives usually added can inhibit the peroxide attack; on the other hand, PP copolymer will react in a different way than iPP homopolymer, but the overall result shows that it is preferable that the blend of iPP/EPDM will be used without peroxide.

c) Ternary blends

The torque-time evolution for ternary blends was investigated for blends having a LDPE content varying over the range 0—100% weight proportion, a iPP/LDPE matrix, for 20 phr of EPDM, and at constant peroxide concentration. The evaluation of T_B and T_C at the equilibrium (see Figure 4) shows that the crosslinking effect starts to be apparent from (50/50) of iPP/LDPE matrix composition, and torque will increase when LDPE content is predominant. This positive deviation is proportional to the degree of crosslinking of LDPE and EPDM. The co-rotating speed choosen can detect the viscosity change of blend melt flow; therefore, the torque will increase. As mentioned previously, there is formation of a complex network and the

evolution of torque is affected by PP degradation (through β-scission reaction); however, this degradation has no apparent effect on crosslinking reaction. On the other hand, the activation energy could not be investigated by using Monsanto method.

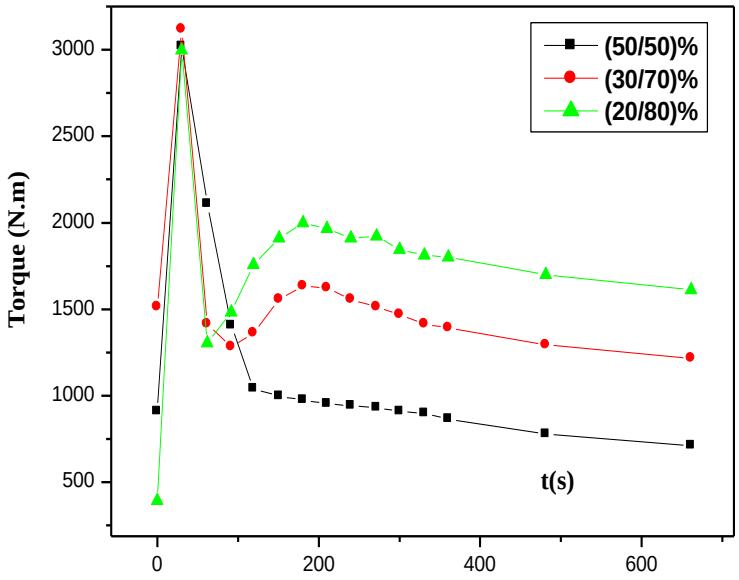

Fig I. 3 :Variation of Torque as function of time for different blends based on (iPP/LDPE) with 20 pcr of EPDM at (0.5 %) of the peroxide at T=200°C

DSC analysis

The DSC results carried out for different compositions of PP/LDPE and for 20 phr of EPDM shows that the T_{melt} of iPP is almost the same as T_{melt} characteristic of raw material and the variation doest exceed 4°C. The enthalpy values of each peak is function of iPP or LDPE proportions in the matrix. Enthalpies of fusion ΔH_f , melting temperature T_{melt} and degrees of crystallinity of each component for different blends have been evaluated; the different values are reported in Table 1 (for the first method) and in Table 2 for the crystalline temperature T_{crist} (using the second method) . It is noticed that the 20/80 of the matrix shows the highest values, but different X_c values are lower than the ones predicted by the additivity law. This result shows that there is no complete process of crystallization of each crystalline part according to crystalline temperatures . This is due to the fact that when iPP starts to

crystallize, LDPE is still in melt state, and then it will affect the nucleation rate. On the other hand, when LDPE starts to crystallize the iPP is in solid state, and it will then affect the growing rate of LDPE crystallites ; as a result the two modes are related to chain dispersion in addition to the fact that EPDM improves close contact, resulting in a decrease of the interfacial tension. Another point has to be mentioned : the networks effect through the crosslinking degree. Therefore, this complex situation will strongly affect the overall crystallization phases, either for the enthalpies or the crystalline temperatures. It is observed an apparition of a new peak at T=123°C which corresponds to HDPE characteristic fusion peak, this appears for the first run case only. This peak is due to shear effect involved even in a plasti-corder or in an extruder. In a melt state, blends undergo high shear and then melt fracture of side chains or branching chains of LDPE will result in regular chains able to crystallize differently compared to raw material: This result could be related to the presence of oxy radicals and macroradicals of both ethylenics chains of EPDM and Polyethylene present in the ternary blends.

Table I. 1 : Evolution of fusion enthalpies and melting temperatures for different blends based on iPP/LDPE/20pcr of EPDM.

Composition of (iPP/LDPE) + 20 phr EPDM	T_{melt} (°C) 1 First Fusion Peak	T_{melt} (°C) 2 Second Fusion Peak	ΔH_f 1 (J/g)	ΔH_f 2 (J/g)	Degree of Crystallinity (%)
100/00 + EPDM	113	165	6	44	23
80/20 + EPDM	111	167	9	47	25
50/50 + EPDM	110	166	28	25	22
20/80 + EPDM	112	164	51	15	22
00/100 + EPDM	114	166	46	15	22
EPDM	53	/	23	/	/

Table I. 2 : Evolution of crystalline temperature for different blends based on iPP/LDPE/20pcr of EPDM.

iPP/LDPE/20pcr of EPDM	100/00	80/20	50/50	20/80	00/100
1st crystalline peak (°C)	110	108	100	92	92
2nd crystalline peak (°C)	95	92	92	80	78

Optical microscopy results

From the optical microscopy analysis (see micrographs in Figure 5) it appears that show that spherulite sizes are dependent on blend compositions. The dimensions are higher for pure iPP and decrease as LDPE proportion increases or when the EPDM is used. This result is in good agreement with the DSC analysis. According to literature, the iPP spherulite sizes are 30 times higher than the LDPE ones [9]. Therefore, in the blend, iPP spherulite dimensions will differ according to the blend composition. This effect will, in turn, affect the crystalline degree, thus inducing a change in the mechanical properties.

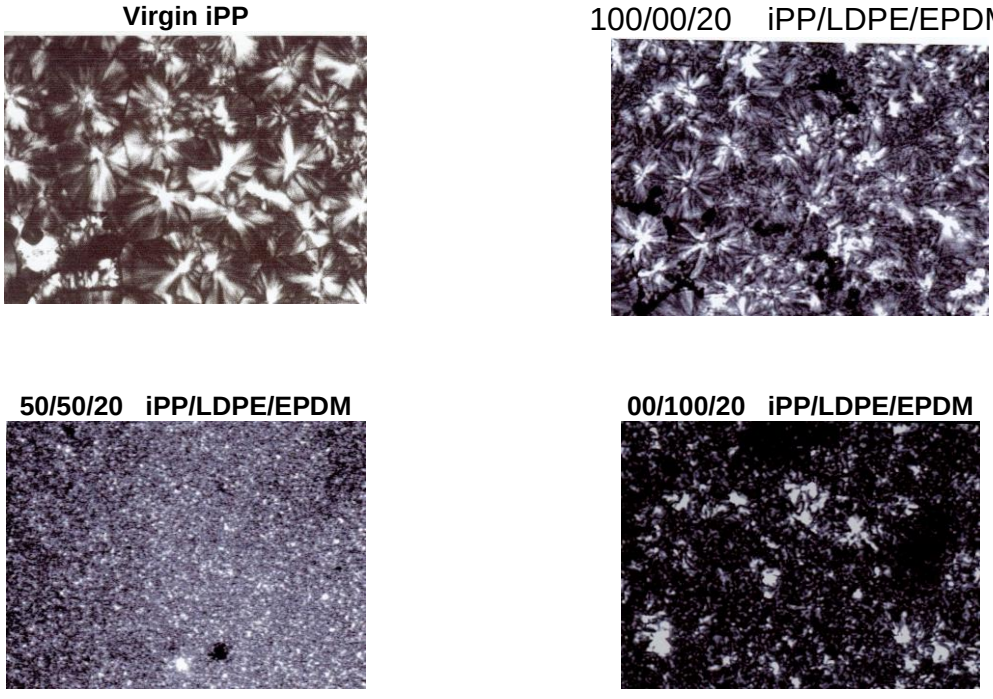

Fig I. 4 : Optical micrographs of different blends based on iPP/LDPE with 20 pcr EPDM parts in presence of 0.5 peroxide under cross polars (300x) .

SEM results

The effect of blend composition is observable on the micrographs of the different blends. For blends containing either LDPE or iPP and EPDM, rough fractured surfaces are obtained (Fig.6 a and e). This is also the case for ternary blend iPP/LDPE/EPDM 50/50 (Fig.6 c).When either composition of LDPE or iPP is the major one, a smooth surface was observed (Fig.6 b and d).

The LDPE/20 pcr EPDM binary blend shows smooth fracture due to good miscibility and the reactive effect. In addition, the LDPE and EPDM will crosslink in presence of peroxide and will form complex network, this could be accompanied by further induced crystallization of crystallizable materials within and between spherulites [9]. Based on optical microscopy and impact strength results for 80/20/20EPDM and 20/80/20EPDM blends, it was observed that as the spherulite radius decreases, the fracture surface becomes more apparent. On the other hand, for the 50/50/20EPDM blend, the networks formed and further crystallization parts induce rougher fracture surfaces of brittle regions. As a result, it could be concluded that there is competition between formation of crystaline parts and crosslinking parts due the presence of EPDM and in particular the double bonds of diene monomer to form network formation [9,11].

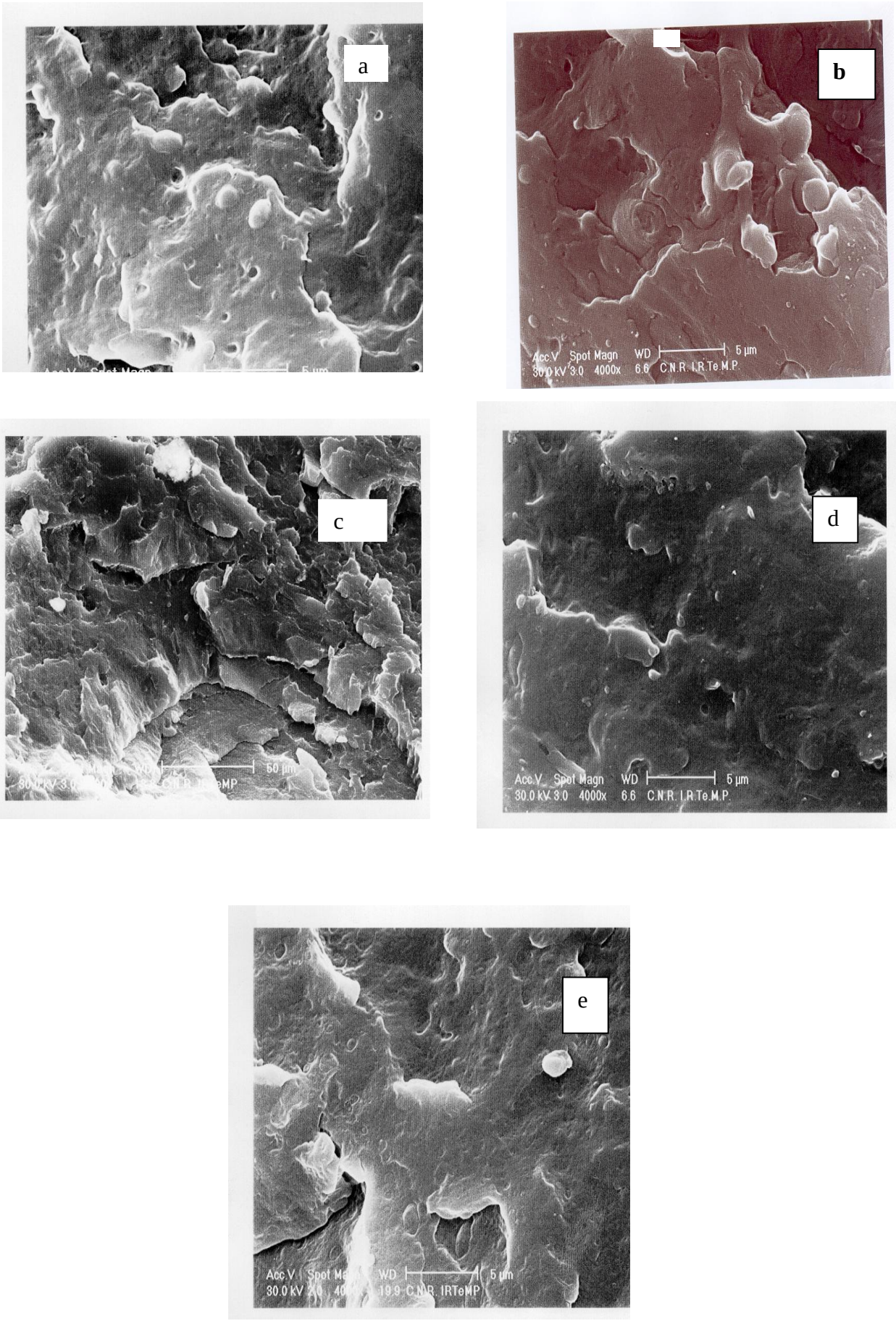

Fig I. 5 : SEM micrograghs of brittle fractured surfaces of different reactive blends based on (iPP/LDPE) with 20 pcr EPDM . (a) 100/00; (b) 80/20; (c) 50/50; (d) 20/80; (e) 00/100.

Impact resistance properties

Figures 6 and 7 show results of impact testing for notched and un-notched specimen, at two different temperatures (almost –15°C, i.e. close to the Tg of iPP , and at room temperature). This methodology is used to see the influence of EPDM on the impact strength. The effect of LDPE content on a_k is apparent for contents above 50% . The curves show relatively low values of a_n and a_k , notably for LDPE contents below 50% , but the additivity law is not verified for all compositions. The critical proportion 50/50 of iPP/LDPE matrix shows a synergysm effect for a_n ; however, an antagonism result is observed for a_k value and the effect is more evident at –15°C. There is a brittle/ductile transition behavior around 70% of LDPE content. This is due to the different modifications that the blend had undergone. The influence of EPDM and reactive blending to form a network have direct effect on impact fracture. The mode of dispersion of the different components, the network architectural structure are positive factors to get more relaxed blends with less residual stresses. As it is known, the EPDM decreases the interfacial tensions due to the ethylenic chains. The LDPE and EPDM increase the impact strength due to the chains high mobility. There are many theories or models in literature [3,11] concerning the interpretation of toughening mechanisms of polymer/rubber blends, mainly : micro-crack theory, multiple-crazing theory, damage competition theory, shear yielding of the matrix and cavitation mechanism ... The results indicate a semi-brittle fracture type for the blends with high proportion of iPP and promoting brittle-ductile fracture transition at around 60 to 70% of LDPE content; the ductile behavior takes place for higher LDPE contents due to a strong interfacial adhesion and high crosslinking degree [12,14].

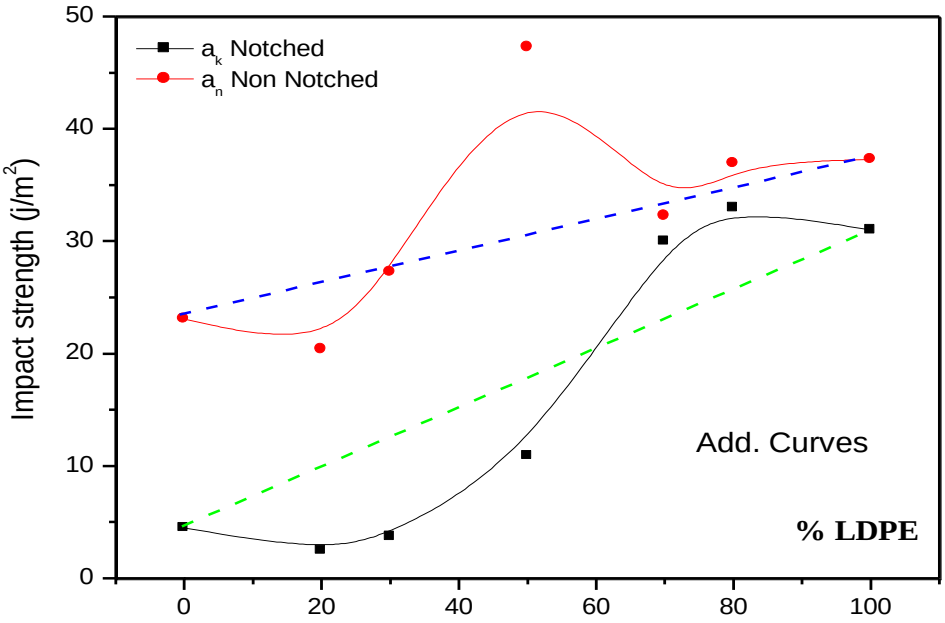

Fig I. 6 :**Variation of impact strength as function of % of LDPE**

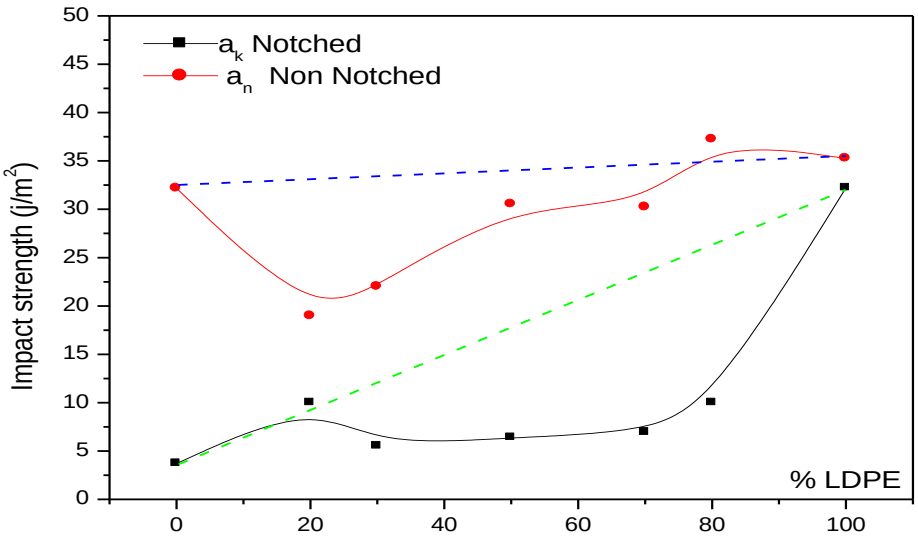

Fig I. 7 : Variation of impact strength as function of LDPE/iPP/20 phr of EPDM at -15°C.

Steady state capillary rheometer

The experimental result of capillary rheometer shown in Figure 9, indicates that the EPDM content does not affect the viscosity whereas the LDPE proportion of the matrix do affect the viscosity. The increase in viscosity is evident from 50/50 and will be higher as the LDPE proportion will be predominant. This result is also observed in Dynamic Rheological Analysis **(**DRA**)** testing and the steady state viscosity; there is a good correlation with the torque values at equilibrium Tc . This could be written as $T_c = K\eta$. The increasing viscosity describes an increase of the networks formed, and according to the result pointed above, it can be concluded that when macroradicals are formed, only a part of them contribute to network formation. Macroradicals efficiency is closely dependent on different parameters (processing conditions an peroxide nature). Network formation is a complex phenomenon; its effect results in a viscosity increase [13,14] .

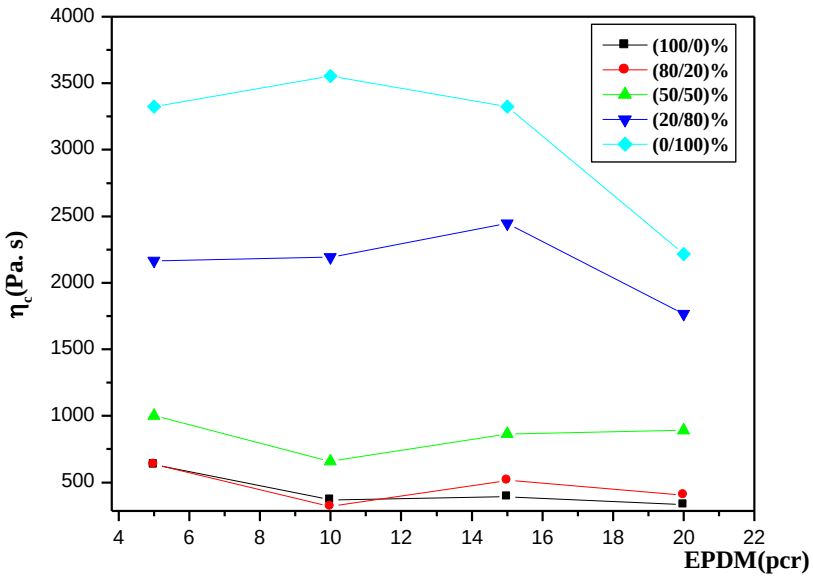

Fig 8 : Variation of corrected viscosity as function of EPDM pcr for different blends based on (iPP/LDPE) matrix at constant shear strain 100$^{-1/s}$)

DMTA results

The result of DMTA for LDPE/EPDM (00/100/20) shows that there is a T_g at - 6°C corresponding to iPP T_g's whereas there no iPP added. This is due to β-scission of propylenic part of EPDM in presence of peroxide which will form a iPP chain, this low M_w is generated from propylenic part contained in ethylenic/propylenic parts of EPDM. Therefore, this low molecular weight of a propylenic part will act as an external lubricant due to repulsive intermolecular forces. Besides this result, different diagrams distinguish differences in characteristic peaks. This could be explained by the fact that the chains are more relaxed for (50/50) LDPE/iPP composition compared to binary blends. This is mainly due to EPDM effect and free volume generated by the complex interpenetrating networks formed.

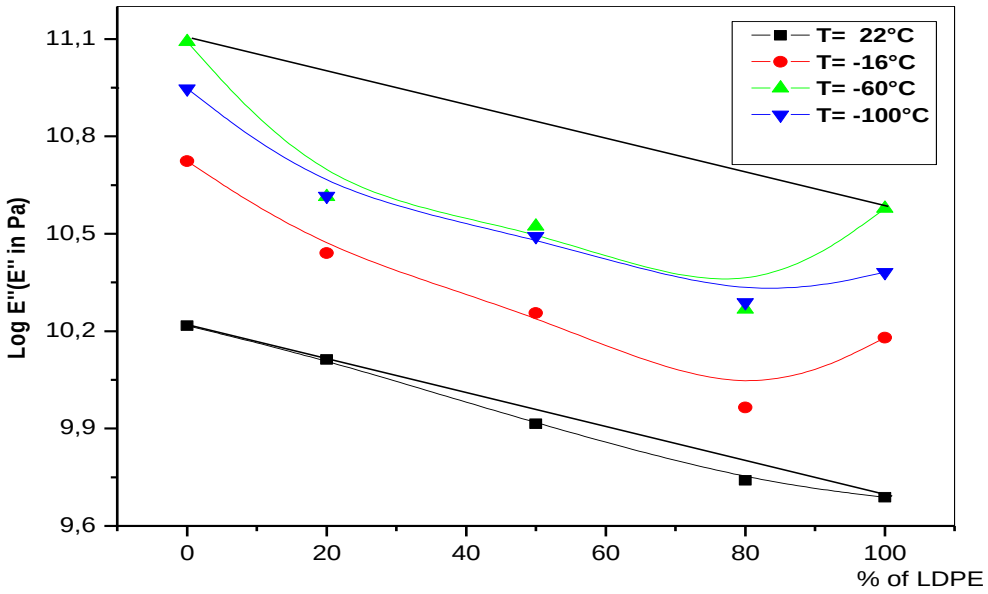

Fig I. 9 : Variation of Viscoelastic modulus as function of blend compositions for different testing temperature.

Beside this result, Figure10 shows the effect of temperature on blend compositions on the visco-elastic modulus (E'') for different testing temperatures. It is observed that as E'' decreases the material is more flexible or presents a rubber like behavior. It is noticed from this curve that E'', taken at 22°C of neat composition based on iPP/EPDM (100/20), presents a corresponding value of E'' taken at –16°C of ternary

blend based on iPP/LDPE/EPDM (50/50/20). This result illustrates the fact that the reactive blending will form a complex structure while improving the stable structure of incompatible components such as iPP and LDPE [13,15]

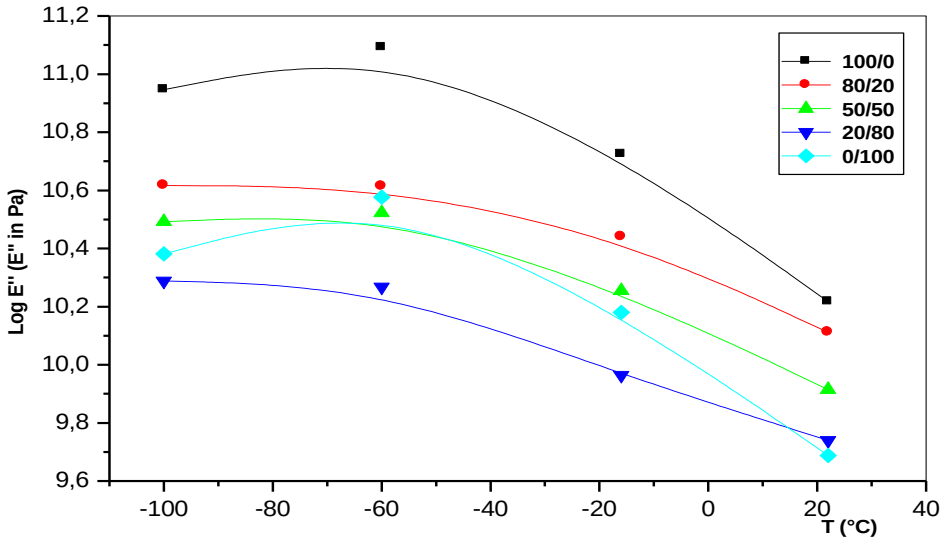

Fig 10 :Variation of viscoelastic modulus as a function of temperature for different blends based on iPP/LDPE/20 Phr EPDM .

Figure 11 shows the effect of composition of iPP/LDPE for different running temperature as a function of E''. It is noticed that the ternary blend of (20/80) iPP/LDPE is the most relaxed blend, and it is more relaxed than the binary blend based on LDPE/EPDM. It could be concluded that than the ternary blends present a rubber like behavior around –50°C. This is an interesting result .

Conclusion

From the different results obtained, it can be concluded that blends prepared through reactive blending react in a different way than traditional ones. Dynamic Rheological Analysis (DRA) results showed that binary blends based on LDPE/EPDM present complex crosslinked reactions, there are at least two separate crosslinking reactions added to the interreaction between the two reactive components. The ternary blends (iPP/LDPE/EPDM) present complex crosslinking reactions accompagnied with a scisssion reaction of iPP. The overall final structure is closely dependant on the peroxide (type and concentration) , the weight content of crosslinkable components (LDPE and EPDM) and iPP scission reaction. These morphological changes will occur mainly in the amorphous regions, affecting slightly the crystalline regions. There is a mass effect on the thermal properties and viscoelastic modulus, characteristic peaks such as T_{crist} and Tg are changed. The spherulite sizes reduction will not obey traditional theory, and mechanical properties will be improved. It may be said that there is a compensatory effect (of such a decrease in spherulite size) by the new final structure (crosslinked network) due to reactive effect. The overall conclusion is that novel blends based on iPP/LDPE/EPDM are useful blends from the mechanical and visco-elastic point of view .

Part II A: Structure and properties of isotactic polypropylene crosslinked in presence of peroxide

1. Introduction.

Branched, crosslinked and interpenetrating polymer networks present improved properties, such as a higher melt strength and a better processability than their linear counterparts [16, 17]. These are important characteristics for the preparation of fibers and materials capable of being processed by blow molding. Polyethylene, PE, is an easily crosslinking polymer by means of an organic peroxide capable of creating radicals by a decomposition reaction [18, 19]. On the contrary, isotactic polypropylene, iPP, has been considered until very recently as a non-crosslinkable polymer. This is due to the fact that, in iPP, the β-scission degradation process predominates over the crosslinking mechanism. Nevertheless, in the last years new methods, in order to achieve the crosslinking of the isotactic polypropylene, have been developed [20].

The present study deals with an innovative method that allows the preparation of reversibly crosslinked isotactic polypropylene [21]. This method, with slight variations, can be used to obtain crosslinked blends of PP and low or high density PE, copolymers of iPP or their blends with elastomers. In addition, the polymers to be crosslinked can be freshly prepared, recycled, restored, etc. The reversible crosslinking reaction is the newest method developed to obtain modified polyolefins. As it is well known, polymer modification contributes to the development of new materials or blends, especially attractive from the recycling and environmental point of view. On the other hand, polyolefins (particularly polyethylene and polypropylene) represent the major part of the total thermoplastic materials consumed.

The materials intervening in the crosslinking process are: isotactic polypropylene, an organic peroxide, sulfur (S), an accelerator (or a mixture of them), and potassium persulfate. The so-called “crosslinking agent” is constituted by the peroxide, the sulfur, and the accelerator. The mixing process used is the extrusion method.

However, all other processes of transformation used for thermoplastics, i.e., blow, injection or compression molding, could be also useful for the subsequent industrial use. Therefore, this kind of modified polymers can be used to manufacture different articles.

The principle of the crosslinking mechanism is to create macro-radicals and cause them to act immediately on sulfur before the reaction of termination occurs. The crosslinking process takes place by a homolytic chemical reaction. The initiation reaction is originated by the peroxide decomposition, which gives rise to the formation of macro-radicals with a very short lifetime. The sulfur atoms link the chains (coupling reaction) through the formation of a tri-dimensional, heat-resistant, network. The inter-chain bridges can be: a sulfur atom, a polysulfide $–(S)_x–$, or a cyclic S-compound. Accelerators increase the sulfur activation rate. In this way, the macro-radicals' formation and their coupling reaction with the sulfur takes place simultaneously, thus obtaining an optimum crosslinking degree for each formulation. The potassium persulfate increases the macro-radicals' lifetime. More details are given in ref. [21].

The composition of the blend has to be deduced by taking into account the degree of crosslinking to be obtained. This, in turn, depends on the radical peroxide efficiency, and on the activation rate. Therefore, in every experiment it is necessary to consider the transformation temperature, and the particular characteristics of the extrusion equipment to be used.

The aims of the present study are two fold:

a) Preparation of samples of crosslinked iPP using different formulations, according to the above described method.
b) Investigation of the influence of the crosslinking process on the mechanical and structural properties of the modified material.

2. Experimental Part.

2.1. Materials.

The materials used in this investigation were:

Isotactic polypropylene (iPP): Sabic-Vestolen 9000-67404, supplied by Chemische Werke Hülls,, Germany.

Dicumyl peroxide: DCP 96% activity, supplied by NORAX.

Sulfur, S, supplied by Wuxi Huasbeng Chemical additives Factory,China.

Potassium persulfate, supplied by Innochem, Belgium.

The three accelerators used were: tetramethyl tiuram monosulphide (TMTM), tetramethyl tiuram disulphide (TMTD) and 2,2', dibenzothiazol disulphide (MBTS). They were supplied by Rhône-Poulenc, France.

The peroxide, the sulfur, and the above accelerators constitute the "crosslinking agent".

Blend preparation.

For the preparation of the blends, the sulfur concentration was always equal to that of the peroxide. The amount of sulfur and peroxide was 0.2 or 0.4 wt %. In all cases, the accelerator was ¼ of the sulfur and peroxide concentration. The six formulations used are shown in Table 1.

Table II. A 1 : Sample composition.

Sample	Polymer	Peroxide content %	Sulfur content %	Accelerator content %
iPP	iPP	---	---	---
1	iPP	0.2	0.2	0.05 (TMTD)
2	iPP	0.4	0.4	0.1(TMTD)
3	iPP	0.2	0.2	0.05 (TMTM)
4	iPP	0.4	0.4	0.1 (TMTM)
5	iPP	0.2	0.2	0.05(MBTS)
6	iPP	0.4	0.4	0.1 (MBTS)

The iPP, the crosslinking agent and the potassium persulfate were firstly mixed in the solid state, using a small quantity of vegetal oil in order to wet and improve the dispersion of the fine powder of the different components within the granules of the iPP. Thereafter, the obtained mixture was inserted into a single screw laboratory extruder (Prolabo 1989) with the following characteristics: L/D = 20; screw diameter = 25 mm; screw speed = 60 turns/min. The residence time was about 3 min. The temperature profile used for the three stages was: feed zone = 155º C; compression zone = 180º C; homogenization zone = 200º C. The extrusion cycle was repeated twice in order to achieve a homogeneous blend.

The impact strength test was carried out in a device equipped with a control of absorption energy. Specimens were prepared by compression molding. Notched (1/10 deep) specimens were submitted to the Izod strength testing. The specimen thickness and width were 3 mm and 9 mm, respectively. Resiliencies a_k (J/m²) and energies of absorption (J) were determined using a hammer of 7 Joules. Measurements were carried at room temperature according to the ASTM D 180 norm.

Specimens for the tensile test were prepared by injection molding at an injection pressure of 200 Kgf /cm² and an injection temperature of 220°C. Moderate cooling rates were used to follow the mechanism of crystallization. Specimens follow ASTM D 638 type 2 shapes. The tensile test was performed in an Instron machine equipped with a control and program unit. A crosshead speed of 10 mm/min at room temperature was used in all samples.

The melt flow index (MFI) was measured by allowing a molten polymer to flow under fixed working conditions (load and temperature), through a standard cylindrical die (2.09 mm diameter, 8 mm length). The MFI is defined as the weight of flow in grams per 10 minutes. The referred norms are ISO R 1138 or ASTM D 1238. In case of iPP, the working conditions were a load of 2.16 kg and a temperature of 230º C.

The microhardness of samples was measured at room temperature using a Leitz tester equipped with a square-based diamond indenter [22]. The H-value was derived from the residual projected area of indentation according to: $H = kP/d^2$. In this expression, d is the length of the impression diagonal in meters, P is the contact load

applied in Newtons, and k is a geometrical factor equal to 1.854. Loads of 0.25, 0.5, 1 and 2 N were used. The loading cycle was 0.1 min. 8 to 10 indentations were made on each sample, and the results were averaged.

Thermal analysis was performed in a Perkin-Elmer differential scanning calorimeter DSC-7, in a N_2 atmosphere. The temperature range studied was 40-220º C. The heating rate was 10 or 20 ºC/min. Typical sample weights were 5-10 mg. The crystallinity measured by calorimetry, α_{DSC}, was derived from the melting enthalpy obtained by DSC using the following expression: $\alpha_{DSC} = \Delta H_m / \Delta H_m^{\infty}$, where ΔH_m and ΔH_m^{∞} are the experimental melting enthalpy, and the melting enthalpy for an infinitely long crystal, respectively.

The WAXS study was performed using a Seifert diffractometer (reflection mode). The working conditions were: voltage: 40 kV; intensity: 35 mA; angular range: 5-30º (2□.□ scan rate 0.01 º/s; slits: 0.3, 0.2). The crystallinity α_{rX} of every sample has been calculated as the ratio of the area corresponding to the crystalline peaks to the total area of the diffractogram.

3. Results

Dynamic Rheological Analysis

A torque-time rheometer was used to study the unmodified iPP sample, as well as the modified samples with the peroxide and the couple peroxide/accelerator, respectively. Experimental results of torque-time evolution (fig. 11a) show that the torque of iPP in presence of peroxide is lower than that of pure iPP. This is due to the attack of the peroxide radicals, particularly at the tertiary carbons of iPP, which are the more reactive sites, to form macro-radicals by disproportionation or by cyclisation of the end groups, i.e., the peroxide causes the scission of the iPP chains. However, the torque of the iPP with the couple peroxide/accelerator is lower than that of pure iPP, but higher than the corresponding to the iPP plus peroxide. It is clear that the couple peroxide/accelerator presents a different effect. In this case, a controlled scission takes place, because the accelerator decreases the peroxide efficiency (the accelerator could then be considered as inhibiting or slowing down the action of the peroxide).

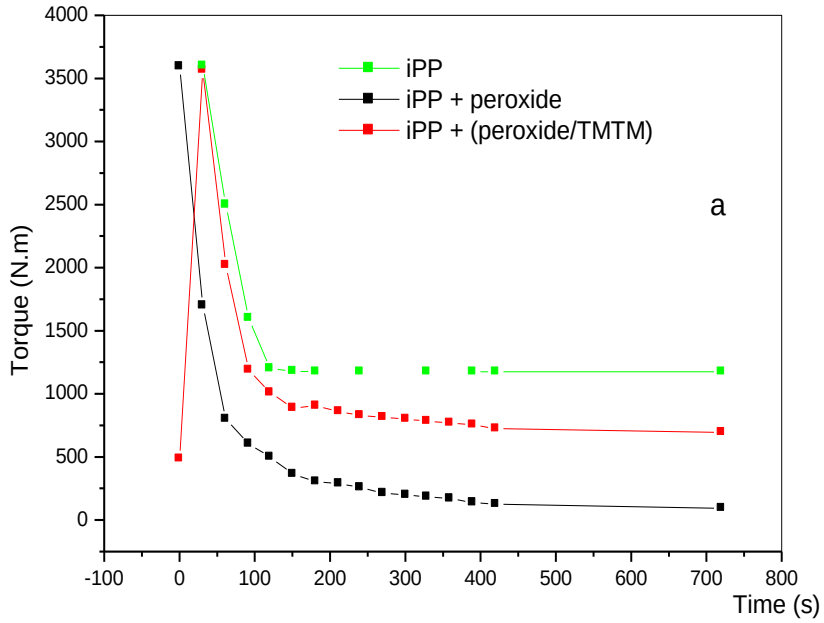

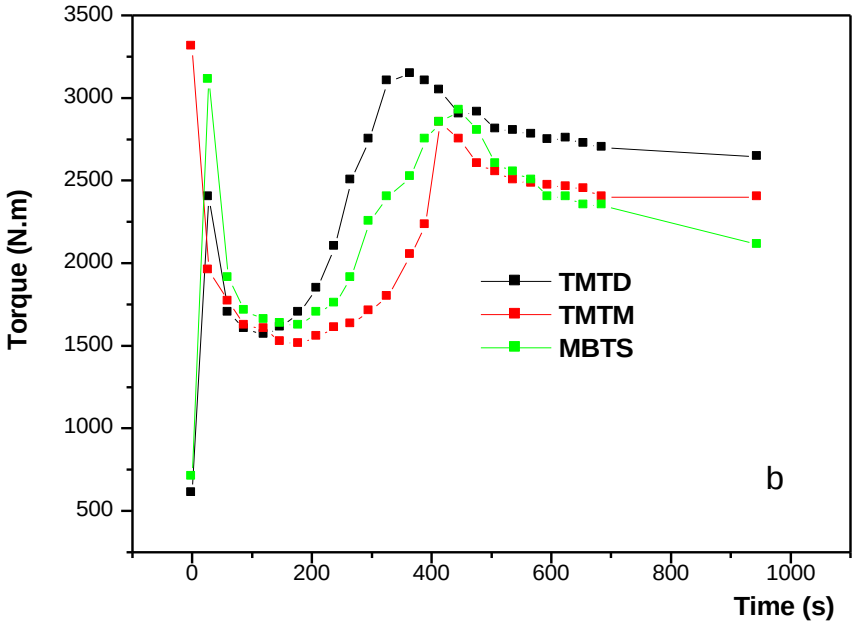

Fig II. A 1 : a) Effect of the peroxide and the couple peroxide/accelerator TMTM on the torque-time evolution of iPP. b) Effect of the accelerator type on the torque-time evolution of iPP in presence of different crosslinking agents (peroxide/sulfur/accelerator).

Consequently with the decrease of the torque in the presence of peroxide, there is a decrease of the molecular weight (M_w). It has been shown that the higher is the peroxide concentration [P], the lower is the M_w obtained [23]. Such a result, not shown here, has also been observed in a MFI study on iPP as a function of the peroxide content. With the couple peroxide/accelerator, a smaller decrease in the MFI, as compared to that observed with only the peroxide, is observed. Therefore, in this case, controlled scission reactions are thought to occur. The M_w of the resulting material is controlled by the accelerator concentration related to, both, the concentration and the activity of the peroxide. However, the weight fraction of the accelerator should not exceed that of the peroxide. By using ¼ weight concentration of the peroxide, which is the common weight fraction used in this study, a constant torque value, and a moderate increase of MFI values compared to those shown by the iPP-peroxide formulations, are obtained [2].

Furthermore, the combination of the peroxide and sulfur agents shows no important effect on the peroxide activity. Because the accelerator has also an activation effect on the sulfur, the combination of the sulfur, the peroxide and the accelerator gives rise to the crosslinking reaction (fig. 11b). Here, it can be seen that the torque-time evolution follows the typical shape for a crosslinked polyolefin material (see chapter experimental part). Using the Monsanto method, developed by Harpell and Walrod [2], it is possible to evaluate how does the crosslinking reaction occur. Fig. 11b additionally shows the effect of the different accelerators used when the three components (peroxide/sulfur/accelerator) are added. It is to be noted that the T_B values (T_B = maximum torque, corresponding to the maximum crosslinking degree) are not so different for the three accelerators used. The maximum degree of crosslinking (maximum T_B) takes place at a shorter time for TMTD, and at a longer time for MBTS. These results are strongly related to the activity temperature of each accelerator. The most interesting aspect here is that the macro-radicals of the iPP chains present a very long lifetime.

Macroscopic mechanical properties

Data concerning the impact strength, the microhardness, the yield stress and the Young's modulus for the studied samples are collected in Table 4.

Table II. A 2 : Mechanical properties (microhardness, H; yield stress, σ_y, Young's modulus, E, and impact strength) of the samples included in this study: isotactic polypropylene iPP unmodified (sample 1), and crosslinked by using different agents. Samples are as in Table 1.

Sample	H (MPa)	σ_y (MPa)	E (MPa)	Impact strength (J/m^2)
iPP	89	7.962	830	4.47
1	78	30.33	1217	19.40
2	72	26.60	1216	15.91
3	79	29.01	1182	24.47
4	70	19.57	1123	18.25
5	88	28.06	1317	30.94
6	81	27.98	1252	19.79

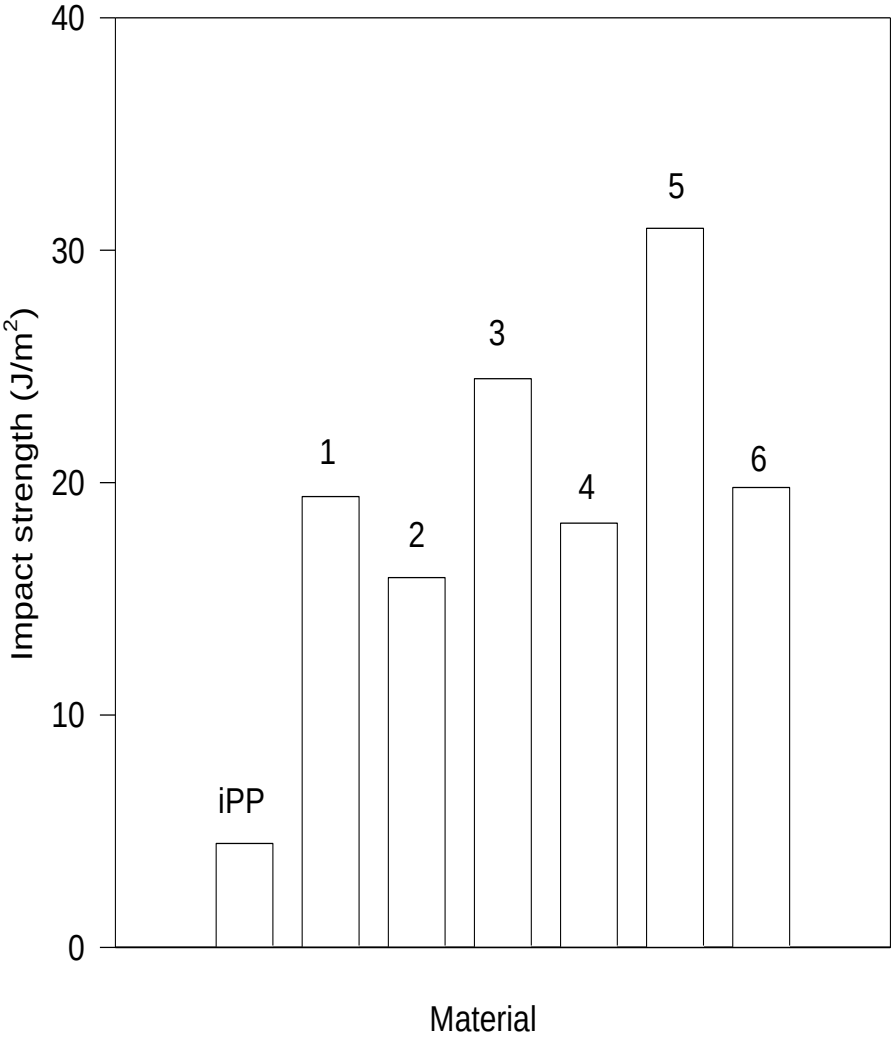

Fig II. A. 2: Impact strength shown by the unmodified iPP and by the crosslinked samples. Sample composition is indicated in Table II. A . 3

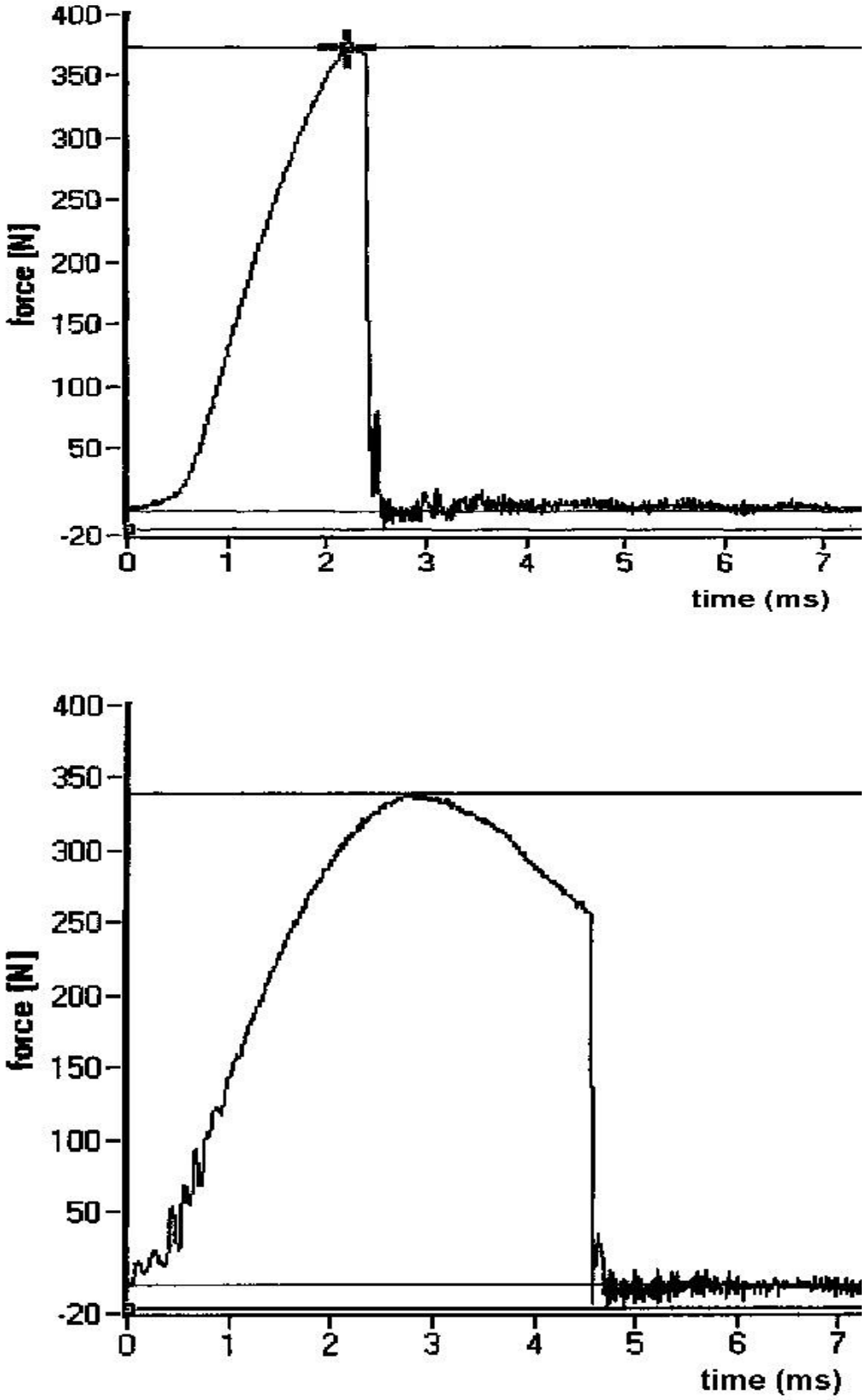

Fig.II.A.3: Plot showing the fracture behavior of: a) unmodified iPP; b) sample number 5. For sample composition, see Table 3.

Figure 3 shows the influence of the crosslinked structure on the impact strength for notched specimens at room temperature. The effect of the different crosslinking agents and of the different weight fractions on a_k is apparent. The histogram clearly shows that the modified material reaches higher impact strength values than those of the raw material. In particular, the impact strength for sample 5 (iPP with a 0.05 % of MBTS added) is as high as 30.94 J/m^2, i.e., about 7 times the value of unmodified iPP (4.47 J/m^2, see table 4, column 5). Also, it is noteworthy the fact that, whereas the iPP raw material presents brittle fracture behavior, for the different crosslinked iPP samples ductile fracture behavior is observed [12, 13, 14]. For instance, compare fig. 13a (unmodified iPP), and 13b (iPP with a 0.05 % of MBTS added). The other crosslinked samples behave similarly.

All samples show hardness values slightly lower than that of initial iPP, except sample 5. The hardness of this sample is almost identical to that of iPP (see Table 4, column 2). None of the samples included in this study showed any elastic recovery. From the plot of the microhardness vs. the yield stress of the modified samples (not shown here), one obtains: $H/\sigma_y = 2.8$. Additionally, for all crosslinked samples, a linear relationship (not shown here) between the Young's modulus E and the hardness H, E/H = 15.6, is obtained.

Differential Scanning Calorimetry

From the calorimetric study, it is seen that the crosslinking process gives rise to a new, low temperature peak, not appearing in the non-modified iPP. For instance, compare fig. 14a, (the thermogram of the non-modified iPP), with fig. 14b and 14c (the thermograms obtained on samples 5 and 6, i.e., crosslinked iPP prepared with 0.05 and 0.1 % of MBTS, respectively).

Table II. A 3: Data obtained in the DSC and WAXS study of samples of isotactic polypropylene normal, and crosslinked by using different agents (TMTM, TMTD and MBTS). T_{m1} and T_{m2}: melting points corresponding to the DSC maxima. l_{c1} and l_{c2}: thermodynamic crystal thickness obtained from the melting points by using the Thomson-Gibbs equation (considering samples being mixtures of PE and PP). ΔH_1, ΔH_2 and ΔH_m total: melting enthalpies corresponding to the first and second DSC maxima, and the sum of these two values, respectively. α_{DSC} total: total crystallinity values derived from the DSC study. α_{rX}: crystallinity data obtained from the WAXS diagrams.

Sample	T_{m1} (º C)	l_{c1} (nm)	ΔH_1 (J/g)	T_{m2} (º C)	l_{c2} (nm)	ΔH_2 (J/g)	ΔH_m total (J/g)	α_{DSC} (total)	α_{rX}
iPP	---	---	---	163.2	19.2	114.1	114.1	0.55	0.48
1	118.4	9.6	30.3	158.5	16.1	82.3	112.7	0.50	0.39
2	117.7	9.3	31.2	157.8	15.7	81.6	112.8	0.50	0.41
3	118.6	9.7	33.7	159.9	16.9	83.3	117.0	0.52	0.42
4	117.6	9.3	25.2	158.6	16.4	75.4	100.5	0.45	0.40
5	117.7	9.3	30.1	160.8	17.5	96.5	126.5	0.57	0.42
6	118.4	9.6	30.2	158.8	16.3	84.3	114.5	0.51	0.42

The new peak, indicated by an arrow, is probably caused by the presence of polyethylene (PE) chains, eventually originated by the action of the peroxide and potassium persulfate on some of the tertiary carbon atoms of the iPP. Table 5 includes the melting temperatures T_m corresponding to the different peaks of every sample. The thermodynamic crystal size l_c has been calculated for each maximum from the Thomson-Gibbs equation:

$$T_m = T_m^0 [1-(2\sigma_e / \Delta H_m^\infty l_c)] \qquad (1)$$

where σ_e is the surface free energy and T_m^0 is the equilibrium melting point of each component. The l_c values, the melting enthalpies ΔH_m, and the crystallinities α_{DSC} for, both, PP and PE are also included in Table 3. In this calculation, we have used the following values: for the iPP, ΔH_m^∞ = 207.33 J/g [24], T_m^0 = 460.7º K [24] and σ_e = 100 erg/cm^2 [25]; for the PE, ΔH_m^∞ = 293.86 J/g [24] and T_m^0 = 414.6º K [24]. For the surface free energy of the PE, we have taken σ_e = 79 erg/cm^2 [26]. However, this σ_e value is probably an upper limit. In fact, according to our results, σ_e on linear PE samples depends on the molecular weight. Thus, for PE samples studied in [16], the surface free energy varies between 79 and 91 erg/cm^2 [26]. On the other hand, the melting point found in our work for the first maximum appearing in the thermograms of the crosslinked samples is 117-118º C. This is a relatively low value, suggesting that the PE originated during the crosslinking process has a low molecular weight and/or is not linear, but branched.

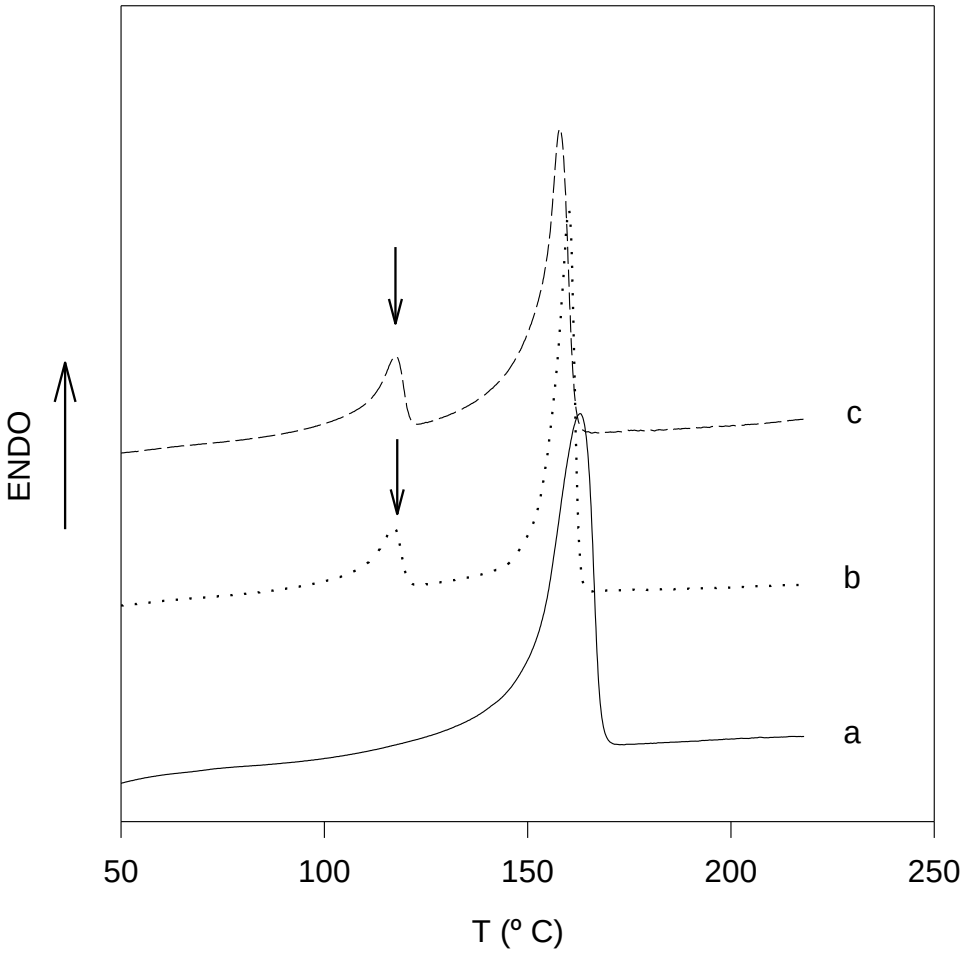

Fig.II.A.4: Thermograms of: a) unmodified iPP; b) sample number 5; c) sample number 6. For sample composition, see Table 3.

X-ray diffraction study

The WAXS patterns taken for the non-modified and crosslinked samples show the characteristic reflections of the monoclinic α-form of isotactic PP (fig. 15) [27]. By comparing the diffractogram of the original iPP (fig. 15a) with that of the crosslinked sample number 6, prepared with a 0.1 % of MBTS (fig. 15b), it is seen that the crosslinking process affects mainly the relative intensity of the first and second diffraction peaks. The other crosslinked iPP samples behave similarly. All crosslinked samples exhibit crystalliny values α_{rX} slightly lower than that of the unmodified iPP. Table 5 includes α_{rX} data for all the samples (column 10). These data show a linear correlation (not presented here) with the hardness values of the samples.

From a closer inspection of the WAXS patterns of the crosslinked material, one observes one new, small intensity reflection appearing at 23.85º (2θ). See, for instance, fig. 15b, corresponding to the crosslinked sample with a 0.1% of MBTS, in which the reflection is indicated by an arrow. This new reflection, not appearing in the original iPP (fig. 15a), could be associated to the (200) planes in PE [28]. In addition, the (111) reflection of the original iPP, at 21.03º (2θ), in the crosslinked material is slightly shifted towards higher angles, and nearly coincides with the peak (110) of PE, at 21.55º (2θ) [28] (compare figs. 15a and 15b). It is also noteworthy that the results obtained in the FTIR study of these samples (not shown here), confirm the presence of ethylenic chains in the modified iPP. For instance, the occurrence of a band at 720 cm^{-1} is attributed to the ethylenic chains induced during the crosslinking process. This band, usually appearing in the range 750-720 cm^{-1}, is characteristic of the “rocking” mode of the $–(CH_2)_n-$ sequences when $n \geq 4$ [29]. In addition, at 650 cm^{-1} a new band appears. This band could be due to the “stretching” mode of the –C-S- groups, thus being directly related to the bridging chains created in the crosslinked material [30].

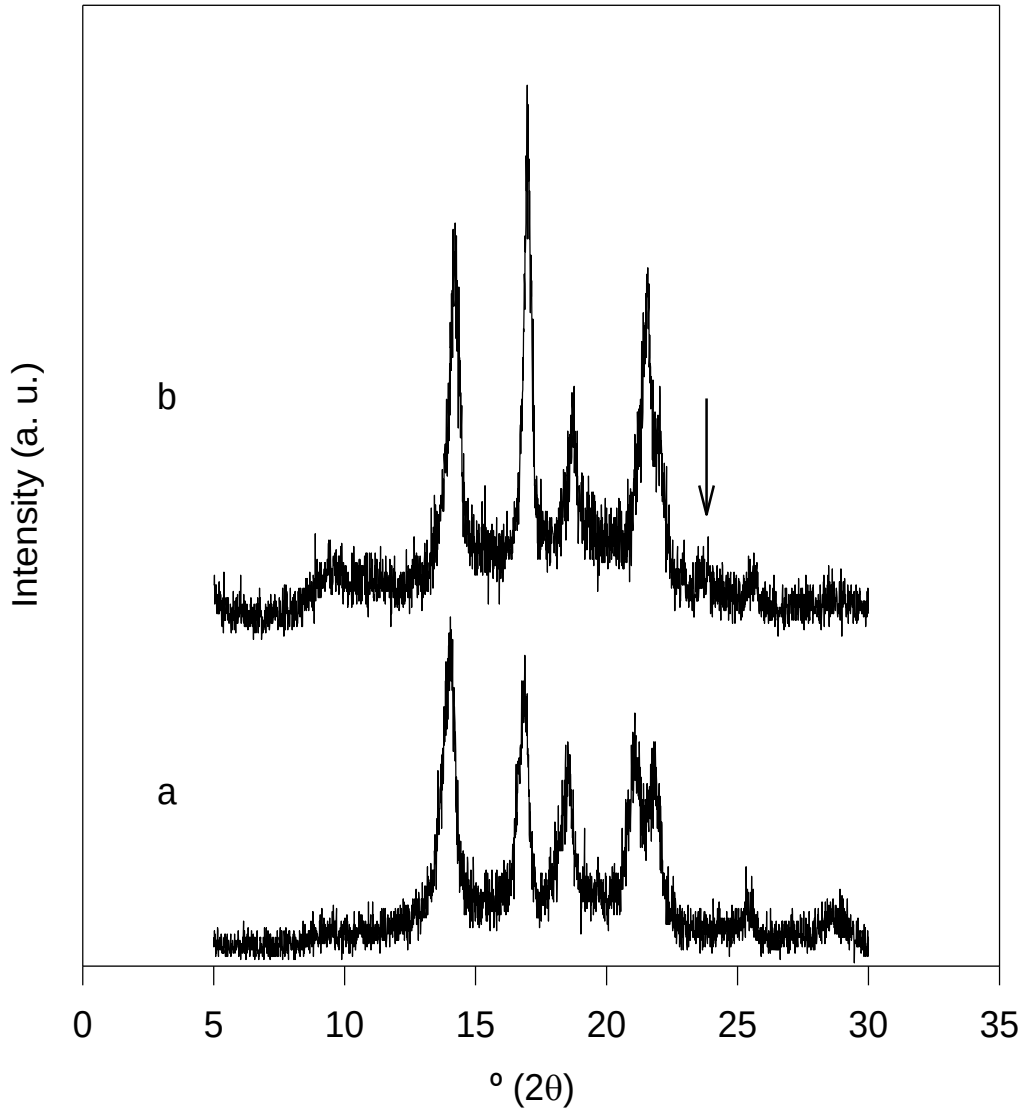

Fig.II.A.5: WAXS diagrams of: a) unmodified iPP; b) sample number 6. For sample composition, see Table 3.

4. Discussion

From the results shown in fig. 11b, it can be seen that the equilibrium torque value T_C, and also the difference between the maximum torque T_B and the equilibrium torque T_C values, are different for each accelerator type. According to the technique of Harpell and Walrod [2], in the torque-time curves the activation energy of the crosslinking has always been calculated between T_B and T_A. However, it is noteworthy that our present study is the first one which shows the decrease from T_B to T_C. This result can be explained as follows: The long macro-radicals' lifetime shown in fig. 11b might be due to the high continuous shearing involved. Therefore, the fast initial crosslinking reaction should result in a high degree of crosslinking, which later undergoes a partial destruction by the high shearing developed just before the equilibrium takes place. The crosslinking degree is determined at the equilibrium torque value T_C, because at this stage there is a stable equilibrium for very long processing times. This is due to the fact that a stable torque value involves a stable viscosity. Consequently, one reaches a stable crosslinking degree during a longer time (~15 min) that corresponds to 5 times the extruder cycle time. Accordingly, a reversible crosslinking reaction will not affect the overall crosslinking degree, even for a multi-repeated processing cycle. The overall network formed will be stable. More details are reported in the patent [21]. This is also an important result from the industrial point of view, because the pumping and shearing involved in a single screw extruder does not provide the same crosslinked iPP as in a twin-screw extruder device.

The data derived from the structural study seem to indicate that the crosslinking process gives rise to a slight decrease in the crystallinity and microhardness of the samples. Furthermore, from the DSC and WAXS results, it is clear that crosslinking gives rise to the appearance of a certain amount of PE (25-29 %). The generation of the ethylenic chains could be explained as follows: The oxy-radicals of the peroxide might eventually attack the tertiary carbons of the iPP. In this case, the alcoholates provided by the peroxide or the peroxidisulfate would stabilize these tertiary carbons (intermediate reaction). The working conditions used are sufficiently strong as to permit the attack of the H of the methyl side group. This is a very stable hydrogen atom, and one needs a very high energy to abstract it.

Nevertheless, the entropy involved in this process is also high. The process would finally lead to the formation of branched ethylenic chains. These chains are thought to be responsible for the melting peak appearing at 117-118º C in the thermograms of the modified iPP.

In addition, the slight decrease in the hardness of the modified material (see Table 2) can be due to a combination of several effects:

a) A decrease in crystallinity of the modified samples (see Table 5, columns 9 and 10).
b) The smaller crystal thickness shown by the crosslinked iPP (see Table 5, column 6).
c) The appearance of a 25-29 % of a crystalline population (probably due to the new branched PE chains), with smaller hardness values than those of pure iPP.

From the study of the mechanical properties of the samples, the obtained value of H/σ_y = 2.8 is quite close to that predicted by the Tabor relation, H/σ_y = 3.0 [31]. Previous investigations carried out in our laboratory on melt-crystallized polyethylene indicate that the Tabor relation is obeyed when the strain rate in the tensile tests is comparable to that employed in the hardness tests [32]. In our samples, the value found of E/H = 15.6 is higher than that obtained by Struik [33] and Flores [34], i.e., E/H = 10.

From Table 4, it can be seen that, even if the hardness of modified iPP is slightly smaller than the value measured in the unmodified material, the crosslinked samples present improved mechanical properties than the original iPP ones. Thus, the crosslinking process is responsible for the improvement of the mechanical properties, especially the high impact strength (see fig. 12 and Table 4, column 5), in the modified samples. The six formulations based on the different accelerators with the two compositions (0.2% and 0.4% by weight) related to the matrix, show a synergistic effect on a_k.

According to the foregoing, the structure of the modified iPP could be considered as a combination of rubber-like and crystalline thermoplastic components. The above results also indicate that crosslinking takes place at a higher scale than crystallite formation. This assumption fits well with the results obtained. Thus, the more bridges are formed (higher crosslinking degree), the higher is the ductile behavior (the rubber like behavior). This transformation from a brittle to a ductile behavior in the modified material is extremely important. As pointed out in the introduction, the bridges present in the modified iPP, basically originated by the sulfur component, act as linking agents of the olefin macrochains involved.

The influence of the accelerator type on the reactive blend to form a network has a direct effect on the impact fracture. The mode of dispersion of the different components and the network architectural structure, are factors that tend to yield blends with less residual stresses. As it has been reported before, a ductile behavior is accompanied by a decreasing of the interfacial tensions due to the high mobility chains [35]. The brittle-ductile fracture transition of iPP is usually promoted either by blending the iPP with EPDM or EPR, or with a 60-70% of LDPE when a peroxide is added [3-5]. Within this context, the high impact strength iPP does not need to be blended to become a ductile material.

Another advantage of the new crosslinking method described above is the possibility of recycling the crosslinked samples a number of times. The samples can be repeatedly molten and used again, which is an important aspect when one compares these products with conventional elastomers. In summary, the reversibly crosslinked iPP is an innovative material from the mechanical point of view. In addition, the reactivity of crosslinked iPP overcomes the problem of recycling. This is another aspect that will probably improve the wide using range of this material.

5. Conclusions

1. The new method developed for the reversible crosslinking of iPP gives rise to a promising material with improved mechanical properties. In particular, the impact strength of the modified iPP is comparable to that shown by conventional elastomers.

2. The crosslinking process originates a transition from brittle to ductile behavior in the modified iPP.

3. The crystallinity, and the micromechanical properties of the crosslinked iPP are slightly lower than those the unmodified material. The microhardness decrease is attributed to the combined effect of a crystallinity decrease, the occurrence of smaller crystals in the modified iPP, and the appearance of a low fraction (25-29 %) of PE crystals.

Part II B: Continuous part of second part of results and discussion dealing with :Study of generated ethylenic Chains

The academic finding of the innovative study deals with the appearance of ethylenic chains part. The study is a complement part of the same study described above and the analysis were done using DMTA, DSC and FTIR. The study is still under investigation to elucidate the mechanism of the reversibly crosslinking reaction.

DMTA results

Dynamic mechanical thermal properties (mechanical loss factors tanδ, and storage Young modulus E') were investigated in the $-150 \leq T \leq 170$ °C temperature and 0.3-30 Hz frequency ranges by using a dynamic mechanical thermal analyzer (DMTA) from Polymer Laboratories. The samples were tested in a double cantilever driven in bending mode with a fixed displacement ($\pm$ 16 μm). A heating rate of 2K/min was employed over the wholly temperature range.

Three well defined relaxation regions, i.e. at $T \approx -110$ °C (γ), in the interval $-10 \leq T \leq 30$ °C (α) and in the interval $50 \leq T \leq 100$ °C (α ') appear. They are associated to local (γ) and segmental (α and α') motions. In the case of original iPP (i.e. without any activator) the low-*T* process is rather spread out towards temperatures higher than −110 °C. In the presence of the catalyst, the temperature range of the γ-process reduces to a rather narrower dispersion region around −110 °C. Thus, the hardest local modes (i.e. those visible at $T > -110$ °C) seem to be suppressed as an effect produced by the introduction of the catalyst.

With regards to the cooperative α-relaxation process (between 0 °C and 30 °C) we observe that in samples 1, 2, 5, and 6 the dispersion peak moves towards higher *T* (by ~ 10 °C) with respect to the original iPP, whereas for the others (samples 3 and 4) the dispersion region appears to be rather spread out.

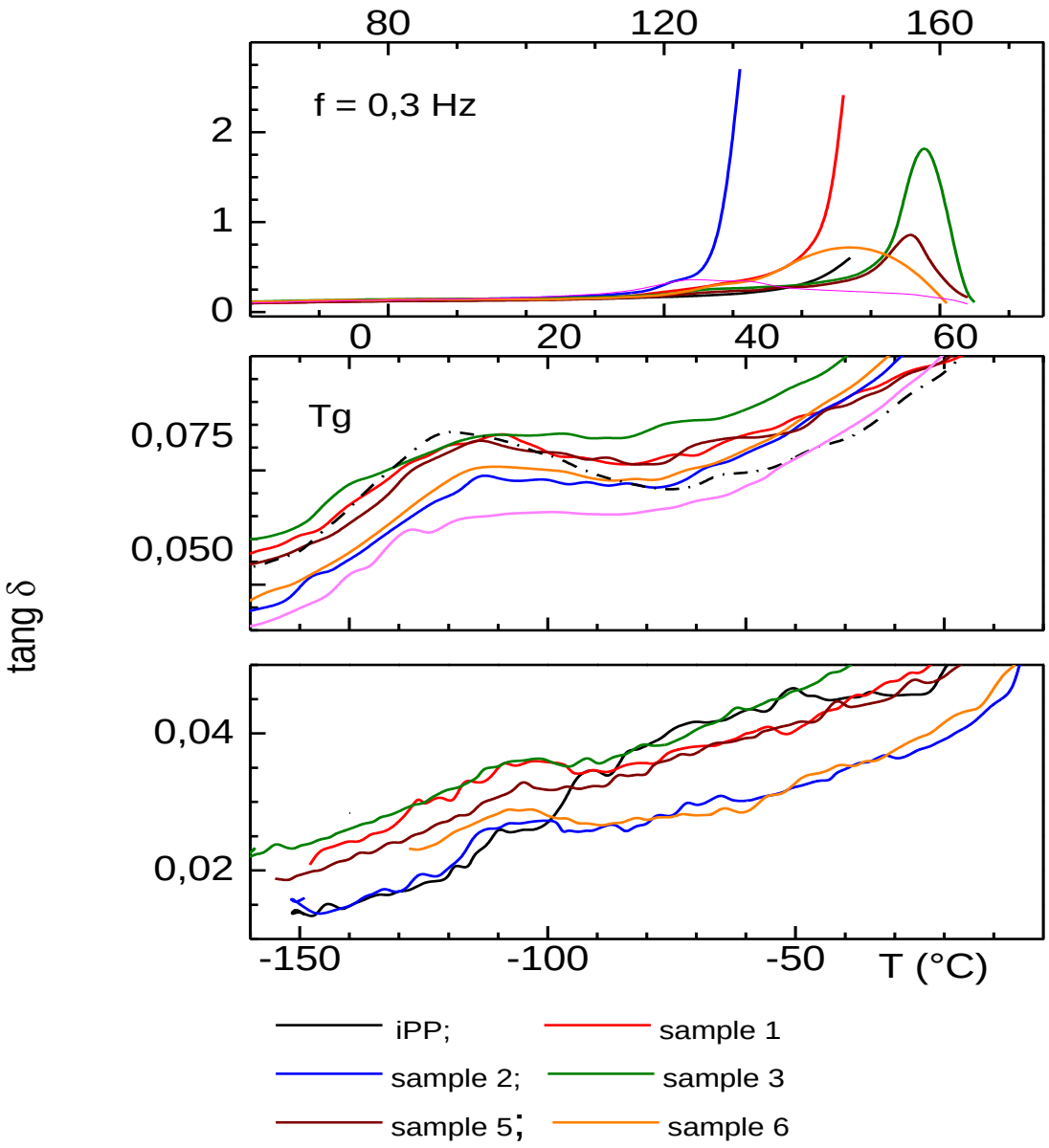

Fig II . B. 1 : DMTA curves for different XiPP compositions

The α'-relaxation process, on the other hand, could be ascribed to the segmental motion occurring within amorphous regions embedded by consecutive crystalline-iPP lamellae.

Finally, in the high *T* region we find the melting processes. For samples 3 and 5 the melting onset is slightly higher than pure iPP. On the other hand, samples 1, 2 and 6 manifest a weakening at temperatures significantly lower than iPP.

In sample 4 we observe from the Log(E') pattern that a hardening process sets in just above 120°C. The latter is a temperature where PE usually melts. Thus the hardening process could probably be ascribed to further iPP crystallization previously hindered by the presence of PE crystals.

The temperature behaviors of the mechanical modulus E', at a frequency of 0.3 Hz, for all the samples is compared to that of net iPP sample. At least three relaxation drops are evident in the mechanical spectra of all the specimens, whose position shifts to higher temperatures with increasing frequency (not shown here) as expected for thermally activated relaxation processes. As the temperature is increased from -150 °C, Log (E') slowly decrease and passes through the γ –relaxation drop, located at about – 90 °C (at 0.3 Hz). Above 0 °C, E' shows for all the samples a second drop which is associated to the glass to rubber transition (α-relaxation or dynamic Tg), exhibiting the familiar shifts to higher temperatures, the higher the driving frequency (not shown here).

Finally, for higher values of temperature the α'-relaxation process appears.

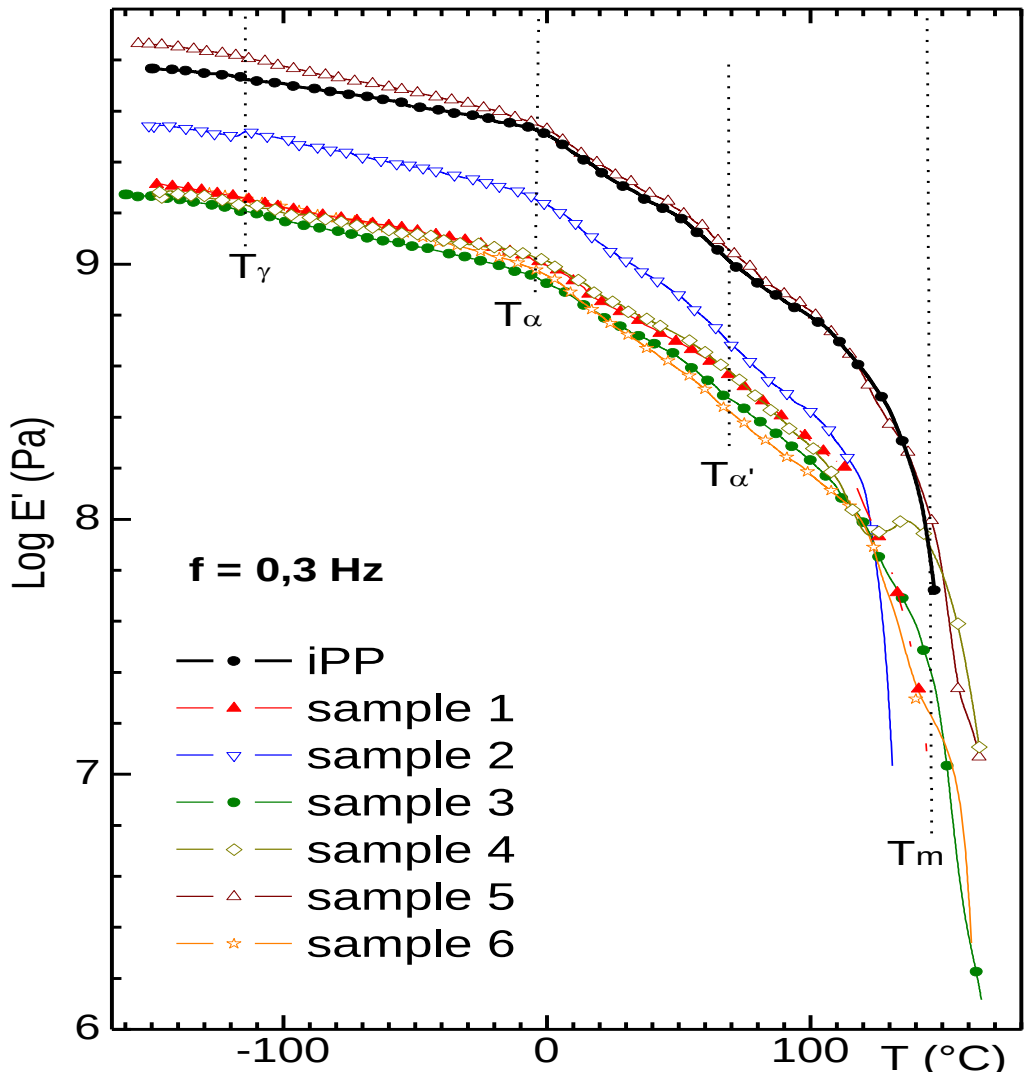

Fig II. B. 2 : Differents Glass transitions Tg's for different XiPP Compositions

Note that the values of Log(E') follow the same trend of the microhardness results reported in the first part. In fact, at room temperatures, all samples have modulus values lower than that of pure iPP, except sample 5, that show a value almost identical to that of iPP.

Table II. B. 1 : Micro- and macro- mechanicals properties for differents XiPP Compositions

Sample	Peroxide content (%)	Sulfur content (%)	Accelerator content (%)	Impact Strength (J/m^2)	Microhardness (MPa)	Mechanical modulus $(E')^{25^\circ}$ (Gpa)	ρ (gr/cm^3)
1	0.2	0.2	0.05 (TMTD)	19.40	78	0.67	
2	0.4	0.4	0.01 (TMTD)	15.91	72	1.10	
3	0.2	0.2	0.05 (TMTM)	24.47	79	0.58	
4	0.4	0.4	0.1 (TMTM)	18.25	70	0.70	
5	0.2	0.2	0.05 (MBTS)	30.94	88	2.24	
6	0.4	0.4	0.1 (MBTS)	19.79	81	0.56	
iPP		--------	----------	4.47	89	2.10	

TMTD: tetramethyl thiuram disulphide -
TMTM. tetramethyl thiuram monosulphide -
MBTS: mercaptobenzothiazole disulfide –

The difference in the values of Log (E') is due to the activation temperature of the accelerator MBTS which has higher activation temperature around 180°C whereas the TMTM and TMTD have activation temperature around 140°C. In this case the overall crosslinking reactions of these three accelerators are different.

DSC results

DSC scans at 20 °C/min have been carried out on all the samples. Bare iPP shows already a small endothermal peak at about T = 115 °C, which can be associated to the presence of small amounts of PE (as confirmed by the IR analysis below). At higher temperature the large melting peak characteristic of iPP is found. The addition of the catalyst has, as a consequence, the enhancement of the PE melting peak and the appearance of a small, spread out shoulder (the origin of which we don't know) in the 50 ≤ T ≤ 90 °C interval. The table reports the values of the peak temperatures and the enthalpies associated to the melting processes observed.

The melting enthalpies of the iPP and PE mono-crystals have been taken to be:

iPP – 207,33 J/gr

PE – 293,86 J/gr

For an initial estimate of the effects of the catalyst, last column to the right in the table reports the ratio X_c of the iPP-component melting enthalpy to the value obtained for bare iPP, i.e.

$$X_c = \frac{\Delta H_{iPP}}{83.3} \quad \text{(J/gr)}$$

Table II. B. 2 : ΔH_{iPP} and X_c by DSC for different XiPP compositions

Sample	ΔH_{PE} (J/gr)	T_{melt} (PE) (°C)	ΔH_{iPP} (J/gr)	T_{melt} (iPP) (°C)	ΔH_{tot} (J/gr)	X_c (cryst. iPP relative to pure)
Sample 1	13.1	125.9	70.6	169.5	83.7	0.85
Sample 2	11.4	124.9	68.4	166.7	79.8	0.82
Sample 3	11.9	125	68.4	168.9	80.3	0.82
Sample 4	14.5	125	64.6	166.7	79.1	0.77
Sample 5	12.5	125	75.3	168.9	87.8	0.9
Sample 6	12.9	125.6	66.5	166.7	79.4	0.95
iPP	negligible	115	83.3	167.3	83.3	1

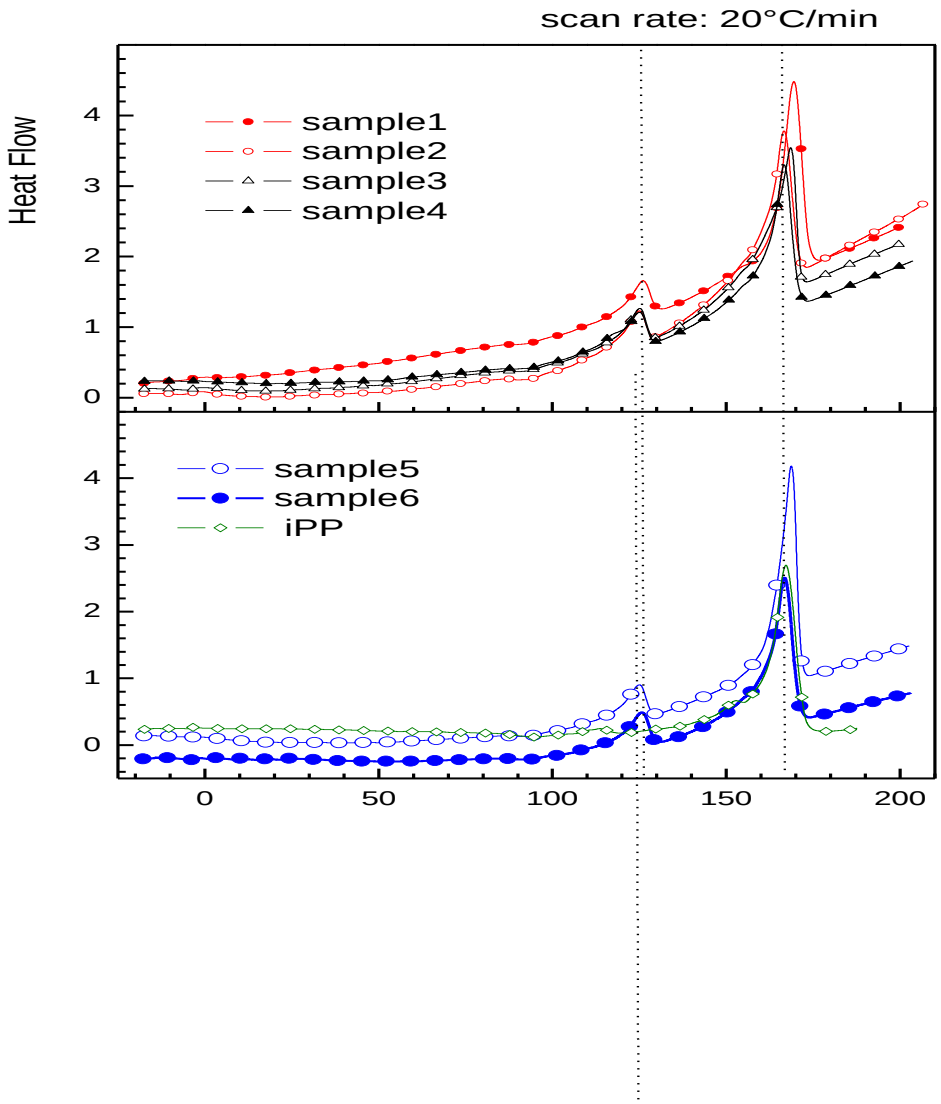

Fig. II. B. 3 : DSC curves for different XiPP compositions

FTIR results

We start from the high energy part of the spectrum, in the interval 2800 – 3000 cm $^{-1}$. With the idea of furnishing just a first, rough estimate of the content of iPP after addition of the catalyst, we consider the heights *h* of the peaks at 2920 and 2950 cm $^{-1}$, which are attributed to the CH_2 and CH_3 antisymmetric stretching modes respectively.

The table below reports the ratios $R \equiv h_{CH2} / h_{CH3}$ for the different samples. From these ratios it is possible to get an estimate of the fraction F_{iPP} of iPP (both in the amorphous and in the crystalline sates) still present in the samples after introducing the catalysts. This is done with the following procedure:

Let R_0 (= 1.28 in the present case) be the value obtained for bare iPP and let R_i be the value of Sample *i*. Then $R_i > R_0$ means that part of the CH_3 groups disappeared (i.e. iPP disappeared) and the relative enhancement of the CH_2 peak height with respect to the CH_3 one, is ascribed to a corresponding PE fraction appearing in the system. So,

$$F_{iPP} = R_0 / R_i$$

(more exactly, R should be estimated from the areas of the peaks, but here we just want to get an approximate evaluation of F_{iPP} , with the aim of tracing a route for a more reliable estimate of the real degree of crystallinity that iPP has in each sample).

From the values of F_{iPP} we can predict how much should be the iPP melting enthalpy of each sample *in the hypothesis that it crystallizes in the same way as in the bare iPP sample*. This estimate (i.e. $\Delta H_{iPP,\,IR} = F_{iPP} \times 83.3$ J/gr) is listed in the last column to the right of the table. The DSC measured melting enthalpies are also reported for an easy comparison.

Table II. B. 3: iPP fraction and $\Delta H_{iPP, IR}$ for different XiPP compositions

Sample	R	F_{iPP} (iPP fraction. From IR)	$\Delta H_{iPP, DSC}$ (J/gr)	$\Delta H_{iPP, IR}$ (J/gr)
1	1.73	0.74	70.6	61.6
2	1.46	0.88	68.4	73.3
3	1.59	0.81	68.4	67.5
4	1.71	0.75	64.6	62.5
5	1.5	0.85	75.3	70.8
6	1.53	0.84	66.5	70
iPP	1.28	1	83.3	83.3

Consider for instance Sample 1. We note that the measured (DSC) melting enthalpy of the iPP component is larger than predicted by the IR analysis. This means that the crystallinity of the iPP component in this sample is larger than in bare iPP. However, also Sample 5 has the same feature, but its mechanical modulus (and its hardness) is significantly larger than that of Sample 1.

A possible explanation may be that even if both the samples are microscopically inhomogeneous, in Sample 5 the "islands" are more efficiently interconnected than in Sample 1.

On the other hand, Sample 6 shows a slight reduction of the iPP crystallinity with respect to Sample 5, which could explain the decrease of both its E' modulus and hardness.

With regards to Sample 2 we note that, although the crystallinity of iPP is lower than in bare iPP sample, the fraction of iPP present is the highest among all. This would explain why its E' modulus is lower than the iPP one, but larger than all the others (except Sample 5, of course).

Other features of the IR spectra

Going to the low frequency part of the spectra, we observe the peaks at 720 and 730 cm^{-1} characteristic of the rocking mode of PE. Note that these peaks are present also in the "bare" iPP sample (which of course is not pure; go back to the DSC thermogram of this sample).

The peak at 870 cm $^{-1}$ is related to the C–C, C–N stretching and is due to the activator. The C–S stretching generates a peak at 1074 cm $^{-1}$, which however is very weak.

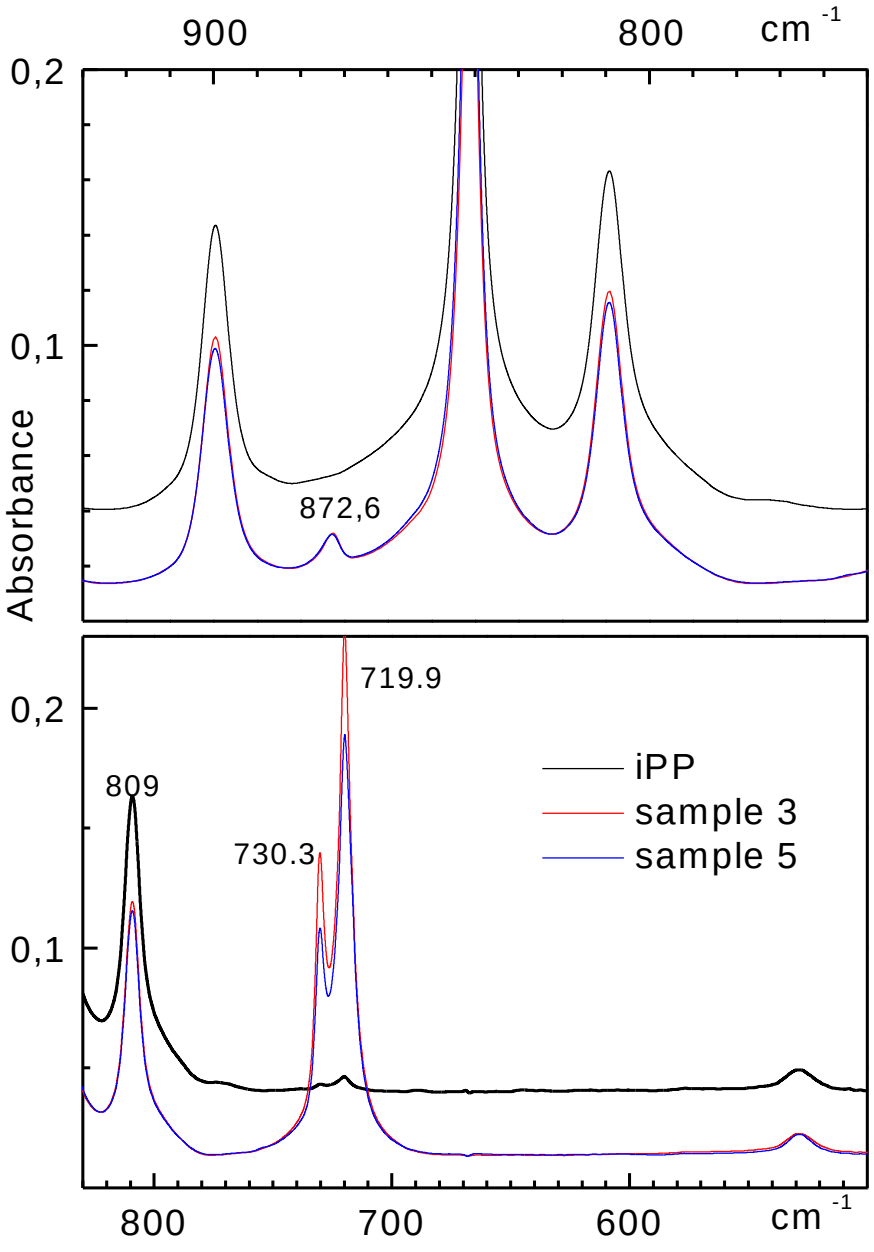

Fig. II. B. 4 : C—N and $(CH)_n$ bonds characteristics for different XiPP compositions

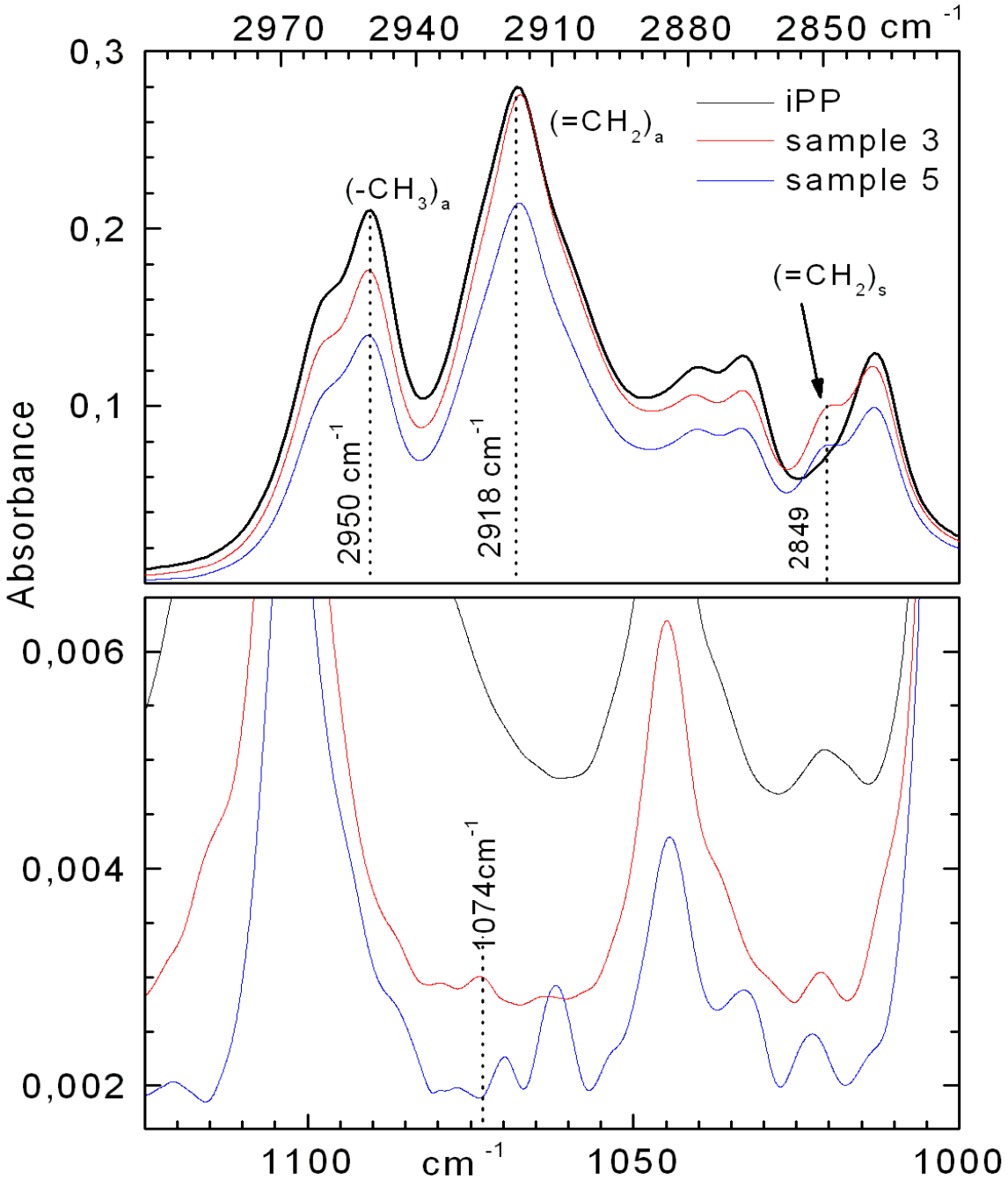

Fig. II. B. 5: Bonds characteristics of iPP fraction and C—S bond characteristic for different XiPP compositions

Discussion

From the different results reported in this part, it will be clear to say that the crosslinking reaction generates ethylenic chains and the chemical mechanism is very complex and need more investigation. In all case the amount of ethylenic chain generated is so high “up to 25%” by weight which is great result and the question is to see which part of this ethylenic chain will be in crystalline region and second point dealing with the participation of this ethylenic part in bridges forming the crosslinked networks. The computation of the different properties let us to say that the material is more ductile and the PE Tg appearing in different compositions shows that is responsible in some case about this behavior. The DSC shows that there is one part of this ethylenic chains will crystallise this is with good agreement with the DRX results where there is appearance of Polyethylene characteristic peaks. Third point dealing with the FTIR results where the generated ethylenic chain is clearly mentioned by the ethylene characteristic groups . For this reason the comparison of FTIR and DSC iPP fraction shows that there is could agreement. Finally, we think that the atomic microscopic forces to see the lamellas of each part and the RMN to see the linking molecules , permit us to see what happen in this reaction.

Part III: Study of crosslinking agent on the properties of iPP/LDPE Blends

Introduction

In the part II, we have presented the experimental method developed for reversibly crosslinking of the iPP, and studied the properties of the modified materials obtained by using several crosslinking agents in different proportions. As it was there indicated, this method is also susceptible to be applied to different kind of polyolefins, and their blends. As polyolefins are among the polymers most widely used in the world, the possibility of solving the problems related with their recovery and recycling is really very attractive.

Thus, we have extended the crosslinking method, initially developed to reversibly crosslink the isotactic polypropylene (iPP), to low density polyethylene (LDPE), and also, to several iPP/LDPE blends with different compositions .

Experimental

The materials used in this investigation were the following:

Isotactic polypropylene (iPP) Sabic-Vestolen 9000-67404: supplied by Chemische Werke Hüls, Germany.

Low density polyethylene (LDPE) B21 sak: supplied by ENIP, Skikda, Algeria

Dicumyl peroxide (DCP) (96% activity): supplied by NORAX.

Sulfur, (S) (vulcanizing agent for rubber) supplied by Wuxi Huasbeng Chemical Additives factory, China

Potassium persulfate: supplied by Innochem, Belgium.

The three accelerators used were: “Super accelerator 500” (tetramethyl thiuram monosulphide, TMTM); “Super accelerator 501” (tetramethyl thiuram disulphide TMTD); and “Quick accelerator 200” (mercaptobenzothiazol disulphide, MBTS). They were supplied by Rhône-Poulenc, France.

The peroxide, the sulfur, and the accelerators constitute our “crosslinking agents”.

Blend preparation

For the preparation of the blends, the sulfur concentration was always equal to that of the peroxide. The amount of sulfur and peroxide was 0.2 or 0.4 wt %. In all cases, the accelerator was ¼ of the sulfur and peroxide concentration. The composition of the samples included in this study is indicated in Tables III.1.1 to 1.4.

The iPP, the LDPE, the crosslinking agent and the potassium persulfate were first mixed in the solid state, using a small quantity of vegetal oil, to wet and improve the dispersion of the fine powder of the different components within the granules of the iPP and the LDPE. Thereafter, the obtained mixture was inserted into a single screw laboratory extruder (Prolabo 1989) with the following characteristics: L/D = 20; screw diameter = 25 mm; screw speed = 60 turns/min. The residence time was about 3 min. The temperature profile used for the three stages was: feed zone = 155º C; compression zone = 180º C; homogenization zone = 200º C. The extrusion cycle was repeated twice to achieve a homogeneous blend.

Table III. 1.1. iPP and LDPE samples

Sample	Polymer	Peroxide content %	Sulfur content %	Accelerator content %
iPP	iPP	---	---	---
1	iPP	0.2	0.2	0.05 (TMTM)
2	iPP	0.4	0.4	0.1 (TMTM)
3	iPP	0.2	0.2	0.05 (TMTD)
4	iPP	0.4	0.4	0.1 (TMTD)
5	iPP	0.2	0.2	0.05 (MBTS)
6	iPP	0.4	0.4	0.1 (MBTS)
LDPE	LDPE	---	---	---
X1	LDPE	0.2	0.2	0.05 (TMTM)
X2	LDPE	0.4	0.4	0.1 (TMTM)
X3	LDPE	0.2	0.2	0.05 (TMTD)
X4	LDPE	0.4	0.4	0.1 (TMTD)
X5	LDPE	0.2	0.2	0.05 (MBTS)
X6	LDPE	0.4	0.4	0.1 (MBTS)

Table III. 1.2. Blends PP/PE 30/70

Sample	Polymer	Peroxide content %	Sulfur content %	Accelerator content %
PP/PE 30/70	PP/PE 30/70	---	---	---
VI1	PP/PE 30/70	0.2	0.2	0.05 (TMTM)
VI2	PP/PE 30/70	0.4	0.4	0.1 (TMTM)
VI3	PP/PE 30/70	0.2	0.2	0.05 (TMTD)
VI4	PP/PE 30/70	0.4	0.4	0.1 (TMTD)
VI5	PP/PE 30/70	0.2	0.2	0.05 (MBTS)
VI6	PP/PE 30/70	0.4	0.4	0.1 (MBTS)

Table III.1.3. Blends PP/PE 50/50

Sample	Polymer	Peroxide content %	Sulfur content %	Accelerator content %
PP/PE 50/50	PP/PE 50/50	---	---	---
IIA	PP/PE 50/50	0.2	0.2	0.05 (TMTM)
IIB	PP/PE 50/50	0.4	0.4	0.1 (TMTM)
IIC	PP/PE 50/50	0.2	0.2	0.05 (TMTD)
IID	PP/PE 50/50	0.4	0.4	0.1 (TMTD)
IIE	PP/PE 50/50	0.2	0.2	0.05 (MBTS)
IIF	PP/PE 50/50	0.4	0.4	0.1 (MBTS)

Table III.1.4. Blends PP/PE 70/30

Sample	Polymer	Peroxide content %	Sulfur content %	Accelerator content %
PP/PE 70/30	PP/PE 70/30	---	---	---
IV1	PP/PE 70/30	0.2	0.2	0.05 (TMTM)
IV2	PP/PE 70/30	0.4	0.4	0.1 (TMTM)
IV3	PP/PE 70/30	0.2	0.2	0.05 (TMTD)
IV4	PP/PE 70/30	0.4	0.4	0.1 (TMTD)
IV5	PP/PE 70/30	0.2	0.2	0.05 (MBTS)
IV6	PP/PE 70/30	0.4	0.4	0.1 (MBTS)

Techniques

We have investigated the influence of the crosslinking process in the microstructure, and the micro- and macromechanical properties of the modified blends. The samples have been characterized by using the following techniques: wide-angle X-ray scattering (WAXS), differential scanning calorimetry (DSC), microhardness measurement, and tensile stress-strain study.

The microhardness of the samples was measured at room temperature using a Leitz tester, equipped with a square-based diamond indenter [22]. The *H*-value was derived from the residual projected area of indentation according to: $H = kP/d^2$. In this expression, *d* is the length of the impression diagonal in meters, *P* is the contact load applied in N, and *k* is a geometrical factor equal to 1.854. Loads of 0.25, 0.5, and 1 N were used. The loading cycle was 0.1 min. 8-10 indentations were made on each sample, and the results were averaged.

Thermal analysis was performed in a Perkin-Elmer differential scanning calorimeter DSC-4, in a N_2 atmosphere. The temperature range studied was 45-220º C. The heating rate was 20 ºC/min. Typical sample weights were 5-10 mg. The crystallinity measured by calorimetry, α_{DSC}, was derived from the melting enthalpy obtained by DSC using the following expression: $\alpha_{DSC} = \Delta H_m / \Delta H_m^{\infty}$, where ΔH_m and ΔH_m^{∞} are the experimental melting enthalpy, and the melting enthalpy for an infinitely long crystal, respectively.

The WAXS study was performed using a Seifert diffractometer (reflection mode). The working conditions were: voltage: 40 kV; intensity: 35 mA; angular range: 5-30º (2θ); scan rate: 0.01 º/s; slits: 0.3, 0.2. The crystallinity α_{rX} of every sample has been calculated as the relation of the area corresponding to the crystalline peaks to the total area of the diffractogram.

Results

The blends properties, obtained from the DSC, WAXS and microhardness study, are listed in Tables III.2.1 to 2.5. These tables include: the melting enthalpies ΔH_m and melting points T_m of every component in the blends, the crystal thickness l_c derived from them, the crystallinities α_{DSC} and α_{rX} obtained from the DSC and WAXS

study, respectively, and the microhardness value *H* of each sample. In addition, the mechanical properties of the crosslinked blends are presented in Table III.2.6.

X-ray diffraction study

The diffractograms of the different samples are shown in Figs. 1 to 3.

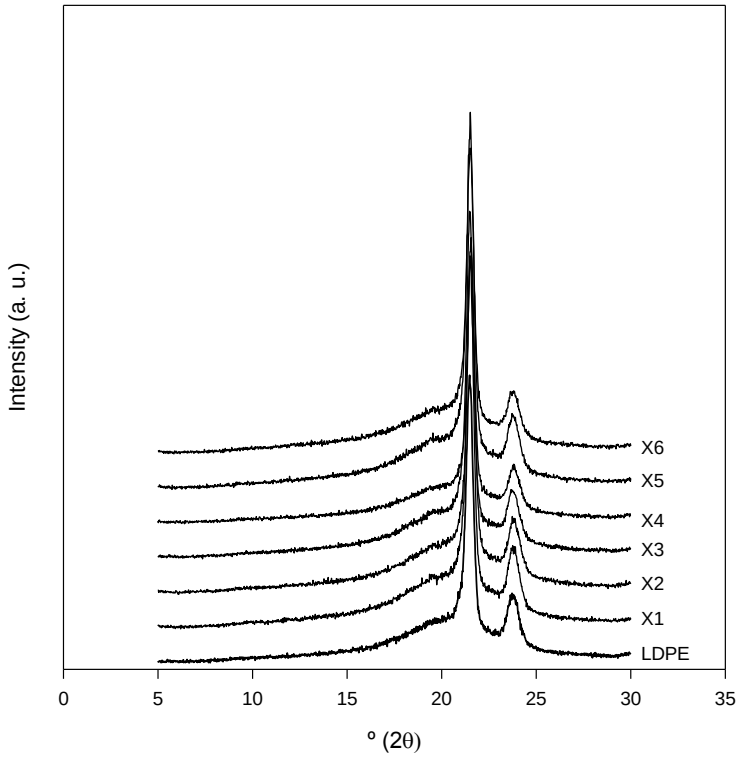

Fig.III. 1. Diffractograms of LDPE original and crosslinked; see Table 1.1 for composition.

The WAXS patterns taken on the non modified and crosslinked samples of LDPE are shown in Fig.III. 1. From the inspection of these diffractograms, and also, from the crystallinity data α_{rX} derived from them (see Table III. 2.1, column 6), the crosslinking process does not seem to affect the crystalline structure of the material. In fact, the diffractograms of all samples are practically identical, and typical of the orthorhombic unit cell of polyethylene [28], their α_{rX} values remaining almost constant.

Fig.III. 2 shows the diffractograms of the original and crosslinked iPP samples. All of them are characteristic of the monoclinic α-form of isotactic polypropylene [27]. By comparing the diffractogram of the original iPP with those of the crosslinked materials, it can be seen that the crosslinking process seems mainly to affect the relative intensity of the first two diffraction peaks. All crosslinked samples exhibit crystallinity values α_{rX} values that are slightly lower than the one shown by the non modified iPP (see Table III. 2.2, column 10). In addition to this, in the WAXS patterns of the crosslinked iPP samples one observes a new, small intensity reflection at about 23.8 º (2θ), not shown in the original iPP diagram [27,30].

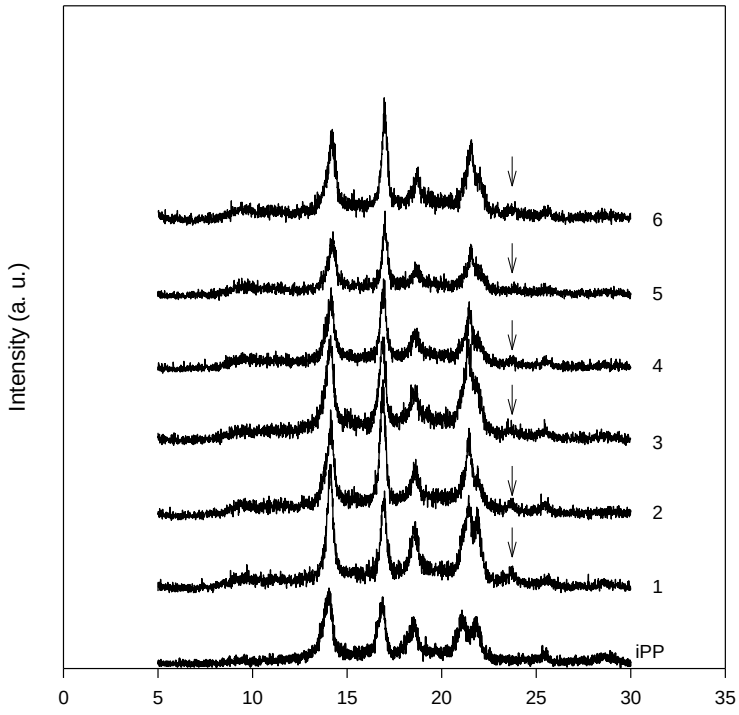

Fig.III. 2. Diffractograms of iPP, original and crosslinked; see table 1.1 for composition.

This reflection, indicated by an arrow, can be related to the (200) planes in PE [ ]. Moreover, the (111) reflection in the non modified iPP, appearing at about 21 º (2θ), is slightly shifted to higher angles, being almost coincident with the (110) reflection of PE, at 21.55º (2θ) [28].

In fig.III. 3, the WAXS patterns of the blends PP/PE 50/50, original and crosslinked, are shown. All the diffractograms present the characteristic reflections of, both, PE and iPP. The crosslinking process seems only to affect the relative intensity

of some reflections. The other blends, with compositions PP/PE 30/70 and 70/30, not shown here, behave similarly.

On the other hand, the crystallinity values α_{rX} of the crosslinked material remain very close to that of the original PP/PE 50/50 blend (see Table III. 2.4, column 11). This is also true for the other PP/PE blends with composition 30/70 and 70/30. The crystallinity data α_{rX} derived for these blends are listed in Table III. 2.3, column 11 and Table III. 2.5, column 11, respectively.

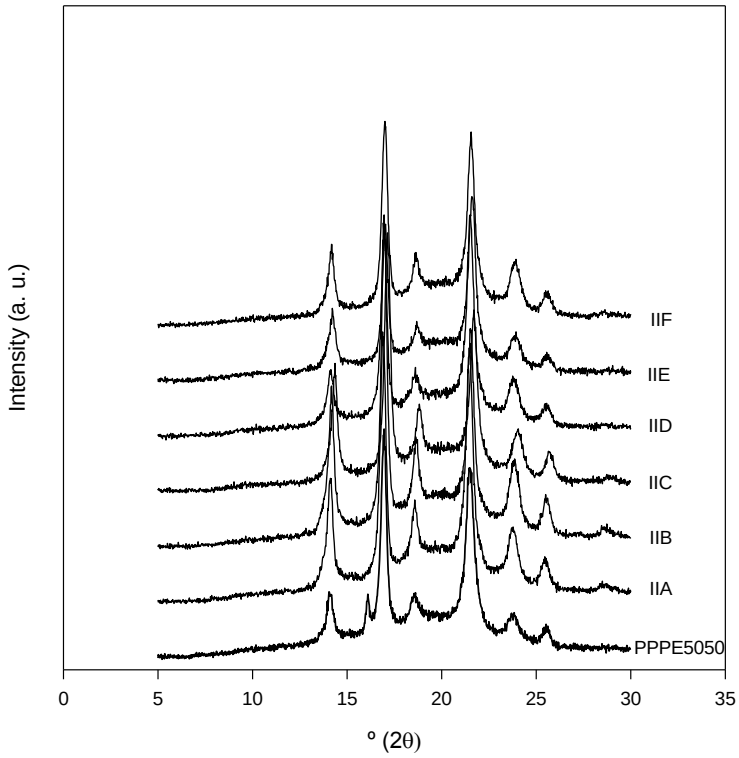

Fig. III. 3. Diffractograms of blends PP/PE 50/50, original and crosslinked; see Table III.1.3 for composition.

Differential scanning calorimetry

The thermograms of all the samples included in this study are shown in Figures III. 4 to III.8.

In Fig. III. 4, it can be seen that the thermograms of all the LDPE samples, either non-modified or crosslinked, are almost equal. The crystallinity values α_{DSC}

derived from them (Table III. 2.2, column 5) remain practically the same (0.38-0.40) after the crosslinking process.

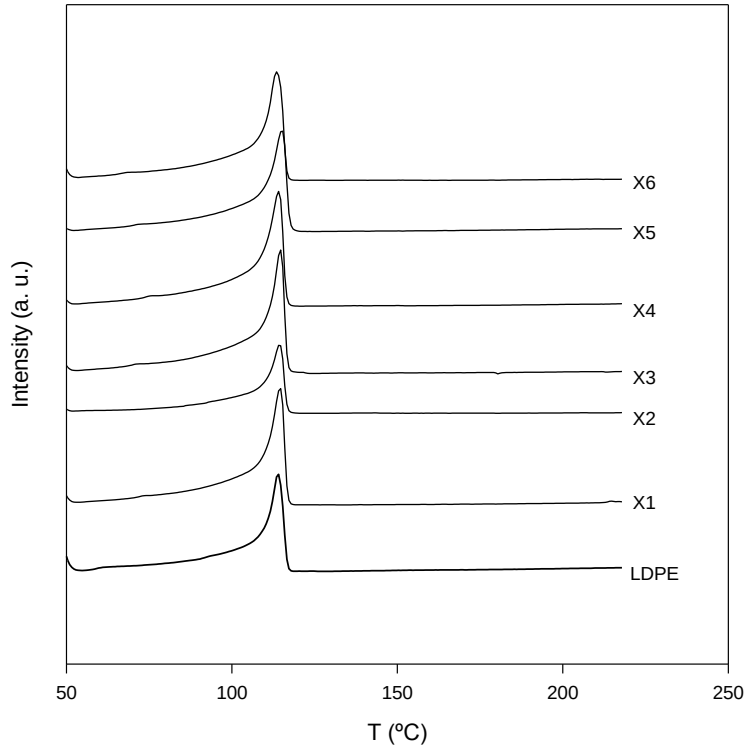

Fig. III. 4. Thermograms of LDPE original and crosslinked; see Table 1.1 for composition.

Table III. 2.1. LDPE samples

Sample	T_m (ºC)	l_c (nm)	ΔH (J/g)	α_{DSC}	α_{rX}	H (MPa)
LDPE	114.0	8.1	116.5	0.40	0.37	21
X1	113.7	8.0	114.1	0.39	0.36	21
X2	113.6	7.9	109.7	0.37	0.40	21
X3	113.8	8.0	113.6	0.39	0.37	20
X4	113.2	7.8	112.6	0.38	0.36	18
X5	114.2	8.1	116.0	0.40	0.38	20
X6	112.7	7.7	110.9	0.38	0.36	21

Fig.III. 5 shows the thermograms of the iPP samples. From the inspection of this figure, one observes a new, low temperature melting peak, appearing in all the

crosslinked iPP samples, but not in the non-modified material. This peak is indicated by an arrow [30]. Its appearance may be due to the presence of PE chains, eventually originated by the action of the peroxide and the potassium persulfate on some of the tertiary carbon atoms of the iPP. Table III. 2.2 includes the melting temperatures T_m corresponding to the different peaks of each sample.

The thermodynamic crystal size l_c has been derived for each maximum by means of the Thomson-Gibbs equation:

$$T_m = T_m^0 [1-(2\sigma_e / \Delta H_m^\infty l_c)] \quad (1)$$

In this expression, σ_e is the surface free energy and T_m^0 is the equilibrium melting point of each component. Table III.2.1 lists, besides the l_c values, the melting enthalpies ΔH_m and the crystallinities α_{DSC} for, both, PP and PE. In this calculation, we have used the following values: for the iPP component, ΔH_m^∞ = 207.33 J/g [24], T_m^0 = 460.7 K [24], and σ_e = 100 erg/cm^2 [25]. For the PE component, ΔH_m^∞ = 293.86 J/g [24], T_m^0 = 414.6 K [24], and for the surface free energy σ_e of the PE, we have taken the value of 79 erg/cm^2 [26]. This value probably represents an upper limit. In fact, according to our results, σ_e on linear PE samples depends on the molecular weight. Thus, for PE samples studied in [26], the surface free energy varies between 79 and 91 erg/cm^2 [26]. On the other hand, the melting point found in our work for the first maximum appearing in the thermograms of the crosslinked samples is 117-118º C. This is a relatively low value, suggesting that the PE originated during the crosslinking process has a low molecular weight and/or is not linear, but branched.

Table III. 2.2. iPP samples

Sample	T_{m1} (º C)	l_{c1} (nm)	ΔH_1 (J/g)	T_{m2} (º C)	l_{c2} (nm)	ΔH_2 (J/g)	ΔH_m total (J/g)	α_{DSC} (total)	α_{rX}	H (MPa)
iPP	---	---	---	159.8	16.8	105.0	105.0	0.51	0.52	86
1	118.6	9.7	33.7	159.9	16.9	83.3	117.0	0.52	0.42	79
2	117.6	9.3	25.2	158.6	16.4	75.4	100.5	0.45	0.40	70
3	118.4	9.6	30.3	158.5	16.1	82.3	112.7	0.50	0.39	78
4	117.7	9.3	31.2	157.8	15.7	81.6	112.8	0.50	0.41	72
5	117.7	9.3	30.1	160.8	17.5	96.5	126.5	0.57	0.42	88
6	118.4	9.6	30.2	158.8	16.3	84.3	114.5	0.51	0.42	81

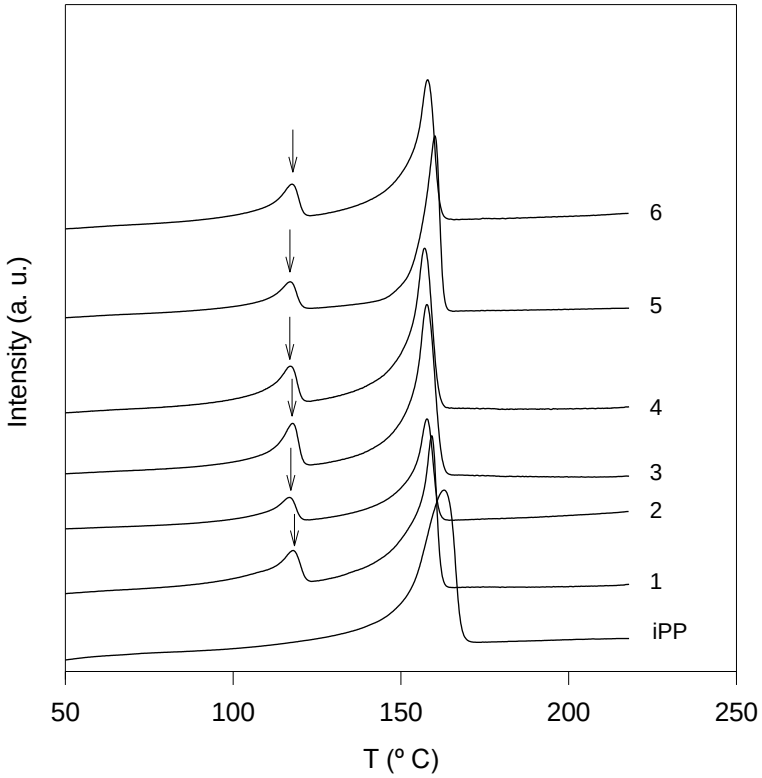

*

Fig.III. 5. Thermograms of iPP, original and crosslinked; see Table 1.1 for composition.

The thermograms of the blends of the two polymers, PP and PE, are shown in Figs.III. 6 to III. 8. It is worth noting that, in the thermograms of the crosslinked blends, the melting peak of the LDPE is wider than in the non-modified ones. This means that the crystal thickness l_{cPE} distribution is more heterogeneous in the crosslinked materials. Also, the l_{cPE} average value increases a little (Tables III. 2.3 to III. 2.5). On the other hand, the proportion of the area of the LDPE melting peak increases notably in all the crosslinked samples, compared to the non-modified ones. For instance, in the non-modified PP/PE blends with compositions 30/70, 50/50 and 70/30, the proportion of the area corresponding to the PE melting peak is 77.4, 49.7 and 39.5 %, respectively. However, in the crosslinked PP/PE blends, the proportion of the PE melting peak varies between 79 and 81 % (series VI), 66 and 69 % (series II), and 49 and 58 % (series IV). Moreover, in the thermograms of the crosslinked

samples with PP/PE compositions equal to 50/50 and 70/30, together with the main melting peak of the LDPE at about 111-113ºC, a shoulder appears at 118-120ºC. Nevertheless, the iPP melting peak in the crosslinked samples looks quite similar to the one in the non-modified ones.

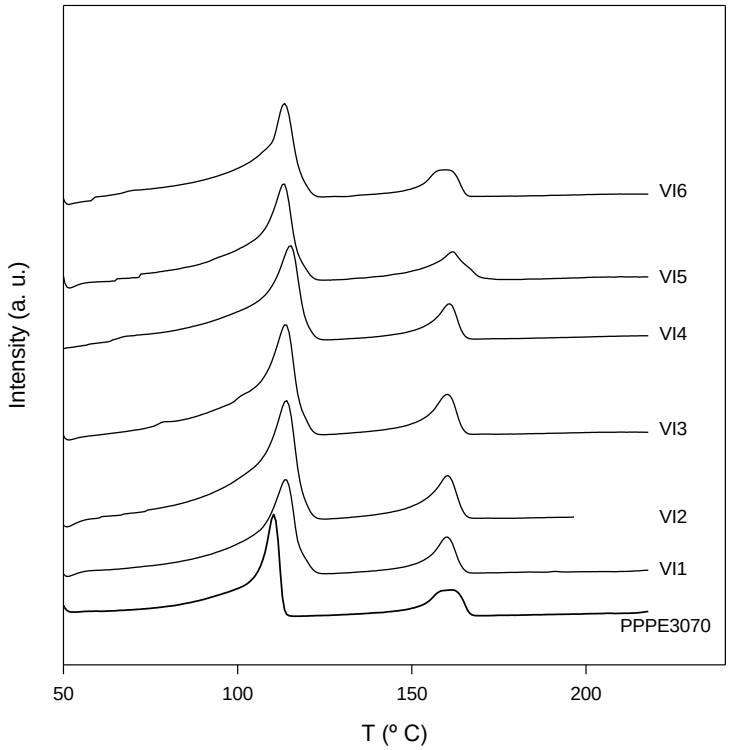

Fig. III. 6. Thermograms of the blends PP/PE 30/70 original and crosslinked; see Table 1.2 for composition.

Table III. 2.3. Blends PP/PE 30/70

Sample	T_{mPE} (ºC)	l_{cPE} (nm)	ΔH_{PE} (J/g)	α_{PE}	T_{mPP} (º C)	l_{cPP} (nm)	ΔH_{PP} (J/g)	α_{PP}	α_{DSC} (total)	α_{rX}	H (MPa)
PP/PE 30/70	109.5	6.9	72.0	0.24	160.6	17.3	21.0	0.10	0.35	0.39	30
VI1	112.8	7.7	89.4	0.30	159.1	16.4	20.9	0.10	0.40	0.40	29
VI2	112.9	7.8	98.1	0.33	159.3	16.5	23.2	0.11	0.45	0.41	30
VI3	112.7	7.7	94.9	0.32	159.2	16.5	23.1	0.11	0.43	0.41	30
VI4	114.1	7.7	100.9	0.34	159.8	16.8	23.7	0.11	0.46	0.39	28
VI5	112.2	7.6	102.2	0.35	160.7	17.4	26.7	0.13	0.48	0.37	32
VI6	112.4	7.6	103.6	0.35	158.8	16.2	24.1	0.11	0.47	0.40	29

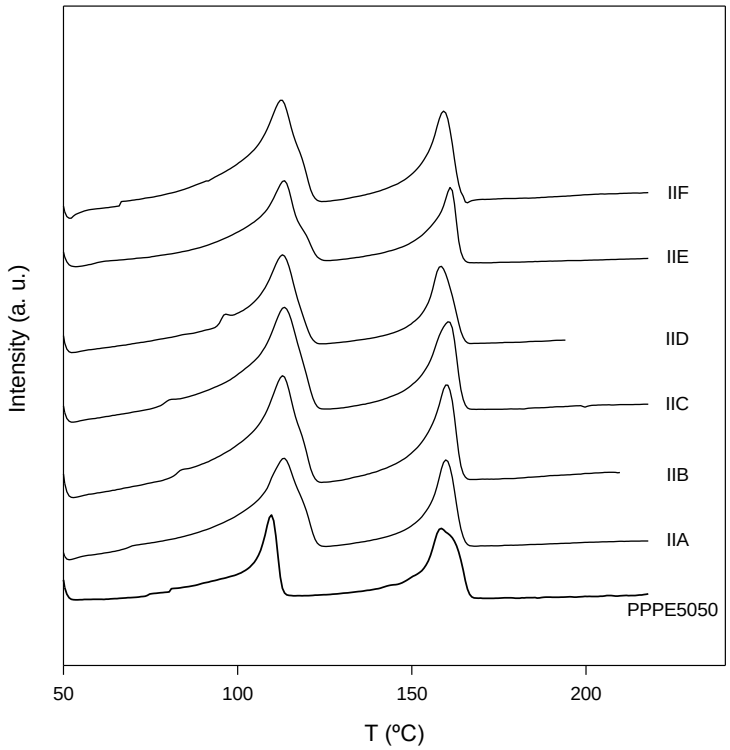

Fig. III. 7. Thermograms of the blends PP/PE 50/50, original and crosslinked; see Table 1.3 for composition.

Table III.2.4. Blends PP/PE 50/50

Sample	T_{mPE} (ºC)	l_{cPE} (nm)	ΔH_{PE} (J/g)	α_{PE}	T_{mPP} (º C)	l_{cPP} (nm)	ΔH_{PP} (J/g)	α_{PP}	α_{DSC} (total)	α_{rX}	H (MPa)
PP/PE 50/50	108.8	6.8	50.3	0.17	157.7	15.6	49.7	0.24	0.41	0.44	33
IIA	112.3	7.6	79.6	0.27	158.8	16.3	36.7	0.18	0.45	0.43	39
IIB	111.9	7.5	72.2	0.25	159.0	16.4	36.2	0.17	0.42	0.45	37
IIC	112.4	7.6	74.8	0.25	159.6	16.7	35.7	0.17	0.43	0.46	40
IID	111.9	7.5	71.2	0.24	157.3	15.5	35.2	0.17	0.41	0.43	34
IIE	112.5	7.6	73.4	0.25	160.2	17.1	37.3	0.18	0.43	0.43	41
IIF	111.5	7.4	82.6	0.28	158.2	15.9	37.3	0.18	0.46	0.42	34

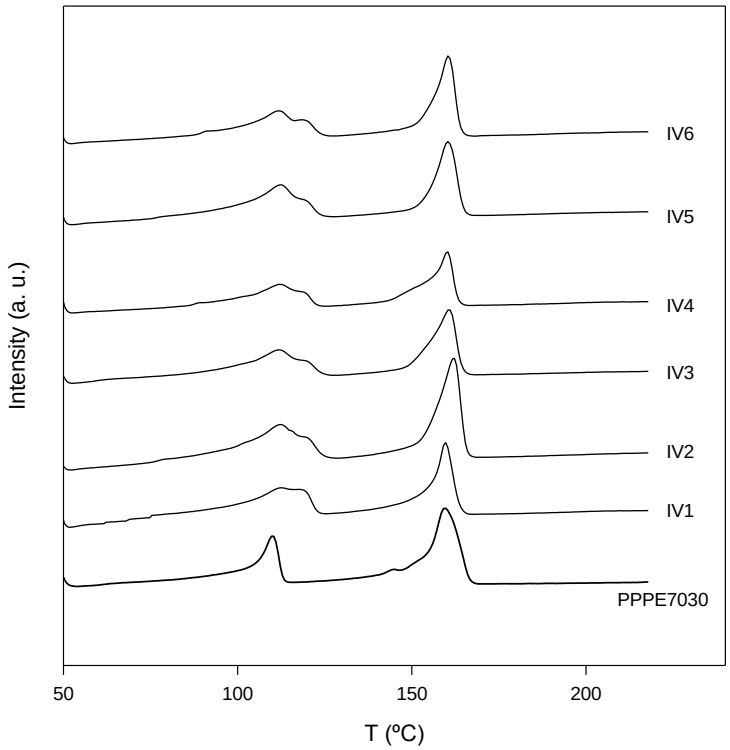

Fig.III. 8. Thermograms of the blends PP/PE 70/30 original and crosslinked; see Table 1.4 for composition.

Table III.2.5. Blends PP/PE 70/30

Sample	T_{mPE} (ºC)	l_{cPE} (nm)	ΔH_{PE} (J/g)	α_{PE}	T_{mPP} (º C)	l_{cPP} (nm)	ΔH_{PP} (J/g)	α_{PP}	α_{DSC} (total)	α_{rX}	H (MPa)
PP/PE 70/30	109.2	6.9	40.1	0.14	158.7	16.2	61.4	0.30	0.43	0.43	45
IV1	111.4	7.4	73.6	0.25	158.6	16.2	54.1	0.26	0.51	0.44	49
IV2	111.2	7.3	56.4	0.19	161.0	17.6	59.9	0.29	0.48	0.45	51
IV3	110.8	7.2	63.0	0.21	159.7	16.8	53.9	0.26	0.47	0.44	53
IV4	111.1	7.3	58.0	0.20	159.2	16.5	55.2	0.27	0.46	0.44	52
IV5	111.3	7.3	65.6	0.22	159.4	16.6	49.2	0.24	0.46	0.49	44
IV6	110.7	7.2	57.4	0.20	159.5	16.6	57.0	0.27	0.47	0.47	59

In addition to this, the crystallinity α_{PE} derived from the DSC study increases in all the crosslinked samples, with independence of the composition, in relation to the non-modified ones. On the contrary, α_{PP} does not vary (blends PP/PE 30/70, see Table III. 2.3), or experiences a small decrease (blends 50/50 and 70/30, see Tables III. 2.4 and III. 2.5). Total crystallinities α_{rX} and α_{DSC}, derived from both methods, show quite similar values.

Mechanical properties

Tables III. 2.1 to 2.5 include, in their last columns, the microhardness *H* values measured for all the samples studied. There is a linear relationship, not shown here, between the crystallinity α_{rX} of the samples and their microhardness values.

On the other side, Table III. 2.6 shows the data of the macromechanical properties obtained in the tensile stress-strain study. It is interesting to note that none of the crosslinked samples showed a yield point.

The crosslinking process does not seem to influence the microhardness of the PE samples (see column 7 in Table III. 2.1). However, crosslinked IPP samples show hardness values lower than the non-modified material, except sample 5, in which hardness slightly increases.

Table III.2.6. Mechanical properties of the crosslinked blends (tensile stress-strain study)

Sample	Elastic modulus (MPa)	Stress at break (MPa)	Strain at Break (%)	Energy at break
VI1	355	16.55	10.3	5.1
VI2	375	17.2	8.8	4.4
VI3	332	12.9	13.5	7.0
VI4	458	17.6	13.2	7.6
VI5	390	17.5	15.9	9.8
VI6	490	18.0	14.8	9.2
IIA	603	22.3	9.5	6.2
IIB	690	22.5	12.5	10.5
IIC	614	21.0	7.9	4.8
IID	650	22.6	10.6	7.5
IIE	667	22.0	9.4	6.1
IIF	976	26.4	9.4	8.0
IV1	1050	27.0	8.3	6.8
IV2	966	56.6	10.7	9.3
IV3	845	25.4	10.1	8.4
IV4	3638	105.8	8.4	7.1
IV5	960	25.9	9.4	7.81
IV6	976	26.4	9.4	8.0

In addition, the crosslinked PP/PE blends present *H* values that are identical (PP/PE 30/70, Table III. 2.3) or even higher (blends PP/PE 50/50 or 70/30, see Tables III. 2.4 and III. 2.5) than those shown by the non-modified material.

Discussion

From Figs.III. 1 and III. 4, and also from the data listed in Table III. 2.1, it can be deduced that the LDPE alone does not seem to be affected by the crosslinking process. In fact, the melting point T_m, the crystallinity α (derived by both methods, DSC and WAXS) and the microhardness *H* values remain practically the same for all the LDPE samples studied. However, from the data included in Table III. 2.2, it is clear that the crosslinking affects the iPP samples, that show α and *H* values slightly smaller than the non-modified counterpart. Most interesting, however, is the fact that the crosslinking process gives rise to the appearance of a certain amount of PE. The ethylenic chains are responsible for the appearance of a low temperature peak in the thermograms of the crosslinked iPP. The area of this new peak represents from 25 to 29 % of the total area of each thermogram, depending on the sample. This is also why, in the diffractograms of the crosslinked iPP samples, a new reflection can be seen at 21º (2θ), which is related to the (200) planes of PE. There are also FTIR studies performed on these samples, reported in part II B, that confirm the presence of ethylenic chains in the crosslinked iPP. The modified samples have impact strength values considerably higher than the original iPP, and have been shown to experience a ductile fracture, instead of the brittle one characteristic of the non-modified material , the result reported in part II A.

Concerning the PP/PE blends, none of them seem to be so much affected by the crosslinking process, for their crystallinity (both α_{rX} and α_{DSC}) and hardness *H* remain practically identical to the values shown by the non- modified materials, as can be observed from the inspection of Tables III. 2.3 to III. 2.5. Again, the biggest differences between the as-prepared and the crosslinked materials arise from their thermograms. As it has been above mentioned, whereas in the crosslinked blends, the iPP melting peak retains more or less their aspect, compared to the non-crosslinked ones, the PE peak seems to be more affected, especially in PP/PE 50/50 and 70/30 compositions, in the sense that its width increases, and also, is shows a shoulder at 118-120º C, together with the LDPE melting peak at 111-113º C. In addition, as it was mentioned in the results section, the percentage of the area of the PE melting peak increases in all the crosslinked blends, compared to the non-modified ones. Probably, these effects are related to the crosslinking process of the iPP, which, as it happens in case of crosslinked iPP samples, gives rise to the

formation of a certain amount of PE that would add to the PE initially present in the samples. The generation of the ethylenic chains could be explained as follows: the oxy-radicals of the peroxide might eventually attack the tertiary carbons of the iPP. In this case, the alcoholates provided by the peroxide or the peroxidisulfate would stabilize these tertiary carbons through formation of double bonds (intermediate reaction), which may react with the hydrogen H atom of the methyl side groups. The working conditions used are sufficiently strong as to permit the attack of this hydrogen atom. This is a very stable hydrogen atom, and one needs a very high energy to abstract it. Nevertheless, the entropy involved in this process is also high. The process would finally lead to the formation of branched ethylenic chains. These chains are thought to be responsible for the melting peak appearing at 117-118º C in the thermograms of the modified iPP. Also, the shoulder appearing on the high temperature side of the PE melting peak and the increase in the proportion of the area of the same melting peak in the crosslinked PP/PE blends are probably due to the newly created PE chains. Similar reversible crosslinking, also observed in other works [37-39], can be explained by chemical reactions of Diels –Alder type. Such a reversible crosslinking will lead to a “self repairing structure” due to the time - temperature dependence of this continuous reaction [39].

Concerning the macromechanical properties of the crosslinked blends, it is noteworthy that none of them presented a yield point. As it was said previously, Table III. 2.6 lists the values found for the elastic modulus E, and the stress, strain and energy at break for the three series of crosslinked samples.

The plot in Fig. III. 9 illustrates the relation between the elastic modulus, E (see Table III. 2.6), and the microhardness H (see Tables III. 2.3 to III. 2.5) , of the crosslinked blends, the corresponding equation gives, for this set of blends, a ratio E/H = 17. This value is higher than that obtained by Struik [33] and Flores *et al.* [34], who found a ratio E/H = 10.

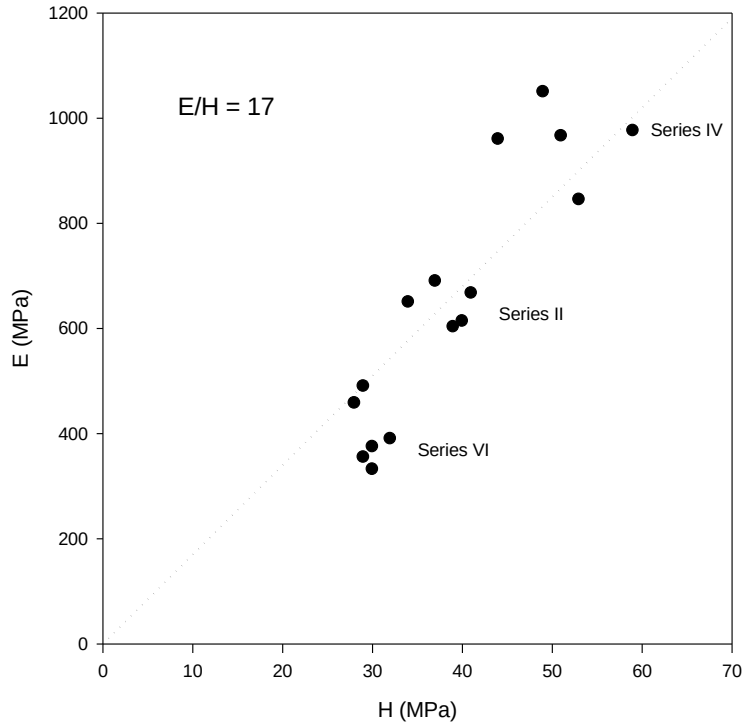

Fig. III. 9. Relationship between the elastic modulus and the microhardness in the crosslinked blends.

Conclusions

1. The new method, initially developed for reversibly crosslink the iPP, has been shown to be also applicable to PP/PE blends having different composition. The modified materials retain their structural and micromechanical characteristics.
2. As a consequence of the crosslinking process, a certain amount of PE chains are created at the expenses of the iPP present initially in the blends, as it has been demonstrated from the WAXS and DSC study. These PE chains have been probably originated by a process similar to the one explained for the case of iPP samples alone.

Conclusions :

What are the most important ideas that could be retained from the present work ?

Materials choice ?

Polyethylenes and Polypropylenes are among the most used polymeric materials. They represent more than 60% of total amount with wide range of end uses. They are now reaching a high ratio of recycled materials.

Technique choice ?

The reactive extrusion could be considered as the technique of the future because the device previously used just to transform raw materials to final shapes, has become the most appropriate equipment to physically-chemically modify conventional plastics. With this processing technique, the equipment; even at an industrial scale, is considered as a reactor. Some structural and chemical modifications, occurring “in situ” (chemical modifications, grafting polymerization, crossslikng …) could be achieved in one single step.

What does iPP crosslinking mean ?

Isotactic Polypropylene has highly regular chains with almost no ramifications,and in presence of oxy radicals or any degradation type, chain-scission degradation predominates in the final product. It is well known that chain - scission reactions will lead to low molecular weights and poor mechanical properties . We found the way to crosslink the iPP with no large expenses ; and this new finding led this material alone to undergo either chain-scission or crosslinking reactions ; this is not the case for other polymers. Adding to that, we made good use of the high shearing and thermo-mechanical operating conditions available in the reactive extrusion equipment. This tool could be considered for any functionalization,

How the crosslinking reaction is reversible ?

Up to now, we are continuing our investigations to further ellucidate such a reaction. The first findings allow us to say there is generation of new chains that will be become parts of the linking chains,. One can deduce that this crosslinking is strong at. low temperatures and weak at. high temperatures (molten state). By analogy we have related this crosslinking reaction to Dials Alder reaction [37]. Such a reversible crosslinking reactionis not only possible but also has been reported for other materials and systems [38-39]

What does this reversibility imply from an academic point of view ?

The formation of this new structure and reverse crosslinked network could be reconstructed in different ways : thus, we may say that we have a « self repairing structure ». Adding to that, the continuous odor arising from the material at room temperature, is a good indicator to show that reactions are continuing to occur; therefore, we suspect that we are dealing with a "new" material that could somehow repair its structure , at low temperatures and for a long time.

What are the industrial and environmental impacts of our results ?

From the different results reported here (and the ones not published yet) we think that there are good perspectives for the XiPP in many applications. Indeed, the XiPP a wide range and flexibility for some principal characteristics such as glassy temperature, elastic modulus , impact strength, ductibility…required for different industrial applications …

From the environmental point of view, this reaction opens the way to a better behaviour of iPP with differents other polymer materials, in order to facilitate the recycling operation . We have extended our method to other polyolefin materials such as polyethylene (low and high density) and also to isobutene 1.To encourage the environmental protection, the best way will be to show that our XiPP is very attractive from the economic side, and that it could be reused and classified, for some applications, as an « engineering material ».

Does the results found for raw materials could be considered as reference for recycled materials ?

Based on the different studies over the last 10 years, we can consider that there is a strong relationship between the present study and the state of recycling in general. In all cases, the last findings show that there is an enhancement of the most useful properties…

Why the use of different techniques such as microhardnes, DMTA, DRX …. ?

The experimental protocole used in our differents studies, was to describe the structure modification phenomena. Beside that, it was very beneficial for us to establish relationships between the macro- and the micro- structure properties. This needs the combination of several different characterization techniques to cover structural as well as thermomechanical properties.

What is the final contribution of the present work ?

The present work is only a part of our ambitious project that needs to be completed and assisted by some new and important scientific equipments. Based on our last findings, we would like to propose a project dealing with the new way of the use and reuse of plastics in general.

In that sense**,** the most important materials that will present big concerns and important challenges are : iPP, PET and the blends of iPP/PET and PET/HDPE.

References

1. D. Braun, S. Richter, G. P. Hellmann and M. Ratzsch, *J. Appl. Polym. Sci*, **68**, (1998), 2019 .

2. R. Gachter and H. Muller, *Plastics Additives Handbook*, 4th Ed., Hanser Publishers, Ed. P.P. Klemchuk Munich, Chap.17 (1993).

3. B. K. Kim, M. S. Kim and K. J. Kim, *J. Appl. Polym. Sci*, **48**, (1998), 1271.

4. B. K. Kim and C. H. Choi, *J. Appl. Polym. Sci*, **60**, (1996), 2199.

5. B. K. Kim and I. H. Do, *J. Appl. Polym. Sci***, 60,** (1996), 2207 .

6. B. K. Kim and I. H. Do, *J. Appl. Polym. Sci*, **61**, (1996), 439.

7. D.W. Mead, *J. Appl. Polym. Sci*, **57**, (1995), 151.

8. K.A. Kunert, H. Soszynska and N. Pislewski, *J. Polym*, **22**, (1981), 1355.

9. J. L. Way, J. R. Atkinson and J. Nutting, J. Mater. Sci., **9**, (1974), 293.

10. B. J. Lovinger and M. L. Williams, *J. Appl. Polym. Sci*, **25**, (1980), 1703.

11. T. Huang and M. R. Kamel, *Polym. Eng. Sci*. , **40**, (2000), 1796.

12. S. Hosoda and Y. Gotoh, *Polym. J.,* **20**, N°1, (1998), 17 .

13. H. P. Blom, J. W. Teh and A. Rudin, *J. Appl. Polym. Sci*, **58**, (1995), 995 .

14. K. Eise, J. Curry and J. Nangeroni, *Polym. Eng. Sci*., (1983). **23**, 642.

15.U. W. Gedde and J. F. Jansson, *Polym. Eng. Sci*., **20**, (1980), 579.

16. H. A. Khonakdar, J. Morshedian, M. Mehrabzadeh, U. Wagenknecht, and S. H. Jafari, *Eur. Polym. J.*, **39**, (2003), 1729.

17. H. A. Khonakdar, S. H. Jafari, U. Wagenknecht, and D. Jehnichen, *Radiat. Phys. Chem*., **75**, (2006), 78.

18. J. P. Mercier, E. Maréchal, Traité des matériaux: *9. Chimie des polymères*, Lausanne (1996). Ed. Presses polytechniques et universitaires romandes, Lausanne (Suisse) Chap. **9**, (2001) pp. 353-391.

19. H. A. Khonakdar, S. H. Jafari, M. Taheri, U. Wagenknecht, D. Jenichen and L. Häussler, *J. Appl. Polym. Sci*, **100**, (2006), 3264.

20. F. Romani, R. Corrieri, V. Braga and F. Ciardelli, *Polymer*, **43**, (2002), 1115 .

21. US Patent Nº 6,987,149; 17January 2006.

22. F.J. Baltá-Calleja and S. Fakirov, *Microhardness of Polymers*, (Solid State Science Series), Ed. Cambridge University Press, Cambridge (2000), pp. 1-237.

23. F. Berzin, B. Vergnes, S. V. Canevarolo, A. V. Machado and J. A. Covas, *J. Appl. Polym. Sci.* (2006),**99**, 2082 .

24. http://web.utk.edu/~athas/databank/html.

25. A. Flores, J. Aurrekoechea, R. Gensler, H. H. Kausch and F. J. Baltá-Calleja, *Colloid Polym. Sci.*, **276**, (1998), .276-786.

26. F.J. Baltá-Calleja, C. Santa Cruz, R. K. Bayer and H. G. Kilian, *Colloid Polym. Sci.* (1990),p.268.

27. J. Karger-Kocsis, *Polypropylene: Structure, blends and composites*, Ed. Chapman and Hall, London, Vol. 1, (1995).

28. F. J. Baltá-Calleja and C. G. Vonk, *X-ray scattering of synthetic polymers*, Ed. A. D. Jenkins, Elsevier New York, (1989). Chap. 3, pp. 94.

29. L.J. Bellamy, *The infrared spectra of complex molecules*, Ed. Methuen and Co. Ltd., John Wiley and Sons, Inc. London, (1964) Chap. 2, pp. 27-29.

30. L.J. Bellamy, *The infrared spectra of complex molecules*, Ed. Methuen and Co. Ltd., John Wiley and Sons, Inc. London, (1964) Chap. 22, pp. 353-355.

31. D. Tabor, *Hardness of Metals*, Ed. Oxford University Press, London (2000).

32. F. J. Baltá-Calleja, L. Giri, I. M. Ward and D. L. M. Cansfield, *J. Mater. Sci*. **30**, (1995), p.1139.

33. L. C. E. Struik*, J. Non-Cryst. Solids* (1991),131-133.

34. A. Flores, F. J. Baltá Calleja, G. E. Attenburrow and D. C. Bassett, *Polymer*, (2000), **41**, 5431.

35. W. Kurtz, J. P. Mercier, G. Zambelli, *Introduction à la science des matériaux*, Séries: Traité des matériaux, 1st ed., Lausanne (1987). Chap. 12, pp. 269-294 and Chap.13, pp. 295-310.

36. G.-M. Kim, G. H. Michler, M. Gahleitner and J. Fiebig, *J. Appl. Polym. Sci*. **60**, (1996), 1391.

37. Y.L. Liu, C.Y. Hsieh and Y.W. Chem; *Polymer,* **47**, (2006) 2581-2586.

38. M. Yamaguchi, S. Ono and M. Terano; *Materials letters,* **61**, (2007) 1396-1399.

39. C.E. Powell, X.J. Duthie and S. E. Kentish, *J. of Membrane Sci.* Article In Press.